Electrode-Based Wireless Passive pH Sensors with Applications to Bioprocess and Food Spoilage Monitoring

by

Sharmistha Bhadra

A Thesis submitted to the Faculty of Graduate Studies of
The University of Manitoba
in partial fulfilment of the requirements of the degree of

Doctor of Philosophy

Department of Electrical and Computer Engineering
University of Manitoba
Winnipeg

Abstract

This thesis purposes and develops inductively coupled LC (inductive-capacitive) pH sensors based on pH-sensitive electrode pair. The LC resonator circuit is based on a varactor and measures the low frequency potential difference. For wireless pH monitoring, the resonator circuit is integrated with a pH-sensitive electrode pair. This sensor demonstrates a linear response over 2 to 12 pH dynamic range, 0.1 pH accuracy and long-term stability. Accurate measurement of pH using electrode-based sensors is affected by temperature variation. A technique of simultaneously measuring two parameters, pH and temperature, with a single RLC resonator based sensor is presented. An algorithm is developed, which applies both pH and temperature measurement to incorporate temperature compensation in pH measurement. For in-fluid applications, an encapsulation method is applied to the LC resonator based sensor to reduce the influence of medium permittivity and conductivity on the sensor measurement. Non-invasive way to obtain reliable pH information from bacterial culture bioprocesses is demonstrated with the fluid embeddable sensor. The pH sensor is remodeled to an acidic and basic volatile sensor by embedding the electrodes in a hydrogel host electrolyte. Tests demonstrate that the volatile sensor has a detection limit of 1.5 ppm and 2 ppm for ammonia and acetic acid vapor, respectively. Application of the volatile sensor to fish spoilage monitoring shows that the sensor is capable of detecting the product rejection level with good sensitivity in real-time. It is important to develop low cost wireless passive pH sensor technologies for embedded applications such as bioprocess and food spoilage monitoring. The electrode-based passive LC sensor approach employed in this thesis overcomes drawbacks of some of the early developed passive pH sensors and can lead to an inexpensive implementation using printed electronics technology.

Acknowledgement

"*If I saw further than others, it is because I was standing on the shoulders of giants*."

- Sir Isaac Newton

I feel blessed that my academic journey has been shaped and guided by a terrific advisor: Dr. Greg E. Bridges. Hopefully my future ventures will reflect his collective wisdom in some way. I would like to express my deep sense of gratitude to him for inviting me to contribute to this multidisciplinary research. With a wonderfully easy-going and balanced character, he has been an exceptional role model for me. He is brilliant, incredibly patient, an engaging and interactive leader, and genuinely concerned about my welfare and progress. I also thank him for providing me opportunities to present at international research conferences, and CMC Texpo. A special gratitude to Dr. Douglas J. Thomson for being an integral part of this research work. He has provided tremendous insight into the physics and engineering of this project. I hope I lived up to their expectations. Many thanks to Dr. Michael S. Freund and Dr. Nazim Cicek for taking time out of their busy schedules to serve as my examining committee members. They provided their vision and knowledge during the project. A special thanks to Dr. Claudia Narvaez for teaching me microbial analysis of food.

I have enjoyed working with highly skilled colleagues – Warren Blunt, Mike McDonald, Chris Dynowski, Cameron Macgregor, Damaris Tan, Xiang Chen, Xuan Zhang and Maria Beijaflor. Their incredible work ethic, enthusiasm and fresh perspectives have continually inspired and energized our efforts. I gratefully acknowledge the University of Manitoba, the Natural Sciences and Engineering Research Council (NSERC) and CMC Microsystems for financial support of this research. I would like to appreciate the assistance of Cory Smit, Zoran Trajkoski, James Dietrich, Dwayne Chrusch and Amy Dario.

For ensuring that I did not become a complete hermit, I wish to thank my office people. Thank you all for enduring my often lengthy rants/stories! With all its mosquitoes and severe wind-chills, the city of Winnipeg has provided a wonderful multicultural (Folklorama is my summer highlight!) atmosphere and some of the most memorable moments in my life.

Finally, I wish to thank my family for their love and unwavering support during this difficult journey. I love them so much. I'm thankful for my life and abilities, which I always hope will contribute positively to the lives of others. Finally, I dedicate this thesis to my father, Satyajit Kumar Bhadra, who passed away when I was finishing this thesis. He encouraged me to be a researcher since I was at high school. My successful completion of this dissertation would have made him the happiest person in the world.

Contributions of Authors

This thesis is comprised of five journal papers. Three of them have been published and two of them are under review. All the papers are multi-authored. S. Bhadra is the first author on all papers. Contributions of all authors for these papers are explained below.

Chapter 2: S. Bhadra, G. E. Bridges, D. J. Thomson and M. S. Freund, "Electrode potential-based coupled coil sensor for remote pH monitoring," *IEEE Sensors Journal*, vol. 11, no. 11, pp. 2813-2819, Nov. 2011.

In this chapter of the thesis, Douglas J Thomson and Greg E. Bridges developed the idea. I have carried out the required background studies, circuit modeling, simulation, fabrication and experiments. Michael S. Freund helped with pH related experiments. I prepared the manuscript, which was edited by Greg E. bridges.

Chapter 3: S. Bhadra, D. S. Y. Tan, D. J. Thomson, M. S. Freund and G. E. Bridges, "A wireless passive sensor for temperature compensated remote pH monitoring," *IEEE Sensors Journal*, vol. 13, no. 6, pp. 2428-2436, June 2013.

In this chapter of the thesis, I developed the idea and carried out the required background studies, circuit modeling, simulation, fabrication, and experiments. Greg E. Bridges and Douglas J. Thomson provided valuable advices on different issues during the work. The work was done in collaboration with researchers from the Department of Chemistry. Damaris S. Y. Tan and Michael S. Freund provided important knowledge on fabrication of pH electrode and assisted with the use of the instruments and chemicals. I prepared the manuscript, which was edited by Greg E. Bridges and Douglas J. Thomson.

Chapter 4: S. Bhadra, W. Blunt , C. Dynowski , M. McDonald , D. J. Thomson , M. S. Freund , N. Cicek and G. E. Bridges, "Fluid embeddable coupled coil sensor for wireless

pH monitoring in a bioreactor," ***IEEE Transactions on Instrumentation and Measurement*****, vol. 63, no. 5, pp. 1337-1346, May 2014.**

The work described in this chapter was accomplished in collaboration with researchers from two different departments: Chemistry and Biosystems Engineering. I designed the sensor and undertook the background studies, circuit modeling, and characterization. Chris Dynowsky helped fabricating the electrical part of the sensor. Greg E. Bridges and Douglas J. Thomson provided useful advices on designing the sensor. The electrode fabrication was done with the help of Mike McDonald and Michael S. Freund. While primarily I conducted the experiments, Warren Blunt and Nazim Cicek handled the bioreactor system. I prepared the manuscript, which was then edited by Greg E. Bridges and Douglas J. Thomson.

Chapter 5: S. Bhadra, D. J. Thomson and G. E. Bridges, "Monitoring acidic and basic volatile concentration using a pH-electrode based wireless passive sensor," ***Sensors and Actuators B: Chemical*****, vol. 209, pp. 803-810, March 2015.**

In this chapter of the thesis, Douglas J. Thomson developed the idea. I designed the sensor and carried out the required background studies, circuit modeling, fabrication, and experiments. Greg E. Bridges provided useful knowledge for conducting the experiments. I prepared the manuscript, and Greg E. Bridges and Douglas J. Thomson edited it.

Chapter 6: S. Bhadra, C. Narvaez, D. J. Thomson and G. E. Bridges, "Non-destructive detection of fish spoilage using a wireless basic volatile sensor," ***Talanta*****, vol. 134, pp. 718-723, March 2015.**

In this chapter of the thesis, I developed the idea and carried out the required background studies, fabrication, and experiments. Claudia Narvaez helped with the microbial analysis of the fish samples. Greg E. Bridges and Douglas J. Thomson provided useful knowledge for conducting

the experiments. I prepared the manuscript, and Greg E. Bridges and Douglas J. Thomson edited it.

Table of Contents

List of Tables

List of Figures

List of Copyrighted Materials for which Permission was Obtained

- S. Bhadra, G. E. Bridges, D. J. Thomson and M. S. Freund, "Electrode potential-based coupled coil sensor for remote pH monitoring," *IEEE Sensors Journal*, vol. 11, no. 11, pp. 2813-2819, Nov. 2011. Chapter 2 of this thesis contains materials from this paper.

- S. Bhadra, D. S. Y. Tan, D. J. Thomson, M. S. Freund and G. E. Bridges, "A wireless passive sensor for temperature compensated remote pH monitoring," *IEEE Sensors Journal*, vol. 13, no. 6, pp. 2428-2436, June 2013. Chapter 3 of this thesis contains materials from this paper.

- S. Bhadra, W. Blunt , C. Dynowski , M. McDonald , D. J. Thomson , M. S. Freund , N. Cicek and G. E. Bridges, "Fluid embeddable coupled coil sensor for wireless pH monitoring in a bioreactor," *IEEE Transactions on Instrumentation and Measurement*, vol. 63, no. 5, pp. 1337-1346, May 2014. Chapter 4 of this thesis contains materials from this paper.

- S. Bhadra, D. J. Thomson and G. E. Bridges, "Monitoring acidic and basic volatile concentration using a pH-electrode based wireless passive sensor," *Sensors and Actuators B: Chemical*, vol. 209, pp. 803-810, March 2015. Chapter 5 of this thesis contains materials from this paper.

- S. Bhadra, C. Narvaez, D. J. Thomson and G. E. Bridges, "Non-destructive detection of fish spoilage using a wireless basic volatile sensor," *Talanta*, vol. 134, pp. 718-723, March 2015. Chapter 6 of this thesis contains materials from this paper.

List of Materials for which Permission from Co-authors was Obtained

- S. Bhadra, G. E. Bridges, D. J. Thomson and M. S. Freund, "Electrode potential-based coupled coil sensor for remote pH monitoring," *IEEE Sensors Journal*, vol. 11, no. 11, pp. 2813-2819, Nov. 2011. Chapter 2 of this thesis contains materials from this paper.

- S. Bhadra, D. S. Y. Tan, D. J. Thomson, M. S. Freund and G. E. Bridges, "A wireless passive sensor for temperature compensated remote pH monitoring," *IEEE Sensors Journal*, vol. 13, no. 6, pp. 2428-2436, June 2013. Chapter 3 of this thesis contains materials from this paper.

- S. Bhadra, W. Blunt , C. Dynowski , M. McDonald , D. J. Thomson , M. S. Freund , N. Cicek and G. E. Bridges, "Fluid embeddable coupled coil sensor for wireless pH monitoring in a bioreactor," *IEEE Transactions on Instrumentation and Measurement*, vol. 63, no.5, pp.1337-1346, May 2014. Chapter 4 of this thesis contains materials from this paper.

- S. Bhadra, D. J. Thomson and G. E. Bridges, "Monitoring acidic and basic volatile concentration using a pH-electrode based wireless passive sensor," *Sensors and Actuators B: Chemical*, vol. 209, pp. 803-810, March 2015. Chapter 5 of this thesis contains materials from this paper.

- S. Bhadra, C. Narvaez, D. J. Thomson and G. E. Bridges, "Non-destructive detection of fish spoilage using a wireless basic volatile sensor," *Talanta*, vol. 134, pp. 718-723, March 2015. Chapter 6 of this thesis contains materials from this paper.

Nomenclature

RFID: Radio-Frequency Identification

SAW: Surface Acoustic Wave

SNR: Signal to Noise Ratio

μ_0: Permittivity of Free Space

ε_0: Permeability of Free Space

f_0: Resonant Frequency

Q: Quality Factor

TVB-N: Total Volatile Basic Nitrogen

TVC: Total Viable Count

V_{pH}: Voltage generated across the pH-sensitive electrode pair

Chapter 1: Introduction

1.1 Research Rationale, Objectives and Scope

Development and application of chemical sensor technology is of growing interest to researchers due to reduced costs for electronic devices and the possibility of miniaturizing sensor systems. pH is one of the fundamental parameters desired in a chemical sensor. It is important to monitor and control pH in numerous fields such as structural health monitoring, environmental monitoring, food quality monitoring, industrial and chemical processing, bioprocess monitoring, and biomedical sensing [1]-[5].

In biomedical sensing pH sensors have received major attention since maintaining proper pH in the blood, digestive tract, tissues and fluids is essential to support optimal health. Numerous efforts have been directed towards the development of pH sensors to facilitate continuous monitoring of blood pH for critically ill patients [6]-[8]. Tissue pH can serve as an indicator of anaerobic metabolism and tissue pH sensors have been applied to assess low blood flow states [9]. An important medical application of pH sensors has been found for diagnosis of Gastroesophageal reflux disease, which refers to symptoms or tissue damage caused by the reflux of stomach contents into the esophagus and pharynx [10]-[12]. pH sensors have also been used for monitoring wound healing processes as the pH level of a wound liquid can be related to the healing process [13].

pH sensors have been used for monitoring pH of the soil, or more precisely pH of the soil solution, since it is a factor that affects a plant's absorption of different essential nutrients (Nitrogen (N), Potassium (K), and Phosphorus (P)) for growth and fighting disease [14]. pH

sensors for high acidity and alkalinity are useful in industries such as manufacturing plants, photographic developers and waste treatment facilities [2], [15], [16].

In structural health monitoring the value of pH is a crucial factor for assessing the deterioration of a reinforced concrete structure. When a structure is first built, a passivation layer is formed on the surface of reinforcing steel which protects it from corrosion. In healthy concrete the pH is around 12.6 and a pH value above 9.5 is required to maintain this passivation layer. Carbon dioxide gas in the atmosphere can be dissolved by the concrete pore solution and react with some calcium compounds to form carbonates. This lowers the pH of the concrete which results in depassivation of the reinforcement steel and initiation of corrosion. In situ measurement of pH at the reinforcing steel/concrete interface has been used for monitoring the corrosion process [17].

For bioprocess applications, optimal cell growth depends on pH control and many cells produce acids as a metabolic by-product. Therefore, monitoring and controlling medium pH during reactor-based bioprocessing is important [4], [5]. They have been applied to monitor pH change during beer fermentation [18]. Microbial growth inside food plays a major role for food spoilage. As microbes grow inside food, the pH level also changes due to the metabolic reactions within the microbes. Hence monitoring pH in food provides a means for food spoilage determination [3].

As delineated by the examples described, there are numerous needs for pH sensors. Our motivation is to develop a new sensor technology that can be beneficial for these applications. In this thesis we specifically concentrate on a pH sensor for applications in bioprocess and food spoilage monitoring.

1.1.1 pH Combination Electrode

The pH combination electrode is the most commonly used, understood and reliable technique of pH measurement. It consists of a sensing electrode and a reference electrode (This is not applicable to glass pH combination electrode. The mechanism of glass pH combination electrode will be discussed later.). The sensing electrode provides a potential that is dependent on pH of the sample while the reference electrode ideally provides a pH independent potential. The potential difference between the sensing and reference electrode, V_{pH}, can be expressed by the Nernst equation as [19]

$$V_{pH} = V_0 - \frac{2.3RT}{nF} pH \ . \qquad (1.1)$$

Here T is the sample temperature in Kelvin, R is the universal gas constant (8.314472 J $K^{-1}mol^{-1}$), F is the Faraday constant (9.64853399×10^4 C mol^{-1}), pH is the pH value of the solution, n is the number of moles of electrons transferred in the electrochemical cell reaction and V_0 is the standard cell potential difference at temperature T. For a constant temperature, a pH combination electrode provides a potential difference which is proportional to the pH value of the sample. The pH combination electrode sensor can provide a linear response over a very wide range of pH values [20]. It is easy to interface with measurement electronics since the output is an electrical potential. Some of the widely used pH sensing electrodes are glass electrode and metal-metal oxide electrode.

Glass electrode:

A glass electrode is a device consisting of a glass bulb membrane and an electrically insulating tubular body, which separates an internal solution and a silver/silver chloride (Ag/AgCl) electrode from the studied solution. The filling solution has constant Cl^-

concentration, which keeps the Ag/AgCl inner electrode at fixed potential. The pH sensing ability of the glass electrode comes from the ion exchange property of its glass membrane. Glass is mostly amorphous silicon dioxide, with embedded oxides of alkali metals. When the surface of glass is exposed to water, some Si–O- groups become protonated

$$\text{Si-O-} + H_3O^+ \equiv \text{Si-O-}H^+ + H_2O$$

The exchange of proton, H^+ between the solid membrane and the surrounding solution, and the equilibrium nature of this exchange, is the key principle of H^+ sensing. As with any interface separating two phases between which ionic exchange equilibrium is established, the glass membrane/solution interface becomes the site of a potential. As the pH of the studied solution changes, the potential across the glass membrane changes. The potential of the electrode contacting the internal solution is measured with respect to a reference electrode and gives a measure of pH. Often, this reference electrode is built in the glass electrode (a combination electrode), in a concentric double barrel body of the device. Fig. 1.1 shows a diagram of such a device.

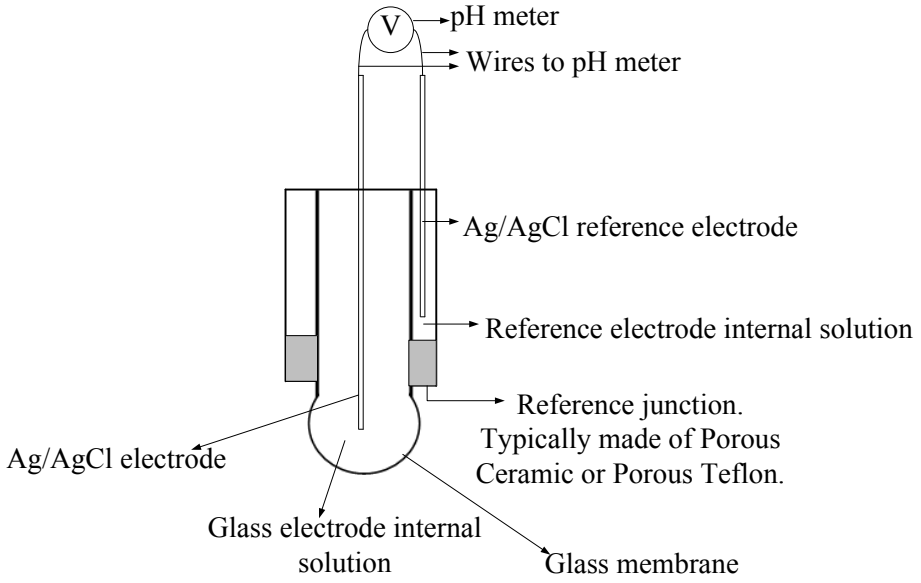

Figure 1.1. pH combination electrode with glass electrode as sensing electrode.

Glass pH electrodes are widely used because of their good sensitivity, selectivity, long-lifetime and stability. However they are easily affected by high alkaline solutions (pH value above 10), have high input impedance and are difficult to miniaturize. Moreover, they cannot be used for food or in vivo applications [21].

Solid state pH metal-metal oxide electrodes:

The basis for using a metal/metal oxide as a pH electrode is that the redox reaction at the metal/metal oxide is reversible in aqueous solutions. The metal oxide as a pH selective electrode must possess excellent corrosion resistance and stable potential response in the test solution. The metal oxides which have been used as pH sensitive electrodes include oxides of Ir, Pt, Pd, Rh, Ti, Sn, Al, Ru, Od, Ta, Mo, W and Co. Usually the potential of metal/metal oxide is measured with respect to a Ag/AgCl reference electrode. Metal-metal oxide electrodes have a number of advantages. They are inexpensive to construct depending on the metal used and fabrication technology, convenient to use, easy to miniaturize. They have low electrical resistance (this makes easy integration with the LC resonator part of our sensor) and can be used for food, biological and in vivo applications [19].

Combination electrode pH sensors typically require a wired electrical connection directly to a potentiometer or pH meter. However, this configuration is not suitable for applications where electrical connection to the measuring device is inconvenient or impossible. For example, for Gastroesophageal reflux disease diagnosis a trans-nasally placed pH recording catheter is commonly used which is very inconvenient for patients [10], [22]. Small bioreactors such as shake flasks and test tubes are regularly used for bioprocess development. The use of wired pH probes for multiple reactors (i.e. simultaneous monitoring of several shake flasks) requires a

proportional increase of wiring, cost and complexity [23]. Wires are also easily damaged during installation or while in service. Wireless passive sensors are an attractive alternative. These sensors have the advantages of requiring no power source on the sensor, and no physical connection between the sensor and the data acquisition system. This allows the sensor to be permanently embedded in the monitoring medium without the need to take out the sensor for battery charging or replacement. Food quality monitoring, bioprocess monitoring, biomedical sensing and concrete pH monitoring are some examples where embeddable wireless passive pH sensors can be advantageous. Some of the widely used wireless passive sensors are described in detail below.

1.1.2 Wireless Passive Sensors

Magnetoeleastic sensor:

Magnetoelastic sensors are typically ribbon-like thick film strips made of amorphous ferromagnetic iron-rich alloys such as $Fe_{81}B_{13.5}Si_{3.5}C_2$ (Metglas 2605SC) ribbons. A conceptual block diagram is shown in Fig. 1.2. When the sensor is exposed to a time-varying magnetic field by an excitation coil, longitudinal vibrations are produced in these sensors. This in turn generates elastic waves. The elastic waves within the magnetostrictive magnetoelastic material generate a magnetic flux that can be detected remotely by a set of pick up coils. These materials have high mechanical tensile strength and high magnetoelastic coupling coefficient. This allows efficient conversion between magnetic and elastic energy and vice versa. For a thin ribbon-like strip of length L, elasticity E, σ is the Poisson ratio and density ρ vibrating in its basal plane the resonant frequency is expressed as [24, 25]:

$$f_0 = \sqrt{\frac{E}{\rho(1-\sigma^2)}}\frac{n\pi}{L} \qquad \text{n=1, 2, 3,…} \tag{1.2}$$

Here n denotes integers. The fundamental resonant frequency, n=1, is of interest due to its relatively large amplitude.

The resonant frequency changes when there is a small mass loading on the surface. A magnetoelastic sensor of mass m_0 with unloaded resonant frequency f_0, when subjected to a mass loading (translational, uniformly applied) of Δm demonstrates a decrease in resonant frequency of [24]:

$$\Delta f = -f_0 \frac{\Delta m}{2m_0} \tag{1.3}$$

Also, upon immersion in a viscous liquid, the resonant frequency of a vibrating sensor decreases due to the dissipative character of the shear forces associated with the viscous liquid. For a low viscosity liquid, the shift in resonant frequency Δf is related to viscosity, η and density ρ_l of the surrounding liquid by:

$$\Delta f = \frac{\sqrt{\pi f_0}}{2\pi \rho_s d} \sqrt{\eta \rho_l} \tag{1.4}$$

Here d is the thickness and ρ_s is density of the magnetoelastic sensor. Thus by changing the surrounding liquid medium with the measurand and monitoring the resonant frequency of the sensor, the measurand can be monitored with the sensor. The sensor can be interrogated either in frequency-domain or in time-domain. In frequency domain the frequency of the interrogation field is swept across over the pre-determined frequency range and the response of the sensor monitored by use of a sensing coil. The output of the sensing coil is fed into a low-noise pre-amplifier, then a lock-in amplifier. The output of the lock-in amplifier provides a frequency spectrum from which the resonant frequency of the sensor can be detected. In time domain the sensor is exposed to a magnetic field impulse and the transient response from the sensor is captured using a run-triggering oscilloscope connected to the sensing coil. The resonant

frequency of the sensor can be determined from a fast Fourier transform (FFT) of the transient response. Typically these sensors operate between 30-100 kHz, have 12-15 cm diameter coil size and 8-12 cm distance of operation [24]. The low cost of the Metglas ribbons allow these sensors to be used on a disposable basis. They have been widely used for measuring a wide range of environmental parameters such as pressure, humidity, temperature, liquid viscosity and density, and chemicals such ammonia and pH [25]. However they are susceptible to stray fields and noise.

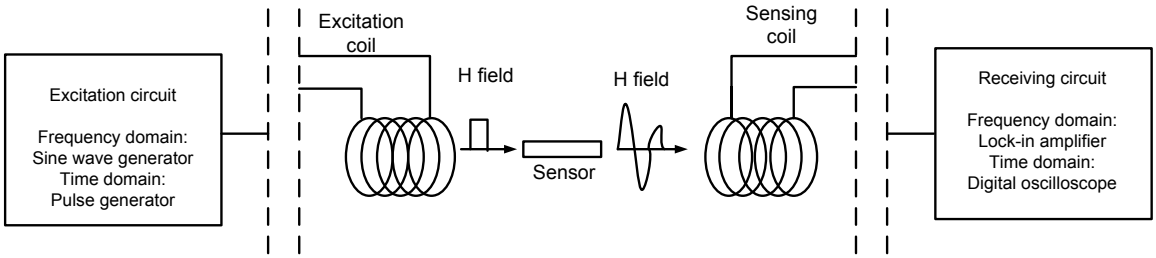

Figure 1.2. Conceptual block diagram a magnetoeleastic sensor.

Surface acoustic wave (SAW) RF sensor:

The materials typically used for SAW sensors are quartz (SiO_2), lithium niobate ($LiNbO_3$), and lithium tantalate ($LiTaO_3$) and new high temperature materials such as berlinite ($AlPO_4$), lithium tetraborate ($Li_2B_4O_7$), langasit ($La_3Ga_5SiO_{14}$), and gallium orthophosphate ($GaPO_4$). Due to the high operational frequency and the high dynamic range for the excitation of surface acoustic waves, it is possible to transfer energy to a SAW sensor using an RF signal. A SAW RF sensor consists of a piezoelectric substrate supporting the metal interdigitated electrodes, and a transponder antenna. The principle of operation is shown in Fig. 1.3. The antenna receives the electromagnetic signal and the interdigital transducer applies the electric field to a piezoelectric material. This generates a surface acoustic wave. The SAW propagates over the surface of the piezoelectric substrate and part of it is reflected from the electrode

reflectors. The reflected acoustic waves are converted back to an electromagnetic field at the interdigital transducer, and emitted back to the reader device by the transponder antenna. The propagation of the SAW depends on temperature, geometry and material of the piezoelectric substrate. The surface is influenced by using a coating material and a mass loading occurs because of absorption or adsorption of the measurand by the coating material. In this manner the measurand can be detected by monitoring the change of the reflected wave from the sensor. SAW RF sensors have been used for applications such as gas sensing, monitoring tire pressure as well as the friction between a tire and the road surface [26], monitoring humidity, pressure and position [27]. High sensitivity, reliability, large temperature range, environmental toughness and competitive price are the benefits of SAW sensors. Typical SAW sensors operate from 25 to 500 MHz. SAW devices using Rayleigh waves (surface-normal waves) are not suited for liquid sensing [28]. Liquid sensing SAW sensors such as pH sensors use wave with horizontal polarization [29].

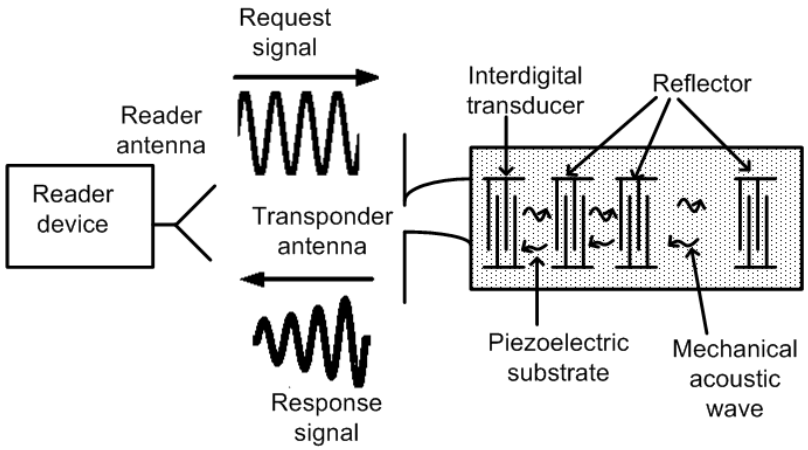

Figure 1.3. Operating principle of surface acoustic wave RF sensor.

Sensor enabled passive RFID tag:

Radio-frequency identification (RFID) has become commercially significant in recent years and it has replaced barcodes in many identification applications. In its simplest form RFID uses a radio frequency electromagnetic field to transfer stored identification information from a tag object. The most common form of RFID is based on the backscattering communication principle (see Fig. 1.4) where the reflected (scattered) signal is modulated by electronics within the RFID tag. Passive RFIDs do not require any internal power supply or battery as energy source. The necessary power required to energize and activate the tag's microchip is drawn from the localised oscillatory magnetic field created by the reader unit's antenna. The reader unit's antenna and the antenna on the tag are inductively or radiatively coupled for passive RFID tags depending on frequency and desired operating distance. The tag backscatters the identification information which is stored in the electronic circuit of the tag. In the case of synchronous tags, the energising RF field also provides the necessary timing pulses for the microchip's internal system clock. In a sensor enabled passive RFID tag, a passive RFID contains a sensor to monitor some physical parameters and sends back the physical parameter information in the modulated backscatter signal (sometimes as identification equivalent information). The read out distance, which is limited by the power need of the integrated circuit (IC), can be up to several metres for these sensors. Limitations are associated with using commercial RFID technology for physical parameter monitoring, the most important being restrictions on what data can be returned to the reader and the reliability of the datastream [30]. Custom RFID circuitry eliminates these issues. Custom RFID circuitry based sensors have been described in [30], [31]. These RFID based sensors use custom active electronics making the sensors expensive for some application e.g. packaged food quality monitoring.

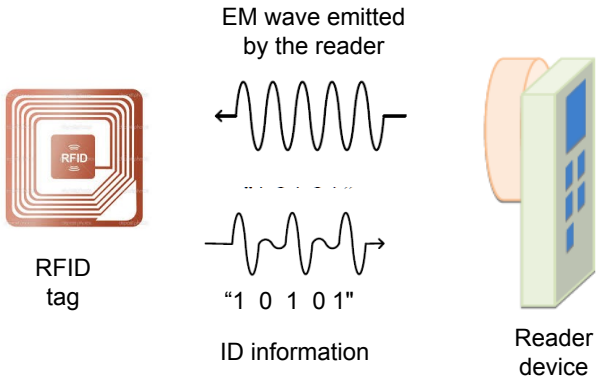

Figure 1.4. Block diagram of a typical RFID Tag.

Inductively coupled LC sensor:

A simpler, low cost alternative to custom RFID circuitry is inductively coupled passive LC sensors. These sensors operate by using a LC resonator whose resonant frequency is a function of the measurand. The sensor is placed in or in proximity of the medium being monitored. The inductance or capacitance of the sensor is designed to be sensitive to a physical quantity and thus the physical quantity affects the resonant frequency of the sensor. In most cases the sensing element is a capacitive transducer, however, inductive transducers are possible. An external interrogator coil is inductively coupled to the sensor coil and tracks the resonant frequency of the sensor. Thus by monitoring the resonant frequency of the sensor, the physical quantity can be monitored. Fig. 1.5 shows the passive LC sensor system. LC sensors are found in many applications e.g., corrosion detection [32], monitoring water content in civil engineering materials [33], strain measurement [34], moisture measurement [35] and food quality monitoring [36]. The sensor does not require any custom IC which makes it amenable to simple printed electronics techniques making potentially very low cost. One weakness is that the read out distance cannot be too large.

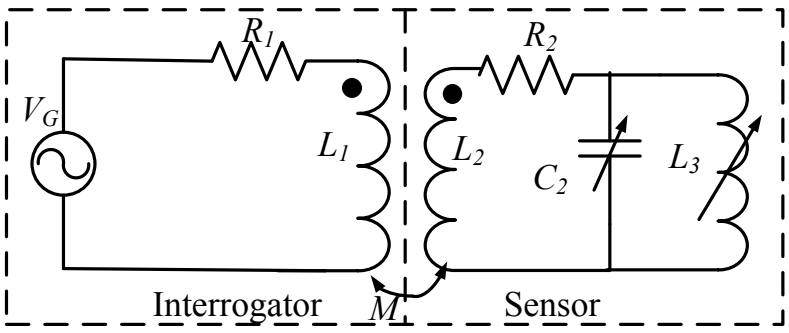

Figure 1.5. Inductively coupled LC sensor system.

Chipless RFID:

The basic operation of the chipless RFID tag system is shown in Fig. 1.6. The RFID reader sends a broadband interrogation signal though the reader Tx antenna which is received by the tag's Rx antenna. The signal is then passed through the tag's multi-resonator and retransmitted back to the reader through tag's Tx and reader's Rx antenna. The multi-resonator is a set of cascaded stop-band filters. Each resonator has a specific resonant frequency. In identification application, each resonant frequency has a 1:1 correspondence with a data bit (n resonators corresponds n bits). The presence of a resonance introduces attenuation in magnitude of the spectrum. These attenuations in amplitude are recognized as '0' and their absence is '1'. In sensing applications, the resonant frequencies of the resonators are functions of the measurand. Thus by the monitoring the frequency response of the signal transmitted by the tag, the measurand can be observed. In a system where the tag has Tx and Rx antennas, they are cross polarized with respect to each other. This is done to maximize isolation between continuous interrogation signal and the encoded tag signal. The chipless tag has advantages over conventional RFID tags, such as lower cost, fully printable and more robust due to the fact it has no IC. It has typically longer operating range than inductively coupled LC sensors. However, it

has smaller number of data bits, shorter reading range and operates at a higher frequency band than conventional RFID tags [37].

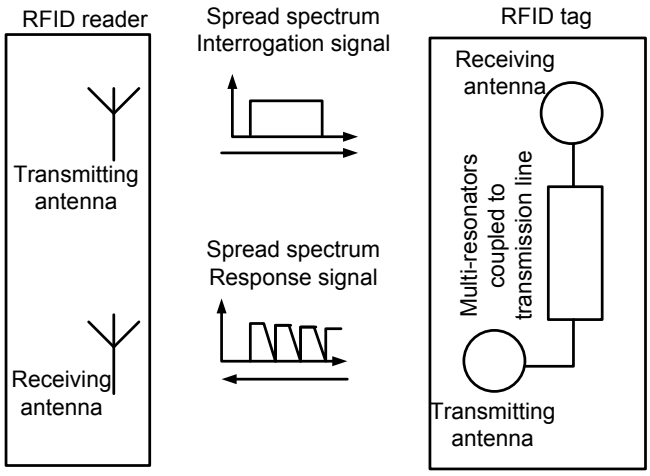

Figure 1.6. A block diagram of the chipless RFID operating principle.

Motivation and objective:

This thesis explores a wireless passive LC sensor based on the pH electrode. The main motivation for my research is the importance of developing a low cost wireless passive pH sensor technology for embedded applications. Another important drive is the drawbacks of some of the early developed polymer-based passive pH sensors which will be discussed later on in this thesis. Electrode-based wireless passive pH sensor is relatively new, leaving room for further analysis and improvements. Only two groups has recently reported wireless passive pH sensor based on the pH-sensitive electrode [3], [38]. These sensors measure pH by measuring the response of a pH combination electrode. The sensor in [3] uses a custom RFID circuitry for wireless communication making the sensors expensive. The sensor in [38] is based on LC sensor and therefore, is cost effective.

Therefore, the objective is to develop a simple cost-effective electrode-based wireless passive pH sensor, demonstrate an appropriate interrogation method where the sensor may be embedded in a lossy medium, determine its operating range, accuracy, response time and long-term stability, incorporate temperature compensation to the sensor measurement (as seen from eqn. 1.1, electrode response depends on temperature) and finally apply the sensor for selected important embedded pH monitoring applications.

1.2 Thesis Organization and Contributions

This thesis is comprised of five journal papers (all of them have been published) and organized in seven chapters as follows:

Chapter 1: Introduction

An introduction to the thesis is given in this chapter, summarizing the research objectives and scope. In addition, a comprehensive literature review providing a summary of different kinds of wireless passive sensors and pH electrodes is given, explaining their principle of operation, advantages and disadvantages.

Chapter 2: Electrode Potential-Based Coupled Coil Sensor for Remote pH Monitoring

This chapter describes a wireless passive pH sensing technique developed. The principal of operation and circuit model of the proposed electrode based wireless passive pH sensor are described. It shows the experimental results of the developed prototype sensor. The contributions of this paper are:

- A varactor based LC resonator circuit is developed to measure low frequency potential difference. An RF interrogation technique is demonstrated to wirelessly monitor the resonant frequency of the LC resonator circuit.
- The LC resonator circuit is integrated with a pH-sensitive electrode pair for wireless pH monitoring.

Chapter 3: A Wireless Passive Sensor for Temperature Compensated Remote pH Monitoring **[40]**

This chapter discusses the temperature dependence of the sensor described in chapter 2. To overcome the pH measurement error due to temperature effect, a method of integrating temperature sensor within the pH sensor and a method of interrogation for this two-parameter case are described. The principal of operation, circuit model and experimental results as well as employing temperature compensation to pH measurement are presented. Application of the sensor to food spoilage monitoring is also presented in this chapter. The contributions of this paper are:

- A technique of measuring two parameters with a single RLC resonator based sensor by varying the resonant frequency, f_0 and quality factor, Q is shown.
- Here pH and temperature of a solution are simultaneously measured by varying the single resonator based sensor's f_0 and Q, respectively.
- An algorithm is developed, which applies both pH and temperature measurement to incorporate temperature compensation in pH measurement.

Chapter 4: Fluid Embeddable Coupled Coil Sensor for Wireless pH Monitoring in a Bioreactor © [2014] IEEE. Reprinted with permission, from [S. Bhadra, W. Blunt , C. Dynowski , M. McDonald , D. J. Thomson , M. S. Freund , N. Cicek and G. E. Bridges, Fluid embeddable coupled coil sensor for wireless pH monitoring in a bioreactor, IEEE Transactions on Instrumentation and Measurement, May 2014] **[41]**

The general pH sensing technique described in chapter 2 is applied to bioprocess pH monitoring and the results are presented in this chapter. For bioprocess monitoring the sensor proposed in chapter 2 was scaled down and embedded in electrically lossy medium. The contributions of this paper are:

- An encapsulation method is applied to the LC resonator based sensor for in-fluid applications. The encapsulation reduces the influence of medium permittivity and conductivity on the sensor measurement.
- The wireless pH electrode-based sensor is miniaturized to fit in a small bioreactor and made autoclavable.
- Demonstration of a non-invasive way to obtain reliable pH information from a bacterial culture bioprocess (*Yarrowia lipolytica* and *Saccharomyces cerevisiae*) is provided.

Chapter 5: Monitoring Acidic and Basic Volatile Concentration Using a pH-electrode Based Passive Sensor © [2015] Elsevier. Reprinted with permission, from [S. Bhadra, D. J. Thomson and G. E. Bridges, Monitoring acidic and basic volatile concentration using a pH-electrode based wireless passive sensor, Sensors and Actuators B: Chemical, March 2015] **[42]**

One issue to apply the sensors described in chapter 2 and 3 is it needs direct contact with food. This is often not desirable due to the risk of electrode fouling and food contamination. Since the sensors can only work for liquid mediums, another issue is detecting spoilage of dry food. To overcome these two issues an acidic and basic volatile sensor based on hydrogel and pH electrode is proposed in this chapter. The principal of operation, circuit model, and response for acidic and basic volatiles are presented. The contributions of this paper are:

- The pH sensor is transformed to a wireless acidic and basic volatile sensor by embedding the pH-sensitive electrode pair in a hydrogel host electrolyte.
- A simple explanation of how the response varies with sensor geometry is developed.
- A study of sensor response to acetic acid and ammonia vapor is provided.

Chapter 6: Non-destructive Detection of Fish Spoilage Using a Wireless Basic Volatile Sensor **[43]**

The general acidic and basic volatile technique described in chapter 5 is applied to fish spoilage monitoring and the results are presented in this chapter. During fish spoilage microbial analysis of fish sample was done and correlated with sensor response. The contributions of this paper are:

- This paper reports the use of the wireless volatile sensor for detecting fish spoilage.
- The sensor response is correlated with bacterial growth pattern in fish and can distinctly identify when the product rejection level occurs.

Chapter 7: Conclusions and Future Work

This chapter summarizes the presented material, outlines the future work of this research.

References

[1] J. M. L. Engels and M. H. Kuypers, "Medical application of silicon sensors," *J. Phys. E: Sci. Instrum.*, vol. 16, no. 10, pp. 987-994, 1983.

[2] J. Lin, "Recent development and applications of optical and fibre-optic pH sensors," *Trends in Analytical Chemistry*, vol. 19, no. 9, pp. 541-552, Sept. 2000.

[3] W. D. Huang, S. Deb, Y. S. Seo, S. Rao, M. Chiao and J. C. Chiao, "A passive radio-frequency pH-sensing tag for wireless food-quality monitoring," *IEEE Sensors J.*, vol. 12, no. 3, Mar. 2012.

[4] P. Harms, Y. Kostov and G. Rao, "Bioprocess monitoring," *Current Opinion in Biotechnology*, vol. 13, no. 2, pp. 124-127, Apr. 2002.

[5] A. S. Jeevarajan, S. Vani, T. D. Taylor and M. M. Anderson, "Continuous pH monitoring in a perfused bioreactor system using an optical pH sensor," *Biotechnology and Bioengineering*, vol. 78, no. 4, pp. 467-472, May 2002.

[6] S. A. Grant and R. S. Glass, "A Sol-gel based fiber optic sensor for local blood pH measurements," *Sensors and Actuators B: Chemical*, vol. 45, no. 1, pp. 35-42, Nov. 1997.

[7] R. Wolthuis, D. McCrae, E. Saaski, J. Hartl and G. Mitchell, "Development of medical fiber-optic pH sensor based on optical absorption," *IEEE Trans. Biomed. Eng.*, vol. 39, pp. 531-537, May 1992.

[8] G. Papeschi, S. Bordi, M. Carlagrave, L. Criscione and F. Ledda, "An iridium-iridium oxide electrode for in *vivo* monitoring of mlood pH changes," *Journal of Medical Engineering & Technology*, vol. 5, no. 2, pp. 86-88, Mar. 1981.

[9] B. R. Soller, N. Cingo and T. Khan, "Fiber optic sensing of tissue pH to assess low blood flow states," in *Proc. IEEE Sensors*, 2002, pp. 266-269.

[10] T. Ativanichayaphong, J. Wang, W.-D. Huang, S. Rao, H. F. Tibbals, S.-J.Tang, S. J. Spechler, H. Stephanou and J.-C. Chiao, "Development of an implanted RFID impedance sensor for detecting Gastroesophageal reflux," in *Proc. IEEE International Conference on RFID*, 2007, pp. 127-133.

[11] T. Ativanichayaphong, , S.-J. Tang, L.-C. Hsu, W.-D. Huang, Y.-S. Seo, H. F. Tibbals, S. Spechler and J.-C. Chiao, "An implantable batteryless wireless impedance sensor for Gastroesophageal reflux diagnosis," in *Proc. of IEEE MTT-S International Microwave Symposium Digest,* 2010, pp. 608-611.

[12] E. I. Gill, A. Arshak, K. Arshak and O. Korostynska, "Investigation of thick-film polyaniline-based conductimetric pH sensors for medical applications," *IEEE Sensors J.*, vol. 9, no. 5, pp. 555-562, 2009 .

[13] V. Sridhar and K. Takahata, "A hydrogel-based passive wireless sensor using a flex-circuit inductive transducer," *Sensors and Actuators: A*, vol. 155, no. 1, pp. 58-65, Oct. 2009.

[14] S. G. Lemos, A. R. Nogueira, A. Torre-Neto, A. Parra and J. Alonso, "Soil calcium and pH monitoring sensor system," *J. Agric. Food Chem.*, vol. 55, no. 12, pp. 4658-4663, June 2007.

[15] A. Dybko, W. Wróblewski, E. Roźniecka, K. Poźniakb, J. Maciejewski, R. Romaniuk and Z. Brzózka, "Assesment of water quality based on multiparameter fiber optic probe," *Sensors and Actuators B: Chemical*, vol. 51 no. 1-3, pp. 208-213, Aug. 1998.

[16] A. A. Panova, P. Pantano, D. R. Walt, "In situ fluorescence imaging of localized corrosion with a pH sensitive imaging fiber," *Anal. Chem.,* vol. 69, no. 8, pp. 1635-1641, Apr. 1997.

[17] R.-G. Du, R.-G. Hu, R.-S. Huang and C.-J. Lin, "In situ measurement of Cl^- concentrations and pH at the reinforcing steel/concrete interface by combination sensors," *Anal. Chem.,* vol. 78, no. 9, pp. 3179-3185, Mar. 2006.

[18] J. A. Ferguson, B. G. Healey, K. S. Bronk, S. M. Barnard and D. R. Walt, "Simultaneous monitoring of pH, CO_2, and O_2 using an optical imaging fiber," *Alatytica Chemica Acta*, vol. 340, no. 1-3, pp. 123-131, Mar. 1997.

[19] P. Kurzweil, "Metal oxides and ion-exchanging surfaces as pH sensors in liquids: state-of-the-art and outlook," *Sensors*, vol. 9, pp. 4955-4985, June 2009.

[20] K. Wilson and J. Walker, *Principles and Techniques of Biochemistry and Molecular Biology*, 7th ed., New York, Cambridge University Press, 2010.

[21] Reagecon, "The theory of pH measurement," http://www.reagecon.com/TechPapers/phfaqv4.pdf, Apr. 21, 2005 [May 04, 2010].

[22] M. K. Jain, Q. Cai and C. A. Grimes, "A wireless micro-sensor for simultaneous measurement of pH, temperature, and pressure," *Smart Materials and Structures*, vol. 10, no. 2, pp. 347-353, April 2001.

[23] J. Buchs, "Introduction to advantages and problems of shaken cultures," *Biochemical Engineering Journal,* vol. 7, no. 2, pp. 91-98, Mar. 2001.

[24] C. A. Grimes, K. G. Ong, K. Loiselle, P.G.S. Stoyanov, D. Kouzoudis, Y. Liu, C. Tong and F. Tefiku, "Magnetoelastic sensors for remote query environmental monitoring," *Smart Materials and Structures ,* vol. 8, pp. 639-646, Oct. 1999.

[25] C. A. Grimes, C. S. Mungle, K. Zeng, M. K. Jain, W. R. Dreschel, M. Paulose and K. G. Ong, "Wireless magnetoelastic resonance sensors: a critical review," *Sensors ,* vol. 2, pp. 294-313, July 2002.

[26] A. Pohl and F. Seifert, "Wirelessly interrogable SAW-sensors for vehicular applications," in *Proc. IMTC*, 1996, pp. 1465-1468.

[27] J. P. Smith and V. Hinson-Smith, "The new era of SAW devices," *Anal. Chem.,* vol. 78, no. 11, pp. 3505–3507, June 2006.

[28] W. Buff, "SAW sensors for direct and remote measurement," in *Proc. IEEE Ultrasonics Symposium,* 2002*,* pp. 435-443.

[29] H. Oh, K. J. Lee, J. Baek, S. S. Yang and K. Lee, "Development of a high sensitive pH sensor based on shear horizontal surface acoustic wave with ZnO nanoprticles," Microelectronic Engineering, vol. 111, pp. 151-159, Nov. 2013.

[30] N. Materer, A. Apblett and T. Ley, *Passive, Wireless Corrosion Sensors for Transportation Infrastaructure*, Oklahoma Transportation Center, OTCREOS7.1-34-F.

[31] W. Leon-Salas, S. Kanneganti and C. Halmen, "Development of a smart RFID-based corrosion sensor" in *Proc. IEEE Sensors,* 2011, pp 534-537.

[32] M. M. Andringa, D. P. Neikirk, N. P. Dickerson and S. L. Wood, "Unpowered wireless corrosion sensor for steel reinforced concrete," in *Proc. IEEE Sensors*, 2005, pp. 155-158.

[33] J. B. Ong, Z. You, J. Mills-Beale, E. L. Tan, B. D. Pereles and K. G. Ong, "A wireless, passive embedded sensor for real time monitoring of water content in civil engineering materials," *IEEE Sensors J.*, vol. 8, issue 12, pp. 2053-2058, Dec. 2008.

[34] J. C. Butler, A. J. Vogliotti, F. W. Verdi and S. M. Walsh, "Wireless, passive, resonant-circuit, inductively coupled, inductive strain sensor," *Sensors and Actuators A ,* vol. 102, no. 1, pp. 61-66, Dec. 2002.

[35] T. J. Hapster, B. Stark and K. Najafi, "A passive wireless integrated humidity sensor," *Sensors and Actuators A ,* vol. 95, no. 2-3, pp. 100-107, Jan. 2002.

[36] K. G. Ong, L. G. Puckett, B. V. Sharma, M. Loiselle, C. A. Grimes and L. G. Bachas, "Wireless passive resonant-circuit sensors for monitoring food quality," in *Proc. SPIE*, vol. 4575, pp. 150-159, Feb. 2002.

[37] S. Preradovic, S. M. Roy and N. C. Karmakar, "RFID system based on fully printable chiplees for paper-/plastic-item tagging," *IEEE Antennas and propagation magazine*, vol. 53, no. 5, pp. 15-32, Oct. 2011.

[38] J. B. E. Horton, S. Schweitzer, A. J. DeRouin and K. G. Ong, "A varactor-based inductively coupled wireless pH sensor," *IEEE Sensors J.*, vol. 11, no. 4, pp. 1061-1066, April 2011.

[39] S. Bhadra, G. E. Bridges, D. J. Thomson and M. S. Freund, "Electrode potential-based coupled coil sensor for remote pH monitoring," *IEEE Sensors Journal*, vol. 11, no. 11, pp. 2813-2819, Nov. 2011.

[40] S. Bhadra, D. S. Y. Tan, D. J. Thomson, M. S. Freund and G. E. Bridges, "A wireless passive sensor for temperature compensated remote pH monitoring," *IEEE Sensors Journal*, vol. 13, no. 6, pp. 2428-2436, June 2013.

[41] S. Bhadra, W. Blunt , C. Dynowski , M. McDonald , D. J. Thomson , M. S. Freund , N. Cicek and G. E. Bridges, "Fluid embeddable coupled coil sensor for wireless pH monitoring in a bioreactor," *IEEE Transactions on Instrumentation and Measurement*, vol. 63, no.5, pp.1337-1346, May 2014.

[42] S. Bhadra, D. J. Thomson and G. E. Bridges, "Monitoring acidic and basic volatile concentration using a pH-electrode based wireless passive sensor," *Sensors and Actuators B: Chemical*, vol. 209, pp. 803-810, March 2015.

[43] S. Bhadra, C. Narvaez, D. J. Thomson and G. E. Bridges, “Non-destructive detection of fish spoilage using a wireless basic volatile sensor,” *Talanta*, vol. 134, pp. 718-723, March 2015.

Chapter 2: Electrode Potential-Based Coupled Coil Sensor for Remote pH Monitoring

2.1 Abstract

We present a coupled coil pH sensor for high-resolution remote pH monitoring. The sensor is based on a passive LC coil resonator whose resonant frequency is monitored remotely by measuring the change in impedance of an interrogator coil coupled to the sensor coil. The sensor resonator consists of an inductive coil connected in parallel with a voltage dependent capacitor and a pH combination electrode. When the pH of the contact solution changes, the electrode potential changes the capacitance, and therefore the resonant frequency of the sensor. A linear response with a 0.1 pH resolution is achieved over a 2 to 12 pH dynamic range at room temperature. The response time of the sensor is demonstrated to be less than 30 sec and is limited by the response time of the pH combination electrode. Effects of varying separation distance and temperature change on the sensor's performance are shown. The described sensor technology has potential application for remote pH monitoring in numerous fields such as biomedical sensing, environmental monitoring, industrial and chemical processing and structural health monitoring.

2.2 Introduction

The importance of monitoring and controlling pH in numerous fields is discussed in section 1.1. The description, advantages and disadvantages of pH combination electrode, the most common types of pH sensors, are also stated in section 1.1. The main disadvantage of pH combination electrode is its wired configuration, which makes it improper for applications where

electrical connection to the measuring device is impossible or inconvenient. Wireless passive pH sensor is appropriate to use for this applications.

Most wireless passive pH sensors developed to date are based on a pH sensitive polymer, for example the polymer-based magnetostrictive magnetoelastic sensor [1], the hydrogel-based LC sensor [2] and the pH sensor based on magnetic higher-order harmonic fields [3]. The common drawbacks of these sensors are the long response time, the highly non-linear response and poor long-term stability [1], [3], [4].

In the paper [5], we present a coupled coil sensor based on the pH combination electrode. The sensor consists of a passive LC coil resonator whose resonant frequency changes with the pH of the solution. Change in the sensor's resonant frequency is detected by measuring the induced change in the impedance of an external interrogator coil that is inductively coupled to the sensor coil. A combination electrode based sensor provides a linear response over a large dynamic range with a fast response time. We present experimental results of a large scale prototype sensor operating over a 2-12 pH range. As the sensor is passive and can be monitored wirelessly, it is suitable for long-term remote pH monitoring.

2.3 Sensor Operation

A block diagram of the coupled coil sensor-interrogator is shown in Fig. 2.1. In the remote sensor, an inductive coil is connected in parallel with a voltage dependent capacitor and a pH combination electrode. Here L_S is the inductance of the sensor coil, $C(V_{pH})$ is the capacitance of the resonant sensing circuit and V_{pH} is the potential difference developed at the pH combination electrode when in contact with a solution. The capacitance, $C(V_{pH})$ changes in

response to the low frequency change of V_{pH}. The sensor coil and capacitor form a resonant circuit with a resonant frequency, f_0, approximately given by

$$f_0 = \frac{1}{2\pi\sqrt{L_S C(V_{pH})}} . \tag{2.1}$$

The sensor coil is inductively coupled to an interrogator coil, whose impedance is monitored using a swept frequency impedance analyzer. The resonant frequency of the weakly coupled sensor coil, f_0, is obtained by measuring the perturbation of interrogator coil impedance. In this manner, the resonant frequency is directly related to the potential difference developed at the pH combination electrode.

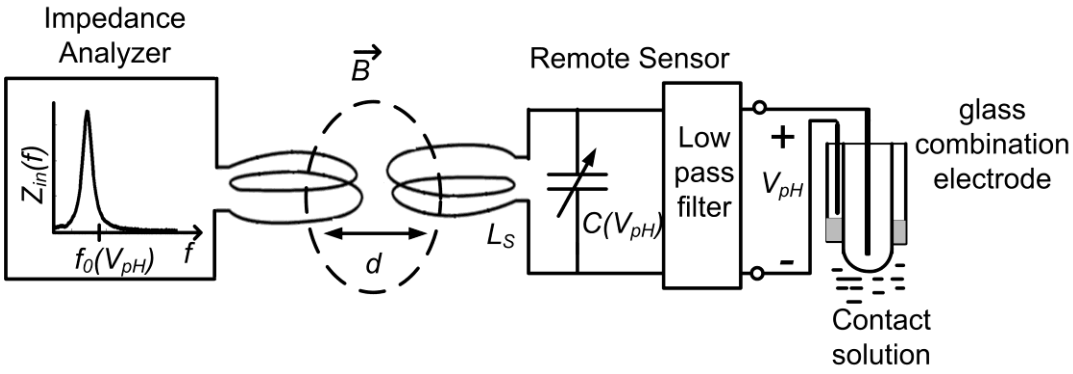

Figure 2.1. Block diagram of the coupled coil pH sensor.

An equivalent circuit diagram of the coupled coil pH sensor is shown in Fig. 2.2. In the circuit, L_S and R_S are the series inductance and resistance of the sensor coil, respectively, with L_1 and R_1 are the series inductance and resistance of the interrogator coil, respectively. M is the interrogator-sensor coil coupling factor. C is the small signal junction capacitance of the voltage dependent capacitor (varactor diode) in the sensing circuit. In the reverse bias state, C is approximated by $C(V_C) = C_0(1 - V_C/\varphi)^{-1/2}$, where C_0 is the junction capacitance at zero bias, φ is the junction built in potential and V_C is the bias voltage applied across the varactor. R_{pH} is the cell

resistance developed at the pH combination electrode when in contact with a solution. In the circuit, R_3 and C_2 act as a low pass filter so that the resonator is sensitive to low frequency variations in the pH electrode potential. For a small source oscillation amplitude, small M, and $R_{pH} << (R_2+R_3)$, $V_C \cong V_{pH}$. Assuming the losses are small and $C_1 >> C(V_C)$, the pH of the contact solution, which is indicated by V_{pH}, can be monitored by tracking the resonant frequency of the sensor [5].

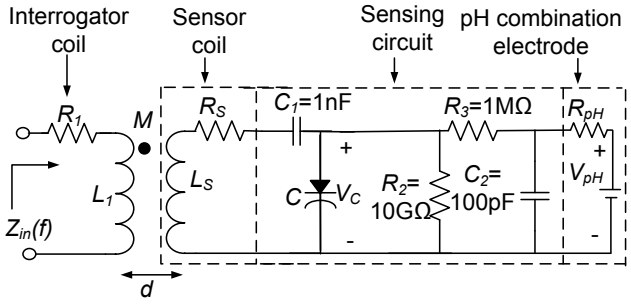

Figure 2.2. Equivalent circuit diagram of the coupled coil pH sensor.

Referring to Fig. 2.2, near and at the resonant frequency the impedance, Z_{in}, seen by the impedance analyzer is given as

$$Z_{in}(f) = Z_1 + Z_T = R_1 + j2\pi f L_1 + \frac{(2\pi f)^2 M^2}{Z_S}, \tag{2.2}$$

where f *is* the source frequency and $Z_S \approx R_S + j2\pi f L_S + (1/(j2\pi f C))$ is the sensor series impedance. In our system the resonant frequency was obtained from the maximum of the real part of the impedance using a quadratic curve-fitting algorithm [6]. The impedance, Z_{in}, in (2.2) consists of two components; $Z_1 = R_1 + j2\pi f L_1$, due to the self impedance of the interrogator coil and $Z_T = j(2\pi f)^2 M^2 / Z_S$, due to the sensor coupling. To remove the self impedance of the interrogator coil a background subtraction, using the measured impedance of the interrogator coil when the sensor was absent, was implemented prior to measuring the sensor response [7]. For two concentric coils (as shown in Fig. 2.5), the mutual coupling, M, can be expressed in terms of

separation distance between the centers of two coils, d, the loop radius of the interrogator coil, r_1, the number of turns of the interrogator coil, n_1, the loop radius of the sensor coil, r_s, and the number of turns of the sensor coil, n_s, as [8]

$$M = n_1 n_S \mu_0 \sqrt{r_1 r_S}\left[\left(\frac{2}{k_1} - k_1\right)K(k_1) - \frac{2}{k_1}E(k_1)\right], \tag{2.3}$$

where $k_1^2 = \frac{4r_1 r_S}{d^2 + (r_1 + r_S)^2}$, $K(k) = \int_0^{\pi/2} \frac{d\varphi}{\sqrt{1 - k^2 \sin^2 \varphi}}$ and $E(k) = \int_0^{\pi/2} \sqrt{1 - k^2 \sin^2 \varphi}\, d\varphi$. Here $K(.)$ and $E(.)$ are the complete elliptic integrals.

2.4 Prototype Sensor and Results

2.4.1 Sensor and Interrogator Description

The prototype sensor, as shown in Fig. 2.3, was constructed using a commercial pH combination electrode. The sensor coil was 6.7 cm in diameter and made of 16 turns of insulated wire of 1 mm diameter, producing L_S=28.91 μH and R_S= 3.12 Ω. The sensing circuit was fabricated on a 2.8 cm x 1 cm printed circuit board with surface mount capacitors and resistors. The varactor (NXP BB202) in the sensing circuit had a junction capacitance that varied in the range of 35.04 pF – 22.95 pF for reverse bias voltages between 0 and 1V, respectively. A PH105: ExStik® (by Extech Instruments) was used as the pH combination electrode. The electrode resistance, R_{pH}, for pH solutions in the range of 2-12 was approximately 150 MΩ. The sensor was designed to have a resonant frequency, f_0, near 5 MHz.

The interrogator coil was 5.1 cm in diameter and constructed of 5 turns of insulated copper wire of 1.2 mm diameter, producing L_1=2.35 μH, R_1=334.13 mΩ and a self-resonant frequency, f_{res}=28.32 MHz. The sensor's resonant frequency was determined by measuring the

real part of the impedance of the interrogator coil when inductively coupled to the sensor coil. The interrogator coil impedance was measured using an impedance analyzer (Agilent 4294A) with the voltage oscillation level of the analyzer set to 25 mV.

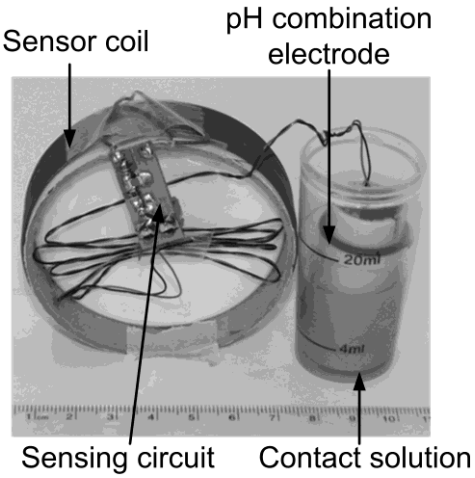

Figure 2.3. Prototype coupled coil pH sensor.

2.4.2 pH Measurement

Solutions with varying pH values between 2 and 12 were made with pH hydration buffer capsules (Micro essential laboratory) and measured with a pH meter (PH150-C-ExStik®) at room temperature. The potential difference developed at the pH combination electrode, V_{pH}, was measured with a high impedance digital voltmeter (Agilent 34401) for each of these solutions. Fig. 2.4 shows the measured V_{pH} at the combination electrode terminals in Fig. 2 and the extracted linear fit which is given by $V_{pH}(mV) = -57.89\,pH + 391.96$. The maximum deviation from the linear fit is less than 0.09 pH. The difference in slope of the measured V_{pH} and that predicted by (1.1) is due to the resistive loading of the sensor and the finite electrode resistance, R_{pH}.

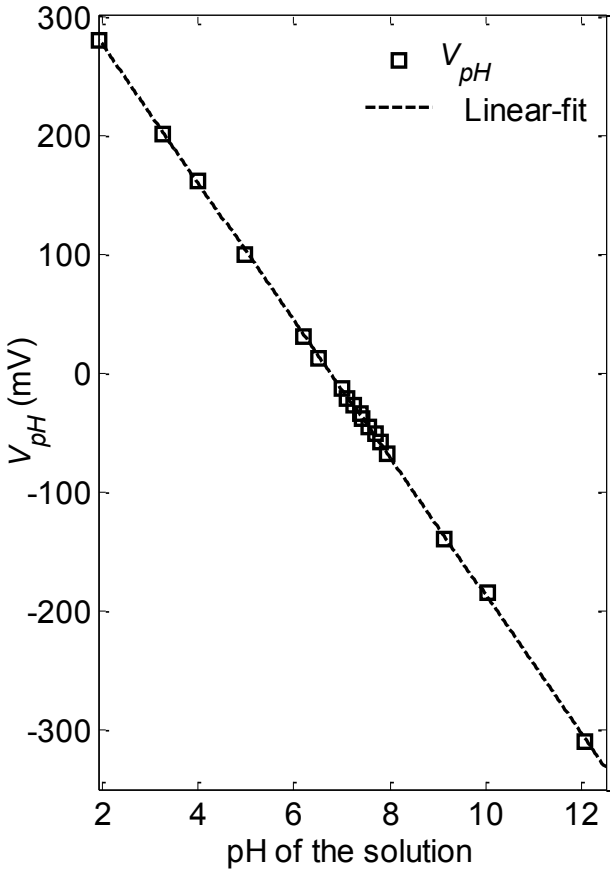

Figure 2.4. Potential difference at the sensor pH combination electrode terminal versus measured pH of the prepared solutions.

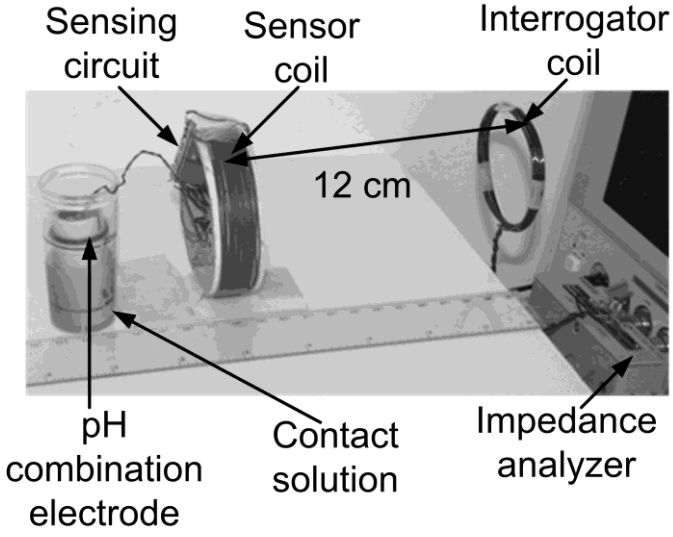

Figure 2.5. Experimental set up with the coupled coil sensor and combination electrode in a prepared pH solution.

The experimental set up for measuring the pH of a solution with the coupled coil pH sensor is shown in Fig. 2.5. For all measurements, the pH was simultaneously measured using the sensor and a commercial pH meter. The sensor coil was aligned concentrically with the interrogator coil with a separation distance d= 12 cm. Fig. 2.6 shows the frequency response of the sensor, Re$\{Z_T\}$, as measured by the impedance analyzer for three different pH solutions. Measurements were performed for pH values between 2 and 12. Fig. 2.7 shows the resonant frequency, f_0, for the different pH solutions as determined from the peaks of their impedance response. Different resonant frequencies are easily distinguishable for changes less than 0.1 pH.

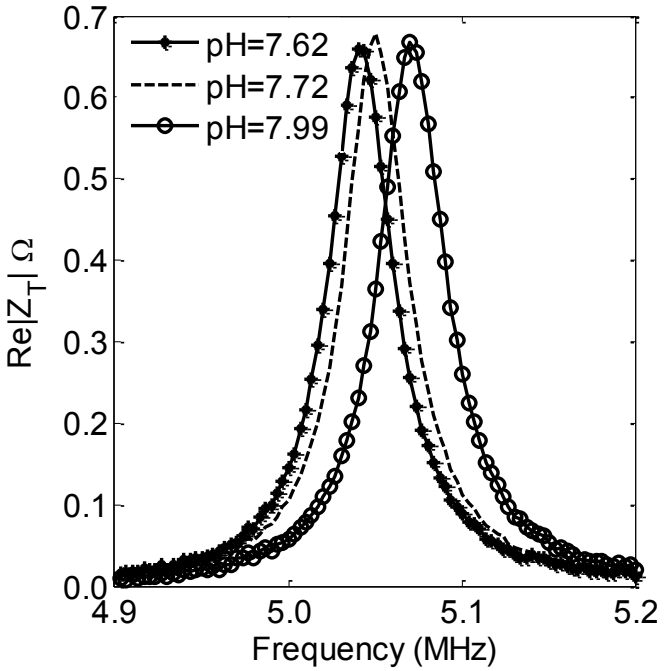

Figure 2.6. Impedance analyzer frequency response for different pH solutions.

The resonant frequency was measured three times for each of the 18 different pH solutions (removing the electrode from the solution between impedance measurements). A linear fit given by

$$f_0(MHz) = 0.073pH + 4.48\,, \tag{2.4}$$

over the 2-12 pH dynamic range indicates a slope of 73 kHz/pH (standard error of 0.23 kHz/pH) and an intercept of 4.48 MHz (standard error of 1.7 kHz). For all measurements a maximum deviation of less than 7.1 kHz from linear-fit (corresponding to a deviation of less than 0.1 pH) was observed.

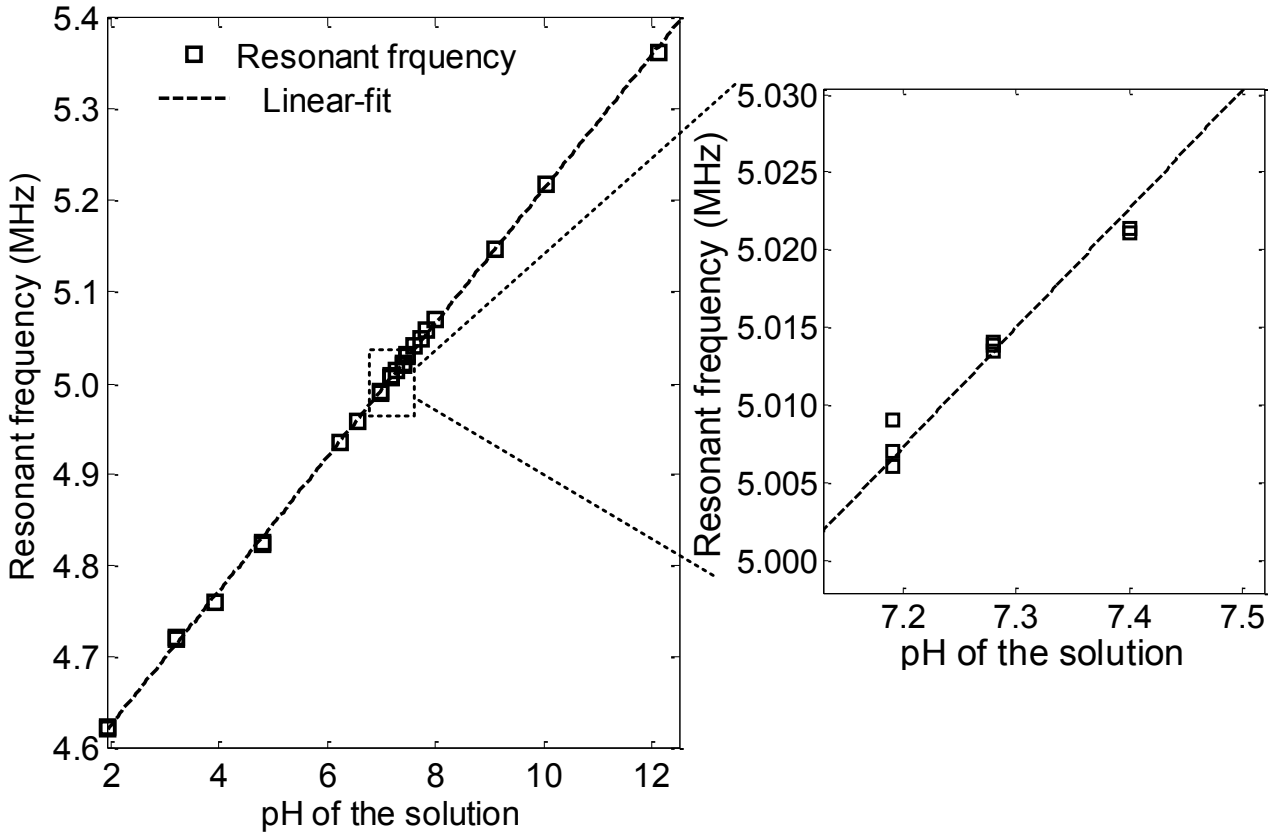

Figure 2.7. Resonant frequency of the sensor versus measured pH of the prepared solutions. The expanded region to the right shows the results of three repeated measurements for each pH solution.

2.4.3 Sensor's Response Time

To determine the response time of the sensor, the pH of the solution was varied in small steps from 9.80 to 9.24 by adding small amount of 7 pH solution in each step while continuously

monitoring the resonant frequency of the sensor. The pH response measured by the sensor was obtained from the resonant frequency using (2.4) and is shown in Fig. 2.8. The pH of the solution also was measured using a commercial pH meter. Since the same combination electrode was used in the commercial meter as in the sensor, the meter's response should be similar to that of the pH combination electrode. Fig. 2.8 shows that the sensor's response follows the pH meter's response with a maximum deviation of 0.088 pH, which is within the 0.1 pH accuracy obtained in the measurements of Fig. 2.7. The time-response of the sensor (see insert in Fig. 2.8) is the same as that of the pH meter, indicating that it is limited by the response time of the pH combination electrode and not by the sensor or interrogator. Fig. 2.8 shows that the response time of the sensor/pH combination electrode is less than 30 seconds.

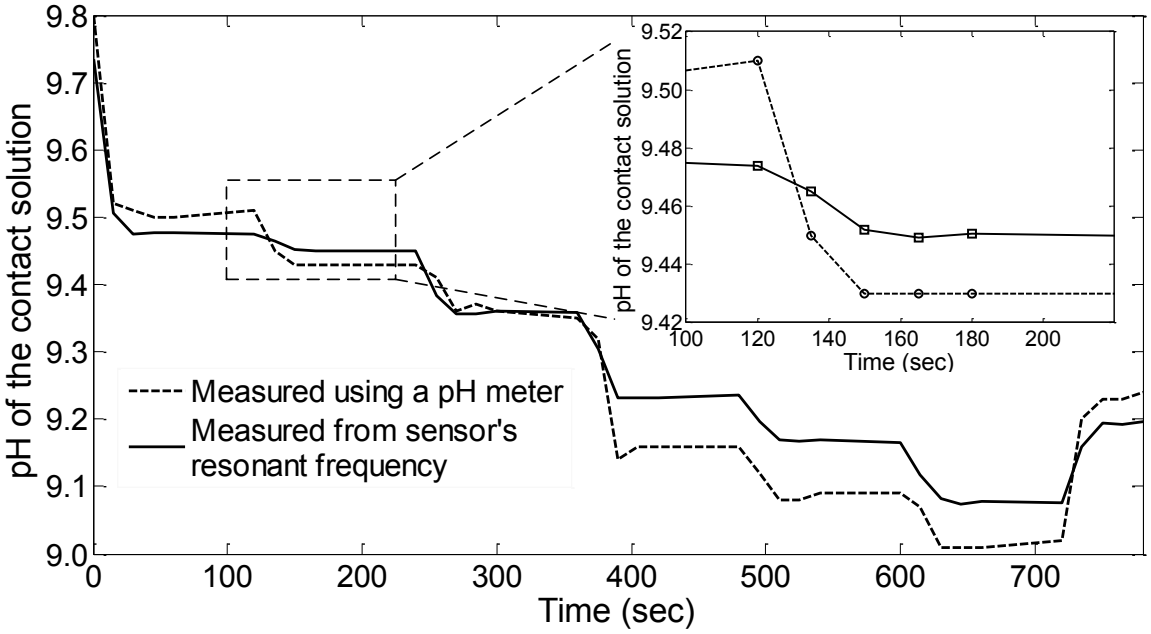

Figure 2.8. Response of the pH sensor and a commercial pH meter over time.

2.4.4 Effects of Varying Separation Distance

As the separation distance between the sensor coil and the interrogator coil increases, the received signal amplitude from the sensor decreases. On the other hand a large mutual coupling coefficient affects the resonant frequency and a minimum sensor-interrogator distance should be maintained for weak coupling. Additionally, for a fixed voltage oscillation level of the analyzer the sensor requires a minimum distance so that the varactor operates in linear region. An experiment was conducted to measure the variation of the sensor's resonant frequency with the separation distance. For all tests the sensor coil was aligned concentrically with the interrogator coil. Fig. 2.9 and Fig. 2.10 show the frequency response of the sensor for different separation distances and the variation of resonant frequency with distance, respectively, when the pH of the contact solution was 3.62 (measured by the pH meter). For voltage oscillation level of the analyzer set to 25 mV, distances less than 8.5 cm set the varactor in a non-linear operating region and a maximum separation distance of 18 cm was needed to maintain a measurement error less than 0.04% (corresponding to 0.03 pH). The separation distance can be improved by increasing the power at the interrogator coil, or by increasing the number of turns and /or radius of the interrogator coil. In the experiments it is important to keep a minimum separation distance between the interrogator coil and the sensor coil so that the sensor remains in a linear operating range.

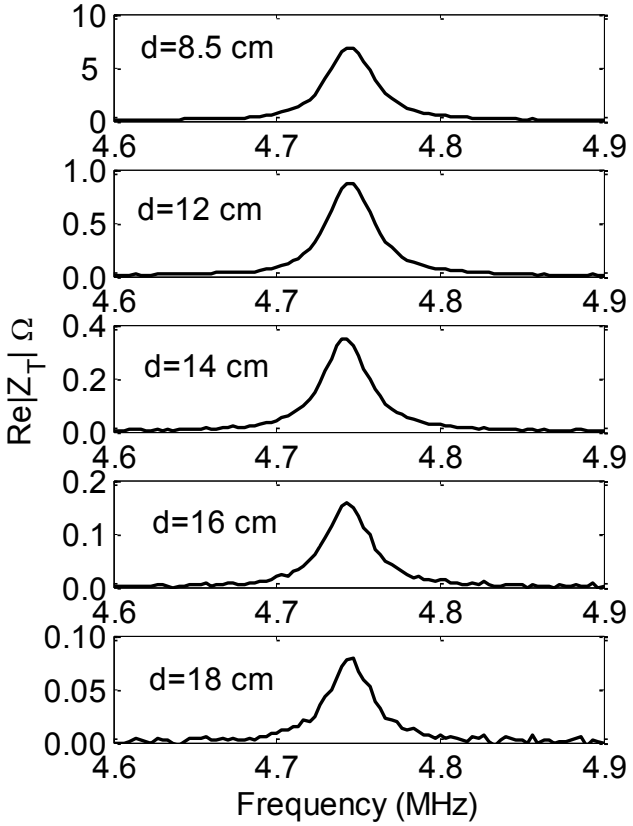

Figure 2.9. Impedance analyzer frequency response for different separation distances.

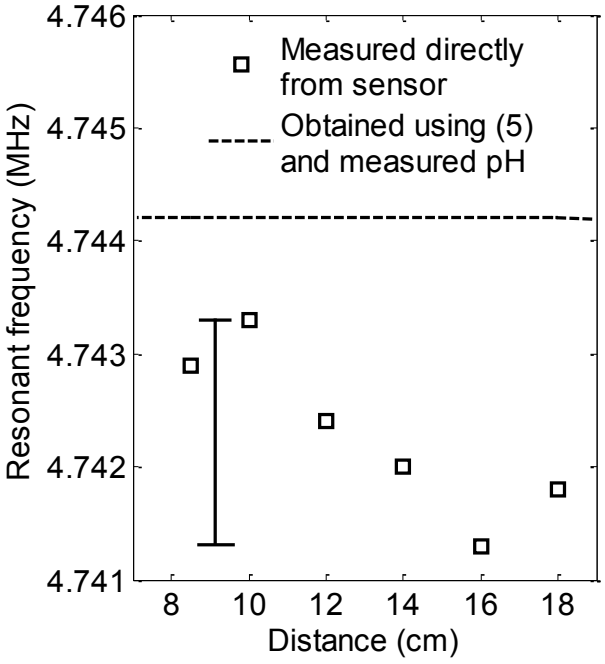

Figure 2.10. Variation of resonant frequency with separation distance. The maximum deviation shown by the error bar corresponds to a 0.03 pH deviation.

2.4.5 Effects of Temperature Change

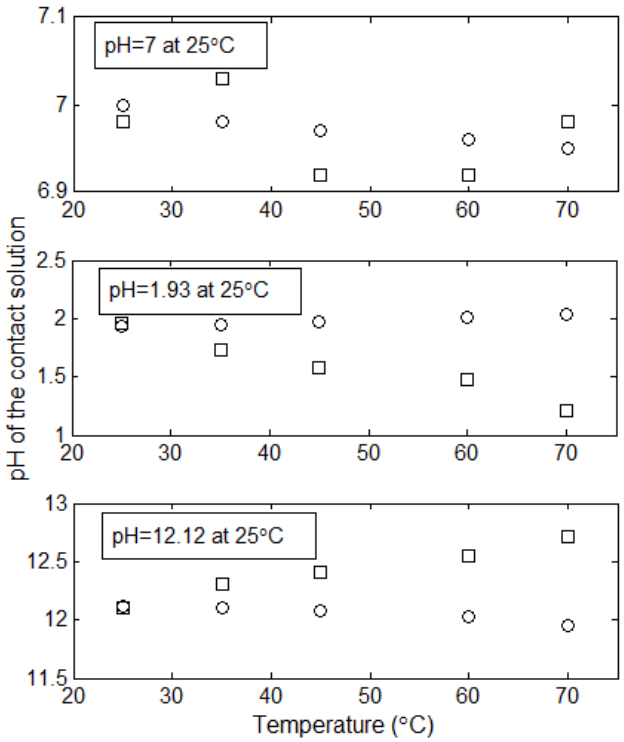

Figure 2.11. Response of the pH sensor and a commercial pH meter as a function of the solution temperature. Squares indicate pH of the contact solution measured from the sensor's resonant frequency and circles indicate pH of the contact solution measured by the pH meter.

All measurements shown previously were performed at a constant room temperature. Accurate measurement of pH is affected by temperature. An increase in a solution's temperature causes a decrease in viscosity and increase in the mobility of its ions in the solution. An increase in temperature may also increase the number of ions in solution due to the dissociation of molecules (this is particularly true for weak acids and bases). As pH is a measure of the hydrogen ion concentration, a change in the temperature of a solution will result in a change of pH. Since this is not an error, there is no need to correct or compensate for this temperature effect. From Nernst equation it can be seen that change in temperature also causes change in the pH combination electrode's response (or sensitivity) to pH [9]. As the sensor is measuring pH by

measuring the response of the pH combination electrode, an experiment was performed to investigate the temperature dependence. The temperature of three different pH solutions were increased from room temperature to 70° C and the resonant frequency of the sensor was monitored. Fig. 2.11 shows the pH response of the sensor obtained from the resonant frequency using (2.4). The pH of the solution was also measured using a commercial pH meter. The change in the pH combination electrode's response with temperature is compensated for by the meter using automatic temperature compensation. Fig. 2.11 shows that sensor's response deviates more from the pH meter's response as the temperature increases. The maximum deviation is 0.05 pH for the 7 pH solution but almost 1 pH for the very acidic and basic pH solutions. This is due to the pH combination electrode's increased temperature sensitivity when the solution's pH is further from 7 and is not due to temperature dependence of the sensor electronics. Results suggest that a temperature compensation technique may have to be implemented in the future. This can be achieved by incorporating temperature compensation into the sensor electronics or by measuring temperature of the solution by a secondary sensor and employing compensation after measurement.

2.5 Discussion and Conclusion

This paper [5] demonstrated a coupled coil pH sensor based on direct measurement of a pH combination electrode's potential difference. Using a simple LC coil resonator, the pH of different solutions could be wirelessly monitored by measuring the change of sensor's resonant frequency. Results obtained for the sensor exhibited a linear relationship between the resonant frequency of the sensor and pH of the solution over a 2 to 12 dynamic range of pH values with a resolution of less than 0.1 pH. The response time of the sensor was shown to be limited by the

response time of the pH combination electrode. The pH combination electrode used in the prototype sensor showed a response time of less than 30 sec.

The described sensor technology is suitable for long-term remote pH monitoring in numerous fields such as biomedical sensing, environmental monitoring, industrial and chemical processing and structural health monitoring. For biomedical implant applications, the size of the sensor coil would be much smaller than the prototype examined in the paper. Further, the orientation of the sensor coil may not be optimal (the experiments described in this paper use concentrically oriented coils) to achieve a good coupling. For implant conditions the interrogator coil size can remain large, and using (eqn. 2.2) and (eqn. 2.3) with $r_1 >> d$ *and* $r_1, d >> r_s$ the coupled impedance signal at resonance is proportional to $f_0^2 n_s^2 r_s^4$. Thus, decreasing the sensor coil size would reduce the coupled signal. This can be compensated for by increasing the number turns of the sensor coil, n_s, and by operating at a higher resonant frequency, f_0. For an unknown orientation of the implanted sensor coil, multiple orthogonal interrogator coils can be used to obtain a reliable signal. Dependence of sensor response to orientation variation is discussed in detail in section 5.5.7 of this thesis.

All measurements shown in this paper were performed at a constant room temperature and do not consider effect of temperature change. As described in section 2.4.5 temperature causes change in the pH combination electrode's response (or sensitivity) to pH. Since the sensor is measuring pH by measuring the response of the pH combination electrode, the temperature dependence of the pH combination electrode should be taken into account for accurate pH measurement. A temperature compensation technique for this electrode based sensor will be described in the next chapter. Another concern with this prototype sensor is its large size. It is using a commercial glass pH combination electrode. Glass electrodes are easily affected by

alkaline or HF solutions, have high cell resistance and are difficult to miniaturize. Because of their brittle nature, they have a risk of breakage. For real embedded application the sensor has to be miniaturized. For miniaturization, metal-metal oxides pH electrodes will be fabricated and integrated with a compact sensor circuit (on printed circuit board) in the next chapter.

References

[1] M. K. Jain, Q. Cai and C. A. Grimes, "A wireless micro-sensor for simultaneous measurement of pH, temperature, and pressure," *Smart Materials and Structures*, vol. 10, no. 2, pp. 347-353, April 2001.

[2] M. Lei, A. Baldi, T. Pan, Y. Gu, R. A. Siegel and B. Ziaie, "A hydrogel-based wireless chemical sensor," in *Proc. Micro Electro Mechanical Systems*, 2004, pp. 391-394.

[3] B. E. Horton, B. D. Pereles, C. Ruan, E. L. Tan and K. G. Ong, "Wireless passive pH sensor based on magnetic higher-order harmonic fields," *Sensor Letters*, vol. 7, no. 4, pp. 599-604, August 2009.

[4] V. Sridhar and K. Takahata, "A hydrogel-based passive wireless sensor using a flex-circuit inductive transducer," *Sensors and Actuators: A*, vol. 155, no. 1, pp. 58-65, Oct. 2009.

[5] S. Bhadra, G. E. Bridges, D. J. Thomson and M. S. Freund, "A wireless passive pH sensor based on pH electrode potential measurement," in *Proc. IEEE Sensors*, 2010, pp. 927-930.

[6] M. P. Robinson and J. Clegg, "Improved determination of Q-factor and resonant frequency by a quadratic curve fitting method," *IEEE Transaction on Electromagnetic Compatibility*, vol. 47, no. 2, pp. 399-402, May 2005.

[7] J. B. Ong, Z. You, J. Mills-Beale, E. L. Tan, B. D. Pereles and K. G. Ong, "A wireless, passive embedded sensor for real time monitoring of water content in civil engineering materials," *IEEE Sensors J.*, vol. 8, issue 12, pp. 2053-2058, Dec. 2008.

[8] F. M. Tesche, M. V. Ianoz and T. Karlsson, *EMC Analysis Methods and Computational Models*, New York: John Wiley & Sons Inc., 1997.

[9] J. J. Barron, C. Ashton and L. Geary, “The effects of temperature on pH measurement,” Technical Services Department, Reagecon Diagnostics Ltd, Shannon Free Zone, County Lake, Ireland, Rep. TSP-01 Issue 1, 2005.

Chapter 3: A Wireless Passive Sensor for Temperature Compensated Remote pH Monitoring

3.1 Abstract

Temperature must be accounted for in order to provide accurate measurements in electrode based pH sensors. We present an integrated wireless passive sensor for remote pH monitoring employing temperature compensation. The sensor is a RLC resonant circuit consisting of a planar spiral inductor connected in parallel to a temperature dependent resistor (thermistor) and a voltage dependent capacitor (varactor). A pH combination electrode consisting of an iridium/iridium oxide sensing electrode and a silver/silver chloride reference electrode, is connected in parallel with the varactor. A potential difference change across the electrodes due to pH variation of the solution changes the voltage-dependent capacitance and shifts the resonant frequency, while temperature of the solution affects the resistance and changes the quality factor of the sensor. An interrogator coil is inductively coupled to the sensor inductor and remotely tracks the resonant frequency and quality factor of the sensor. The sensor was calibrated for temperature over a range of 25°C-55°C and pH over a 1.5-12 dynamic range. By employing temperature compensation, a measurement accuracy of less than 0.1 pH was achieved and the response time of the sensor was demonstrated to be less than 1 sec. The sensor overcomes the pH measurement error due to the temperature dependence of electrode based passive pH sensors and has applications in remote pH monitoring where temperature varies over a wide range.

3.2 Introduction

Section 1.1 describes the areas where monitoring and controlling pH is important. The main disadvantage of pH combination electrode, the most common types of pH sensors, is it's wired configuration. This is not suitable in situations where electrical connection to the measuring device is inconvenient or impossible as in embedded monitoring applications. Wireless passive sensors can provide measurements even when no direct connection is possible. Food quality monitoring, bioprocess monitoring and concrete pH monitoring are some examples where embeddable wireless passive sensors are advantageous. Wireless passive sensor technologies, such as optical sensors based on absorbance or fluorescence from pH-sensitive dyes, have been successfully used inside bioreactors. These sensors are desirable when high accuracy is needed over a narrow dynamic range. However, optical sensors typically suffer from a limited dynamic range and long-term drift [1], [2]. Another type of wireless passive pH sensor that has been recently reported is based on the pH sensitive electrode [3], [4], [5]. These sensors measure pH by measuring the response of a pH combination electrode.

Accurate measurement of pH using electrode based passive sensors is affected by temperature. pH sensors based solely on electrode potential are not suitable for measuring pH when the temperature of the solution varies over a wide range. Also, for fixed temperature processes they require calibration every time the process temperature changes. As examples, in food spoilage monitoring, the temperature of food can change significantly during storage, transportation and consumption stages, and temperature inside concrete has a large variation during the curing process. Many bioprocesses are carried out at different constant temperatures and a sensor with means of temperature compensation would be advantageous so that calibration

is not necessary every time the process temperature changes.

An increase in a solution's temperature causes a decrease in viscosity and increase in the mobility of its ions in the solution. An increase in temperature may also increase the number of ions in solution due to the dissociation of molecules (this is particularly true for weak acids and bases). As pH is a measure of the hydrogen ion concentration, a change in the temperature of a solution results in a change of pH. Since this is not an error, there is no need to correct or compensate for this temperature effect. The Nernst equation describes the effect of temperature on the pH combination electrode's response (or sensitivity) to pH [6], [7]. The temperature sensitivity of the combination electrode increases when the solution's pH is further from the isothermal point [6]. For accurate measurement of pH, this change of sensitivity needs to be compensated by measuring pH and temperature of the solution simultaneously. Temperature compensation was previously demonstrated for measuring chemical and physical parameters with wireless sensors [8], [9].

In this paper [10], we present an integrated wireless passive pH and temperature sensor for temperature compensated remote pH monitoring. The sensor consists of a passive RLC resonator whose resonant frequency and quality factor change with the pH and temperature of the solution, respectively. Changes in the sensor's resonant frequency and quality factor are detected by measuring the induced change in the impedance of an external interrogator coil that is inductively coupled to the sensor inductor coil. Simultaneous measurements of pH and temperature of the solution are used for employing temperature compensation in pH measurement and thus the sensor overcomes the pH measurement error due to temperature dependence of the electrodes.

3.3 Sensor Operation

A block diagram of the wireless passive pH and temperature sensor is shown in Fig. 3.1. In the remote sensor, a spiral inductor is connected in parallel with a temperature dependant resistor (thermistor) and a voltage dependent capacitor (varactor) based voltage sensing circuit. A pH combination electrode is connected in parallel with the varactor and provides a biasing voltage to the varactor. The pH combination electrode in our sensor consists of an iridium/iridium oxide sensing electrode and a silver/silver chloride reference electrode. An Iridium/iridium oxide electrode has the advantages of easy preparation, small size, continuous detection, fast and stable response in aqueous, non-aqueous, non-conductive, and even corrosive media, linear response to pH with reference to a silver/silver chloride electrode over 1.5-12 pH range, low impedance, no requirement for pretreatment and negligible interference of ions and complexing agents. It has been used for pH measurements in technical media, such as fuels, food applications and in biological media [5], [6], [11], [12].

In the sensor shown in Fig. 3.1, L_S is the inductance of the spiral inductor, $R_T(T)$ is the temperature dependent resistance, T is the temperature of the contact solution, $C(V_{pH})$ is the capacitance of the voltage sensing circuit and V_{pH} is the potential difference developed at the pH combination electrode when in contact with a solution. The capacitance, $C(V_{pH})$ changes in response to the low frequency change of the biasing voltage, V_{pH} while variation of temperature, T varies the resistance, $R_T(T)$. The spiral inductor, resistor and capacitor form a resonant circuit with a resonant frequency, f_0, and a quality factor, Q, given by (with no magnetic coupling) [13]

$$f_0 = \sqrt{1-\frac{1}{4Q^2}} \times \frac{1}{2\pi\sqrt{L_S C(V_{pH})}}, \tag{3.1}$$

$$Q \cong R_T(T)\sqrt{\frac{C(V_{pH})}{L_S}} \,. \tag{3.2}$$

An interrogator coil is inductively coupled to the sensor inductor and is used to track the resonant frequency and quality factor of the sensor. In this manner, the measured resonant frequency and quality factor are directly related to the potential difference developed at the pH combination electrode and temperature of the solution, respectively.

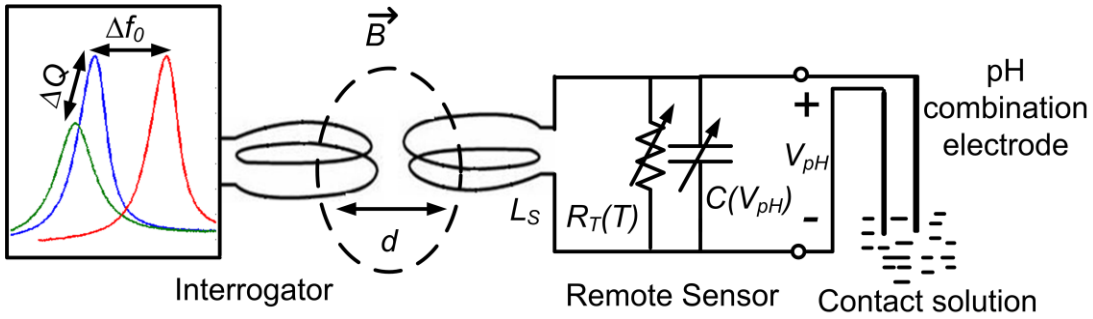

Figure 3.1. Conceptual block diagram of the combined wireless passive pH and temperature sensor.

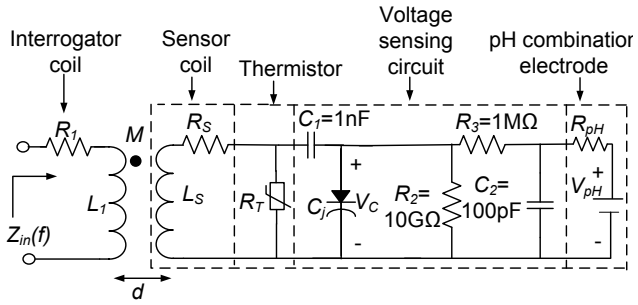

Figure 3.2. Equivalent circuit diagram of the wireless passive combined pH and temperature sensor.

An equivalent circuit diagram of the fabricated wireless passive temperature and pH sensor is shown in Fig. 3.2. Except R_T all other circuit components are described in section 2.3. R_T is the resistance of the temperature dependent resistor (thermistor), which decreases with

increasing temperature. The pH of the contact solution, which is indicated by V_{pH}, and temperature of the solution, T, can then be monitored by tracking the resonant frequency and quality factor of the sensor, respectively [14]. Referring to Fig. 3.2, near and at the resonant frequency of the sensor the impedance, Z_{in}, is given as

$$Z_{in}(f) = Z_1 + Z_T = R_1 + j2\pi fL_1 + \frac{(2\pi f)^2 M^2}{Z_S}, \tag{3.3}$$

where f is the interrogator source frequency and $Z_S \cong R_S + j2\pi fL_S + (R_T/(1 + j2\pi fCR_T))$ is the sensor series impedance. In our system the resonant frequency and quality factor were obtained from the real part of the impedance, Z_{in}, using a quadratic curve-fitting algorithm [15], [16]. A background subtraction method same as described in chapter 2.3 was implemented to remove the self impedance of the interrogator coil [17].

3.4 Design and Fabrication

3.4.1 pH Combination Electrode

The iridium/iridium oxide (Ir/IrO_x) sensing electrode was prepared by direct oxidation method. Ir metal wire (0.5 mm in diameter, 99.8% purity, obtained from Alfa AESAR) of about 10 mm in length was ultrasonically cleaned with 6M HCl solution followed with de-ionized water. The clean wire was then oxidized by bringing it to a temperature of 800ºC in an electric oven for 45 minutes after wetting its surface with 1M NaOH solution. The wetting and heating process was repeated six times until a blue-black coating was formed on the surface [11], [18]. The electrode was immersed in boiling DI water for one hour and then in DI water at room temperature for 30 days to reduce aging effects [19], [12]. A small area of (about 2 mm in length) iridium oxide film at one end was scrapped off and connected to an insulated wire using

silver epoxy. Silicone sealant (GE Silicone I) was applied over the connection area for electric insulation.

The silver/silver chloride (Ag/AgCl) reference electrode (obtained from DOCXS biomedical products and accessories) was 0.5 mm in diameter and 8 mm in length. Soft silver wire was attached to the electrode for electrical connection. An insulated wire was connected to the silver wire and the connection area was electrically insulated with silicone sealant.

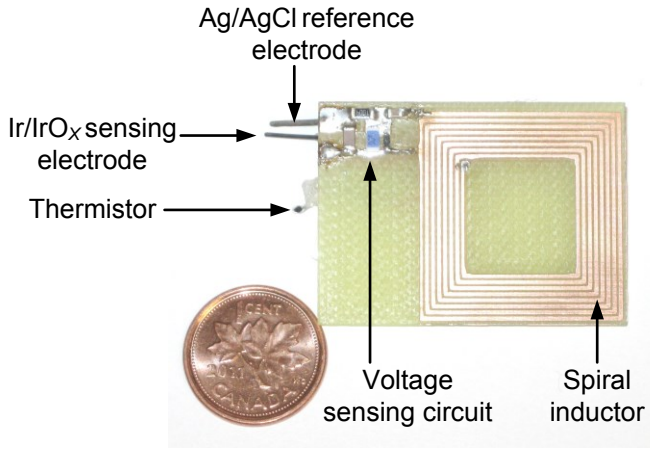

Figure 3.3. 18 MHz wireless passive temperature and pH sensor.

3.4.2 Sensor and Interrogator

The sensor, as shown in Fig. 3.3, was constructed using the Ir/IrO$_x$ and Ag/AgCl electrodes described above. The sensor was designed to have a resonant frequency, f_0, near 18 MHz. The sensor inductor and the voltage/temperature sensing circuit were fabricated on a 4 cm x 3 cm single sided FR4 printed circuit board (PCB) with surface mount capacitors and resistors. The inner and outer dimensions of the square, eight-turn planar spiral inductor were 1.45 cm and 2.68 cm, respectively, producing L_S=2.1 μH and R_S= 2.2 Ω at 18 MHz. The resistance of the thermistor (Honeywell 112-105PAJ-B01), R_T, varied in the range of 0.015 MΩ - 0.008 MΩ at 18

MHz for temperatures between 25°C and 55°C, respectively. The junction capacitance of the varactor (NXP BB202) used in the voltage sensing circuit, C_j, varied in the range of 35.04 pF - 22.95 pF for reverse bias voltages between 0 and 1V, respectively. The electrode resistance, R_{pH}, for pH solutions in the range of 1.5-12 was approximately 3.16 MΩ. The Ag/AgCl and Ir/IrO_x electrodes were connected to the positive and negative terminals of the voltage sensing circuit, respectively. The interrogator coil and interrogation method is same as the one described in section 2.4.1.

3.5 Results

For all calibration tests, solutions of different pH were made by adding 0.01M NaOH to 0.03M HNO_3. During the tests, the pH and temperature of the solutions were continuously monitored using a commercial pH-meter with automatic temperature compensation (PH150-C-ExStik®) and a thermometer, respectively.

3.5.1 Calibration of pH Combination Electrode

The potential difference between the sensing and reference electrodes, V_{pH}, was measured as a function of pH of the test solutions using a high impedance digital multimeter (Agilent 34401). Each solution was heated from 25°C to 55°C in 5°C steps. Fig. 3.4 shows that at a fixed temperature V_{pH} has a linear response to pH. The slope was -58.19 mV/pH at 25°C which was very close to the Nernstian slope (-59.16 mV/pH at 25°C). The slope increases with temperature. The linear fits for three different temperatures (25°C, 40°C and 55°C) were used to determine the isothermal point, 2.2 pH, for the pH combination electrode.

3.5.2 Response Time of pH Combination Electrode

To investigate the response time of the pH combination electrode, rapid step changes in pH of the test solutions were performed by quickly adding NaOH to the test solutions. The tests were carried out at a room temperature of 23±0.3ºC. The solution was stirred vigorously during the test. For step changes of 1.6 pH (from pH 2.2 to pH 3.8), 2.4 pH (from pH 3.8 to pH 6.2), 3.5 pH (from pH 6.2 to pH 9.7) and 5.2 pH (from pH 2.2 to pH 7.4), the pH combination electrode response time was less than 1 sec for an accuracy of 0.1 pH. The dynamic response for a step change of 1.6 pH (from pH 2.2 to pH 3.8) is shown in Fig. 3.5. The small variations in the V_{pH} values after 1 sec (see insert of Fig. 3.5) may result from the solution mixing process.

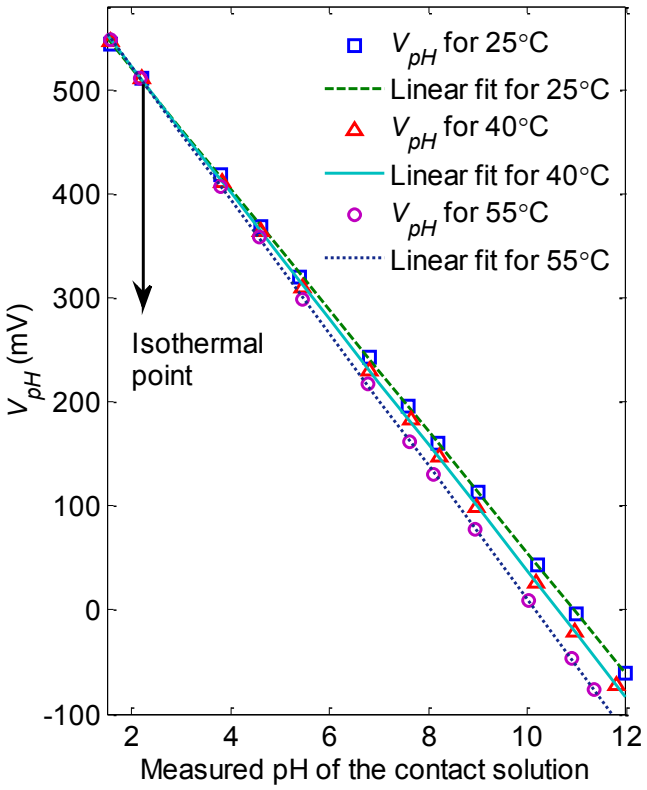

Figure 3.4. Potential difference of the pH combination electrode versus pH of the contact solution for different solution temperatures.

3.5.3 Stability of pH Combination Electrode

Drift of the electrode potential difference, V_{pH}, over time could cause error in pH measurements that cannot be eliminated by calibration. A two day long test was performed to identify the stability of V_{pH}, with time. Fig. 3.6 shows V_{pH} of the combination electrode monitored for a solution of 11.65 pH over 54 hours along with temperature (measured with a thermometer). The value of V_{pH} was almost constant, centered at -42.25 mV, with a deviation of less than ±2 mV (±0.03 pH) over the 54 hours period. The temperature variation (±1°C) during this time accounts for a V_{pH} deviation of ±2.5 mV. This indicates that the pH combination electrode has high stability making it suitable for continuous measurement without frequent calibration.

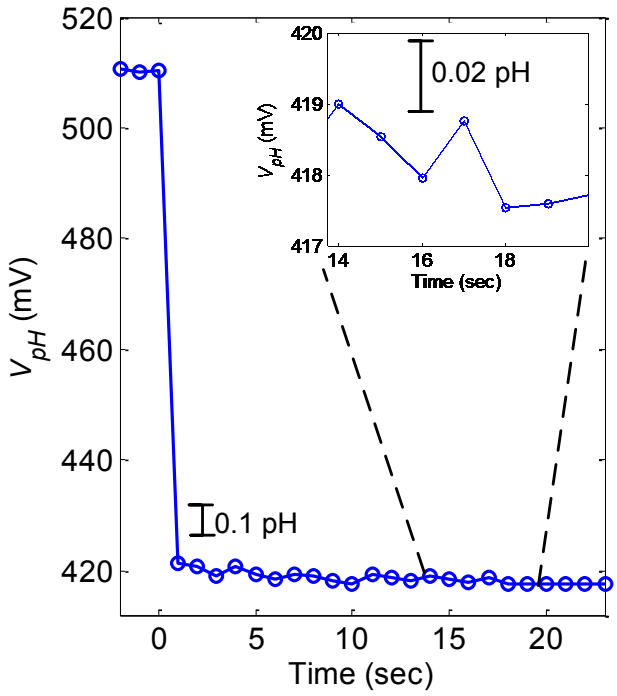

Figure 3.5. Electrode potential difference response to a step change in solution pH (from pH 2.2 to pH 3.8) at a temperature 23±0.3ºC.

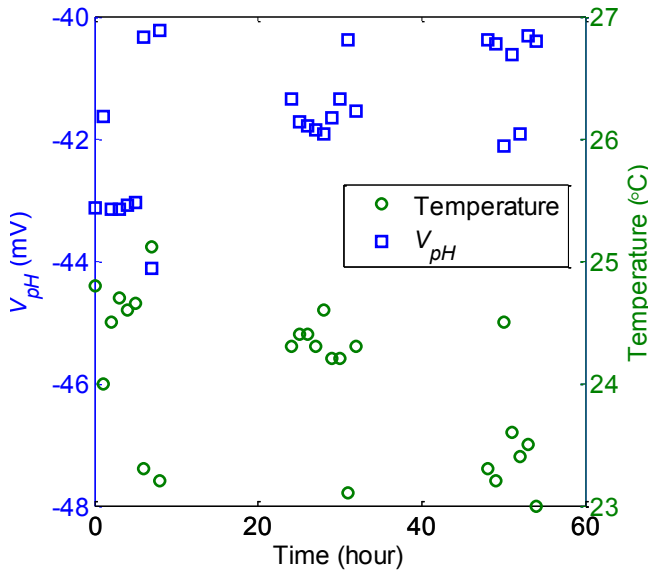

Figure 3.6. Stability of the pH combination electrode in a 11.65 pH solution at a temperature 24±1ºC.

3.5.4 Calibration of pH Sensor

The experimental setup with the wireless passive sensor is shown in Fig. 3.7. Ten different pH solutions were measured with each solution's temperature varied from 25°C to 55°C in 5°C steps. The resonant frequency, f_{0meas}, and the quality factor, Q of the sensor were remotely monitored. Fig. 3.8 shows the frequency response of the sensor, $\mathrm{Re}\{Z_T\}$, as measured by the impedance analyzer for two different pH solutions at two different temperatures. The resonant frequency and quality factor of the sensor were obtained from the maximum and the full-width half-max of $\mathrm{Re}\{Z_T\}$, respectively, using a quadratic curve-fitting algorithm [15], [16]. Fig. 3.9 shows the measured quality factor, Q at different temperatures for different pH solutions. The temperature of the solution can be extracted from the linear fit to data as

$$T[^{\circ}C] = -2.61Q + 166.5\,. \tag{5}$$

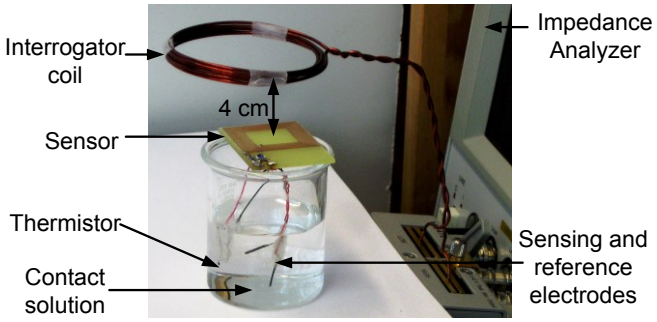

Figure 3.7. Experimental set up with the wireless passive pH/temperature sensor.

According to (eqn. 3.1) the resonant frequency of the sensor depends on L_S, C and Q. For our sensor, loss increases (Q goes down) as the temperature increases and thus the resonant frequency, f_{0meas}, decreases with Q. Fig. 3.10 shows the shift of f_{0meas} due to Q for the isothermal point pH 2.2 solution. As the electrode's response, which in turns changes the junction capacitance, C_j, does not change with temperature for a pH 2.2 solution, a quadratic fit (see Fig. 3.10) was used to adjust the measured f_{0meas} value to compensate for the change in Q. The quadratic fit providing the Q-adjusted resonant frequency is given by

$$f_{0Qadj}[MHz] = f_{0meas}[MHz] - 1.54x10^{-4}Q^2 + 0.0011Q + 0.4\,. \tag{6}$$

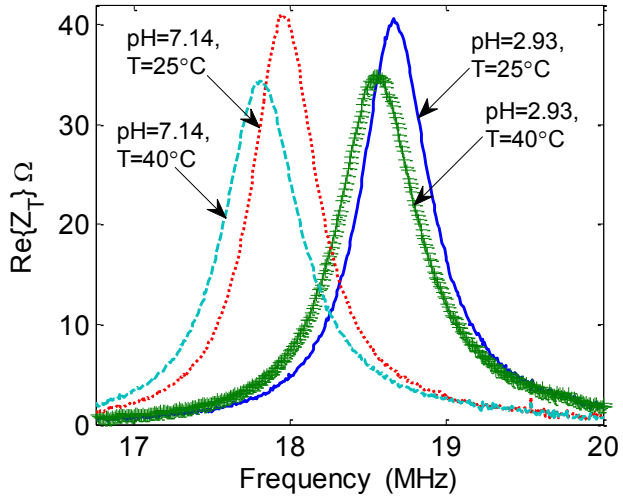

Figure 3.8. Frequency response of the sensor at different operating conditions.

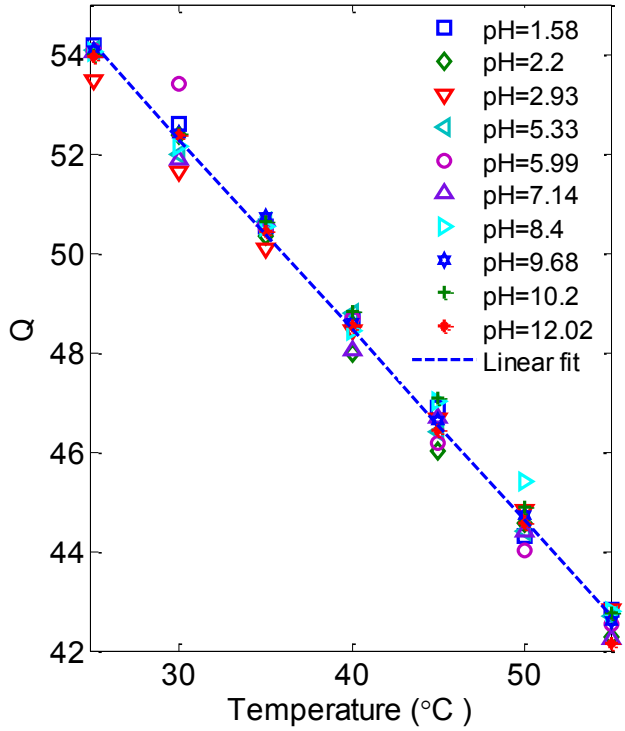

Figure 3.9. Quality factor as a function of solution temperature for different pH solution.

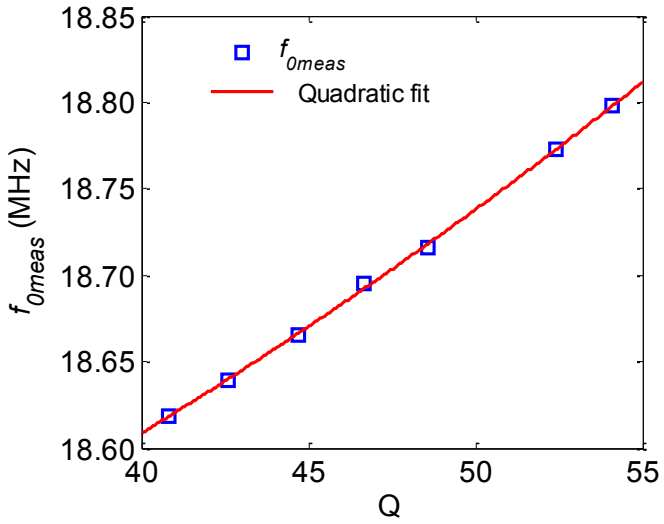

Figure 3.10. Resonant frequency versus quality factor for pH 2.2 (isothermal point) solution.

Fig. 3.11 shows the *Q*-adjusted resonant frequency, f_{0Qadj}, for different pH solutions. It can be seen that, at a fixed temperature, f_{0Qadj} has a linear response to pH. At 25ºC the linear fit over the 1.5-12 pH dynamic range indicates a slope of 174 kHz/pH and an intercept of 19.180 MHz. The slope of the linear fit increases with increase in temperature as 0.6612 kHz/ºC (0.0038 pH/ºC)

centered at 25ºC. After compensating Q, the isothermal point is pH_{Iso}=2.15 (f_{0Iso}=18.806 MHz). The temperature compensated pH can then be found from the sensor resonant frequency as

$$pH = pH_{Iso} - \frac{1}{0.174}\left(1 - 0.0038\left(T[^{\circ}C] - 25\right)\right)\left(f_{0Qadj}[MHz] - f_{0Iso}\right). \quad (7)$$

Fig. 3.12 shows the measured pH of a solution (prepared as pH=9.68 at 25ºC) as a function of temperature (as determined from the quality factor of the sensor). The solution pH was measured with the wireless sensor and a commercial temperature compensated pH meter. Both temperature compensated and non-compensated sensor pH values are shown. This demonstrates that the sensor can measure the pH of the solution with a 0.1 pH accuracy when employing temperature compensation.

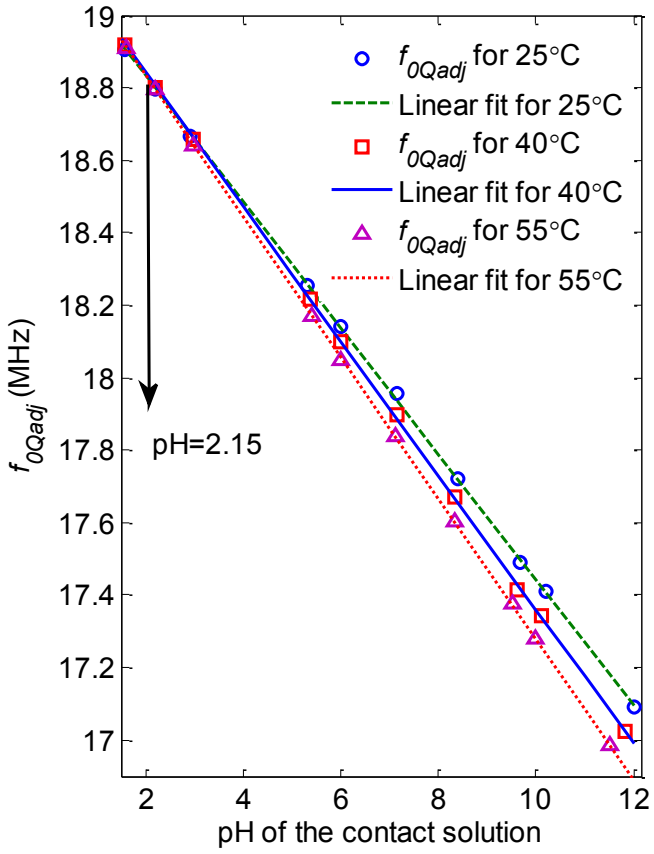

Figure 3.11. Resonant frequency (adjusted for Q change) versus pH of the contact solution (as measured by commercial meter) for different solution temperatures.

The cyclic stability of the sensor was determined by repeatedly immersing the sensor's electrodes and thermistor into solutions of pH 4, 7 and 10 at 25°C. The sensor's resonant frequency and quality factor were measured at each step. The results, shown in Fig. 3.13, indicate that the sensor has high cyclic stability with maximum 9 kHz deviation of resonant frequency and maximum 1.5 deviation of quality factor. This corresponds to a maximum temperature deviation of 3.9°C and a maximum deviation of 0.05 pH

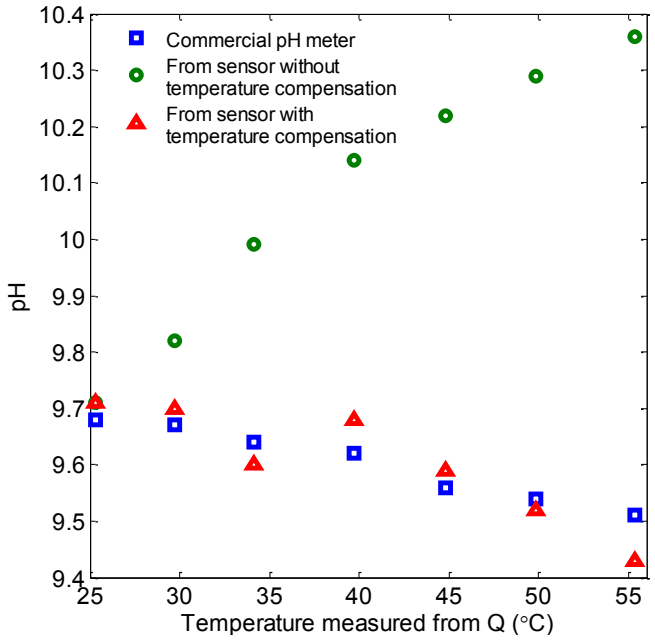

Figure 3.12. Response of the temperature compensated pH sensor and commercial pH- meter as a function of the solution temperature (measured from quality factor). Both temperature compensated and non-compensated results are shown.

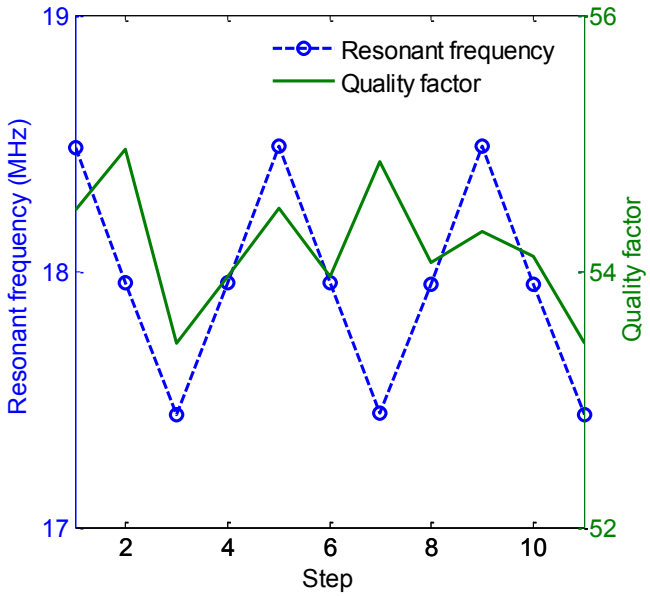

Figure 3.13. Resonant frequency and quality factor of the sensor when exposed to repeated cycles of pH 4, 7, and 10 solutions.

3.5.5 Effect of Interrogator-Sensor Separation Distance

Table 3.1. Variation of resonant frequency, quality factor and signal-to-noise ratio with interrogator-sensor distance

Distance (cm)	Resonant frequency (MHz)	Quality factor	Signal-to-noise ratio (for a bandwidth of 39.8 Hz)
2.5	17.360	53.54	498.45
3.3	17.365	54.42	306.28
4.0	17.361	54.32	159.15
5.5	17.367	54.31	52.90
6.5	17.368	54.07	22.63
7.5	17.367	54.43	9.00
8.5	17.362	54.86	4.56

As the separation distance between the sensor and the interrogator coil increases, the received signal amplitude from the sensor decreases. An experiment was conducted to measure the variation of the sensor's resonant frequency, quality factor and signal-to-noise ratio with the separation distance. For all tests the sensor coil was aligned concentrically with the interrogator coil. Table 3.1 shows the resonant frequency, f_0, quality factor, Q, and signal-to-noise ratio for different distances. The pH and temperature of the contact solution was 10.48 (measured by a pH meter) and 24.8ºC (measured by a thermometer), respectively. The signal-to-noise ratio was determined using the peak value and the rms deviation of $\mathrm{Re}\{Z_T\}$ when measurement time per sampling point was 25.12 mSec (for a bandwidth of 39.8 Hz). For separation distances of 2.5 cm to 8.5 cm a resonant frequency variation less than 8 kHz (corresponding to 0.04 pH) and a quality factor variation of 1.32 (corresponding to 3.4 ºC) were obtained. Distances less than 2.5 cm put the varactor in a non-linear operating region. Larger separation distances can be achieved by increasing the power at the interrogator coil, or by increasing the number of turns and/or radius of the interrogator coil [17]. However, to determine the error in measuring resonant frequency ($f_0 \pm \Delta f_0$) and quality factor ($Q \pm \Delta Q$), n samples of resonant frequency and quality factor need to be measured. The standard deviation of those n samples will determine Δf_0 and ΔQ.

3.5.6 Effect of Embedding Media on Sensor Response

Different materials were placed between the interrogator coil and the sensor to investigate the effect of different media on the sensor's resonant frequency, quality factor and signal-to-noise ratio. For all tests the sensor coil was aligned concentrically with the interrogator coil with distance, d= 4cm. The solution pH was 10.48 and temperature was 24.6°C. Three different dielectric media (air, plexiglass and concrete) of 3 cm thickness were placed between the interrogator and the sensor (6 mm away from the sensor and 4 mm away from the interrogator as

shown in Fig. 3.14). A large ferromagnetic interfering material (a 2.5 cm diameter and 30 cm long steel bar) was also placed 9 cm away from the center of the interrogator coil with concrete as medium in between. Table 3.2 lists the measured resonant frequency, quality factor and signal-to-noise ratio for these cases.

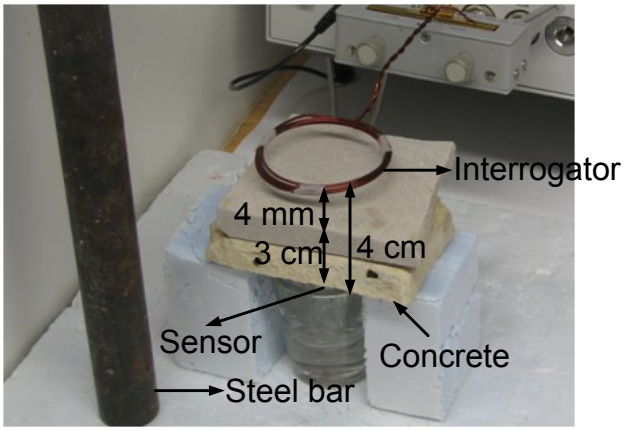

Figure 3.14. Experimental set up for testing the effect of different embedding media and an iron material interferer on sensor response.

Table 3.2. Variation of resonant frequency and quality factor for different embedding media and interferers.

Medium	Resonant frequency (MHz)	Quality factor	Signal-to-noise ratio
Air	17.362	54.59	150.78
Plexiglass	17.360	54.79	147.26
Concrete	17.358	54.86	146.91
Concrete and a rebar in close proximity	17.360	54.92	148.11

The maximum deviation in the resonant frequency, quality factor and signal-to-noise ratio was less than 0.02%, 0.61% and 2.63%, respectively, for these cases. This indicates that if

the sensor coil is packaged appropriately in order to reduce local parasitic effects, the effect of embedding media and interferers will be negligible. One potential application of the sensor is concrete pH monitoring. For concrete pH monitoring, the sensor will be embedded in concrete structures with iron reinforcement and the sensor response may be affected if it is directly tied in place to the rebar [17]. This study shows that the sensor can operate in this environment as long as the reinforcement steel is not in the immediate vicinity of the interrogator-sensor coils.

3.5.7 Wireless Milk Spoilage Monitoring

Bacteria growth is a major source of milk spoilage [5], [20], [21]. As bacteria grows during spoilage, the pH of milk changes. The sensor was used to monitor milk spoilage. A beaker containing 2% milk (initially at 6°C) with a very small amount of yogurt (used for rapid bacteria growth) was left at room temperature for 4 days. The sensor was placed so that the electrodes and the thermistor of the sensor were in contact with milk and the sensor coil/electronics were above the fluid. The resonant frequency, f_0, and quality factor, Q, of the sensor were monitored at a distance of 4 cm using the interrogator coil and the impedance analyzer. From the quality factor, Q, temperature, T, was obtained using (5). Then T and f_0 were used to find the pH using (6) and (7). The pH and temperature of the milk were also measured using a commercial temperature compensated pH-meter and thermometer, respectively. Variations of milk temperature (measured using the sensor's quality factor and thermometer) and pH (measured using the sensor's resonant frequency and temperature compensated pH-meter) are shown in Fig. 3.15. For first few hours (see inset of Fig. 3.15) the uncompensated sensor pH measurement has large deviation (>0.35 pH) as compared with the commercial temperature compensated pH-meter. This is due to the initial temperature increasing from 6°C to room temperature (after removal from a refrigerator). Results indicate that with temperature

compensation the sensor was able to monitor the milk spoilage with a maximum deviation of 0.1 pH as compared with the commercial temperature compensated pH-meter result.

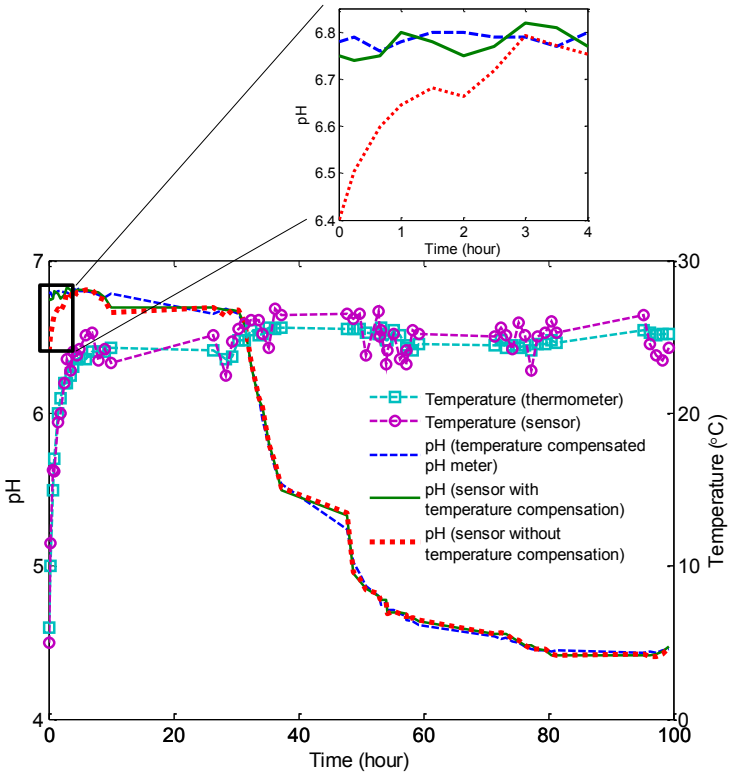

Figure 3.15. Milk pH (measured with a temperature compensated pH-meter and with the sensor) and temperature (measured with a thermometer and with the sensor) over time. The inset shows the compensated and uncompensated pH as temperature increases from 6°C to room temperature.

3.6 Discussion and Conclusion

This paper [10] presented an integrated wireless passive sensor capable of simultaneous temperature and pH measurement. This simple and cost effective multivariable sensor was based on a passive RLC coil resonator. pH and temperature of different solutions could be wirelessly monitored by measuring the change of sensor's resonant frequency and quality factor,

respectively. The sensor was calibrated for temperature over a range of 25°C-55°C and for pH over a 1.5-12 dynamic range. Using the calibration the sensor was able to perform temperature compensated pH monitoring with 0.1 pH accuracy. The accuracy of the sensor can be improved by fabricating a sensor with larger quality factor, improving the sensitivity of the varactor (larger dC/dV) and the thermistor (larger dR/dT), operating the sensor in a higher frequency range and using a reference electrode with better stability. The time-response of the sensor is limited by the response time of the pH combination electrode and not by the sensor electronics or interrogator. Our sensor demonstrated a response time less than 1 sec for a 0.1 pH accuracy. The drift of the combination electrode potential was less than ±2 mV (±0.03 pH), tested over 54 hours, however, longer term drift should be tested. The sensor corrects the pH measurement error due to the temperature dependence of electrode based pH measurement. The measurement accuracy of electrode based pH sensors is also dependent on other factors such as ionic strength and composition of the solution and the cross sensitivity of the pH sensitive electrode to other ions present in the solution [6], [22]. With its temperature compensation ability and simple design the sensor is suited to integration using printed technologies and has potential application for remote pH monitoring in different fields such as food spoilage monitoring, concrete pH monitoring, and industrial and chemical processing.

In this paper the sensor is applied for milk spoilage monitoring only by immersing the electrodes in the milk. The electronics part of the sensor was outside the milk to remove the effect of lossy fluid medium on sensor measurement. However, for any pH monitoring application, it is desirable to embed the whole sensor in the medium. In the next chapter, for in-fluid monitoring, the sensor will be encapsulated in a manner to reduce the influence of the

permittivity and conductivity of the medium, and applied for bioprocess monitoring. The sensor will also be miniaturized to fit inside a small bioreactor or test tube.

References

[1] W. -L Tsai, J. L. Autsen, J. Ma, T. Hudson and J. Luo, "Noninvasive optical sensor technology in shake flasks for mammalian cell cultures," *BioProcess International*, vol. 10, no. 1, pp. 50–56, Jan. 2012.

[2] H. R. Kermis, Y. Kostov, P. Harms and G. Rao, "Dual excitation ratiometric fluorescent pH sensor for noninvasive bioprocess monitoring: development and application," *Biotechnology Progress*, vol. 18, no. 5, pp. 1047-1053, Sept. 2002.

[3] J. B. E. Horton, S. Schweitzer, A. J. DeRouin and K. G. Ong, "A varactor-based inductively coupled wireless pH sensor," *IEEE Sensors J.*, vol. 11, no. 4, pp. 1061-1066, April 2011.

[4] S. Bhadra, G. E. Bridges, D. J. Thomson and M. S. Freund, "Electrode potential based coupled coil sensor for remote pH monitoring," *IEEE Sensors J.*, vol. 11, no. 11, pp. 2813-2819, Nov. 2011.

[5] W. D. Huang, S. Deb, Y. S. Seo, S. Rao, M. Chiao and J. C. Chiao, "A passive radio-frequency pH-sensing tag for wireless food-quality monitoring," *IEEE Sensors J.*, vol. 12, no. 3, Mar. 2012.

[6] P. Kurzweil, "Metal oxides and ion-exchanging surfaces as pH sensors in liquids: state-of-the-art and outlook," *Sensors*, vol. 9, pp. 4955-4985, June 2009.

[7] J. J. Barron, C. Ashton and L. Geary, "The effects of temperature on pH measurement," Technical Services Department, Reagecon Diagnostics Ltd, Shannon Free Zone, County Lake, Ireland, Rep. TSP-01 Issue 1, 2005.

[8] C. Surman, R. A. Potyrailo, W. G. Morris, T. Wortley, M. Vincent, R. Diana, V. Pizzi, J. Curter and G. Gach, "Temperature-independent passive RFID pressure sensors for single-use bioprocess components," in *Proc. IEEE RFID,* 2011, pp. 78-84.

[9] R. A. Potyrailo, T. Wortley, C. Surman, D. Monk, Monk, W. G. Morris, M. Vincent, R. Diana, V. Pizzi, J. Carter, G. Gach, S. Klensmeden and H. Ehring, "Passive multivariable temperature and conductivity RFID sensors for single-use biopharmaceutical manufacturing components," *Biotechnology Progress*, vol. 27, no. 3, pp. 875-884, May 2011.

[10] S. Bhadra, D. S. Y. Tan, D. J. Thomson, M. S. Freund and G. E. Bridges, "A wireless passive sensor for temperature compensated remote pH monitoring," *IEEE Sensors Journal*, vol. 13, no. 6, pp. 2428-2436, June 2013.

[11] G. Papeschi, S. Bordi, M. Carlagrave, L. Criscione and F. Ledda, "An iridium-iridium oxide electrode for in *vivo* monitoring of blood pH changes," *Journal of Medical Engineering & Technology*, vol. 5, no. 2, pp. 86-88, Mar. 1981.

[12] S. Yao, M. Wang and M. Madou, "A pH electrode based on melt-oxidized iridium oxide," J*ournal of the electrochemical society*, vol. 148, no. 4, pp. 29-36, 2001.

[13] K. Zeng, K. G. Ong, C. Mungle and C. A. Grimes, "Time domain characterization of oscillating sensors: Application of frequency counting to resonance frequency determination," *Review of Scientific Instruments*, vol. 73, no. 12, pp. 4375-4380, Dec. 2002.

[14] S. Bhadra, G. E. Bridges, D. J. Thomson and M. S. Freund, "A wireless passive sensor for pH monitoring employing temperature compensation," in *Proc. IEEE Sensors*, 2011, pp. 1522-1525.

[15] R. Nopper, R. Niekrawietz and L. Reindl, "Wireless readout of passive *LC* sensors," *IEEE Transaction on Instrumentation and Measurement*, vol. 59, no. 9, pp. 2450-2457, Sept. 2010.

[16] M. P. Robinson and J. Clegg, "Improved determination of Q-factor and resonant frequency by a quadratic curve fitting method," *IEEE Transaction on Electromagnetic Compatibility*, vol. 47, no. 2, pp. 399-402, May 2005.

[17] J. B. Ong, Z. You, J. Mills-Beale, E. L. Tan, B. D. Pereles and K. G. Ong, "A wireless, passive embedded sensor for real time monitoring of water content in civil engineering materials," *IEEE Sensors J.*, vol. 8, issue 12, pp. 2053-2058, Dec. 2008.

[18] R. A. Macur, "Iridium-iridiumoxide electrode for measuring pH of blood and other fluids," U.S. Patent 3 726 777, April 10, 1973.

[19] R.-G. Du, R.-G. Hu, R.-S. Huang and C.-J. Lin, "In situ measurement of Cl^- concentrations and pH at the reinforcing steel/concrete interface by combination sensors," *Anal. Chem.,* vol. 78, no. 9, pp. 3179-3185, Mar. 2006.

[20] K. G. Ong, J. S. Bitler, C. A. Grimes, L. G. Puckett and L. G. Bachas, "Remote query resonant-circuit sensors for monitoring of bacteria growth: application to food quality control," *Sensors*, vol. 2, pp. 219-232, June 2002.

[21] N. Nicolaou and R. Goodacre, "Rapid and quantitative detection of the microbial spoilage in milk using Fourier transforminfrared spectroscopy and chemometrics," *The Analyst*, vol. 133, no. 10, pp. 1424-1431, July 2008.

[22] A. D. Wiesner, L. E. Katz and C. -C. Chen, "The impact of ionic strength and background electrolyte on pH measurements in metal ion adsorption experiments, " *Journal of Colloid and Interface Science*, vol. 301, no. 1, pp 329-332, May 2006.

Chapter 4: Fluid Embeddable Coupled Coil Sensor for Wireless pH Monitoring in a Bioreactor

4.1 Abstract

A passive embeddable coupled coil sensor for remote bioprocess pH monitoring is described. The sensor is sterilizable, able to operate in a fluid medium and small enough to fit inside a small bioreactor or test tube. It consists of a planar spiral inductor connected in parallel to a varactor forming a LC resonant circuit. A pH combination electrode made of an iridium/iridium oxide sensing electrode and a silver/silver chloride reference electrode, is connected in parallel to the varactor. A potential difference change across the electrodes due to pH variation of the medium changes the voltage-dependent capacitance and shifts the resonant frequency of the sensor. An interrogator coil is inductively coupled to the sensor coil and remotely tracks the resonant frequency of the sensor. For in-fluid monitoring the sensor is encapsulated in a manner that reduces the influence of the permittivity and conductivity of the medium. The sensor, calibrated over 2-12 pH range, exhibits a rapid response with 2.477 MHz/pH sensitivity. The sensor was used for remote pH monitoring of *Yarrowia lipolytica* and *Saccharomyces cerevisiae* fermentation in a shake flask over 63 hours and 25 hours, respectively. Experiments demonstrate that the medium pH can be monitored repeatedly with an accuracy of 0.08 pH.

4.2 Introduction

In recent years, numerous efforts have been dedicated to develop pH sensors for fields such as industrial and chemical processing, environmental and bioprocess applications, food

quality monitoring, structural health monitoring and biomedical sensing [1]-[7]. Bioprocesses are most commonly carried out in bioreactors to produce many commodities and chemicals. During bioprocess, optimal cell growth depends on pH control and many cells produce acids as a metabolic by-product. Therefore, monitoring and controlling medium pH during bioprocess is important [1], [8]. Conventionally, sterilizable electrochemical pH probes are used for bioprocess monitoring. They, however, need wired connections for data exchange and are inherently invasive. Small bioreactors such as shake flasks and test tubes are regularly used for bioprocess development. The use of wired pH probes for multiple reactors (i.e. simultaneous monitoring of several shake flasks) requires a proportional increase of wiring, cost and complexity. Fiber-optic probes are an alternative, but are fragile when mechanically stressed and not sterilizable [9]. Embeddable wireless sensors are an attractive alternative for many of these situations [10]-[13].

Although a large number of studies have been done on developing wireless pH sensors, only a small fraction can be used inside bioreactors. Many sensors do not endure in the harsh bioprocess environment as the medium can permeate through and damage the sensor. Often the fluid medium culture is not well defined and interferes with sensor readings. Moreover, sensors used in bioprocess need to be sterilizable and their components should not leach out into the medium to avoid medium contamination and interference with metabolism [1]. Another challenge is that the sensors have to perform measurement without recalibration, replacement or manual attention over the operational period [8]. Non-invasive optical sensors based on absorbance or fluorescence from pH-sensitive dyes have been successfully used inside bioreactors. They can be affixed to sterile vessels [8], [10], [14]-[16]. Several commercially available systems, [17], [18], [19], use these optical based sensors for online pH monitoring of cultures. The advantages they offer over conventional electrochemical probes are high sensitivity

and accuracy, ease of miniaturization, embeddable in a wide range of vessel types, and most importantly wireless monitoring [20]. However, optical sensors suffer from a narrow operating range and drift due to photobleaching over time [1], [14], [17], [20].

In the paper [21] we present a coupled coil pH sensor that can be integrated with and embedded inside a bioreactor. It employs a varactor based passive LC resonator whose resonant frequency changes with the pH of the medium. This voltage dependent frequency shift type sensor has been previously proposed for pH measurement [22], [23] as well as biopotential transmission [24]. We show how the varactor based LC sensor can be embedded in a fluid so that the resonant frequency is insensitive to the electrical properties of the lossy medium. As the sensor is passive, it requires no internal power source. Therefore, once embedded inside the bioreactor there is no need to remove the sensor for battery charging or replacement. An interrogator coil is inductively coupled to the sensor inductor and change in the sensor's resonant frequency is remotely detected by measuring the induced change in the impedance of the interrogator coil (Z_{in} as shown in Fig. 2). The design of the sensor is simple and inexpensive to manufacture, making it a cost effective solution to remote bioprocess pH monitoring.

4.3 pH Sensor Operation

A block diagram of the coupled coil pH is shown in Fig. 4.1. In the remote sensor, a spiral inductor is connected in parallel with a voltage dependent capacitor (varactor) based voltage sensing circuit. A pH combination electrode is connected in parallel with the varactor and provides a biasing voltage to the varactor. In the sensor shown in Fig. 4.1, L_S is the inductance of the spiral inductor (sensor coil). C_f is the interwinding parasitic capacitance between the traces of the spiral inductor, $C(V_{pH})$ is the capacitance of the voltage sensing circuit

and V_{pH} is the potential difference developed at the pH combination electrode when in contact with a solution. The capacitance, $C(V_{pH})$ changes in response to the low frequency change of the biasing voltage, V_{pH}. The spiral inductor and capacitors form a resonant circuit with a resonant frequency, f_0, approximately given by

$$f_0 = \frac{1}{2\pi\sqrt{L_s(C(V_{pH})+C_f)}} \tag{4.1}$$

The sensor inductor is inductively coupled to an interrogator coil, whose impedance is monitored using a swept frequency impedance analyzer. The resonant frequency of the weakly coupled sensor coil, f_0, is obtained by measuring the perturbation of interrogator coil impedance. In this manner, when the interwinding capacitance is small and fixed (C_f <<C), the resonant frequency is directly related to the potential difference developed at the pH combination electrode.

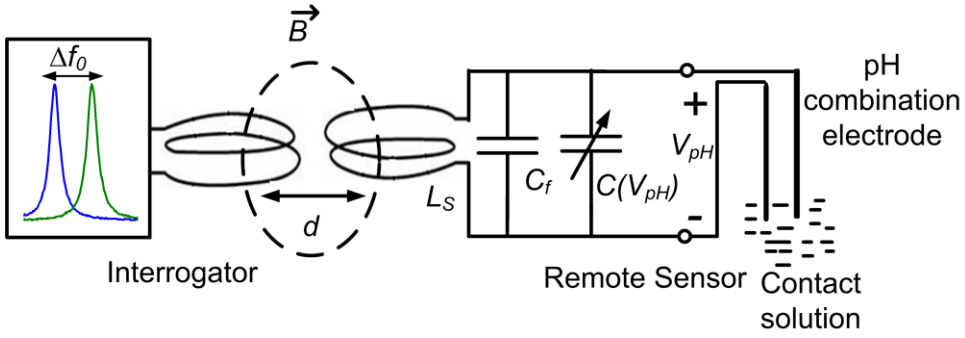

Figure 4.1. Conceptual block diagram of the coupled coil pH sensor.

An equivalent circuit diagram of the fabricated wireless passive temperature and pH sensor is shown in Fig. 4.2. Except C_f all other circuit components are described in section 2.3. C_f is the interwinding capacitance between the traces of the sensor coil. Assuming the losses are small, C_f is small and fixed, and C_1>>$C(V_C)$, the pH of the contact solution, which is indicated by V_{pH}, can be monitored by tracking the resonant frequency of the sensor [25]. Referring to Fig. 4.2, near

and at the resonant frequency of the sensor the impedance, Z_{in}, is given as

$$Z_{in}(f) = Z_1 + Z_T = R_1 + j2\pi fL_1 + \frac{(2\pi f)^2 M^2}{Z_S}, \tag{4.2}$$

where f is the interrogator source frequency and $Z_S \cong R_S + j2\pi fL_S + 1/(j2\pi f(C+C_f))$ is the sensor series impedance. In our system the resonant frequency was obtained from the maximum of the real part of the impedance using a quadratic curve-fitting algorithm [26]. A background subtraction method same as described in chapter 2.3 was implemented to remove the self-impedance of the interrogator coil [27].

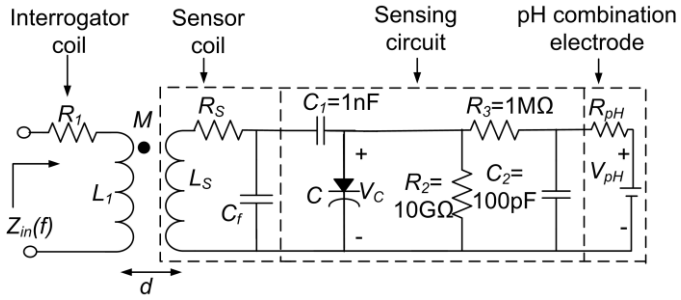

Figure 4.2. Equivalent circuit diagram of the coupled coil pH sensor.

4.4 pH Sensor Design and Fabrication

4.4.1 pH Combination Electrode

A pH combination electrode generally consists of a sensing and a reference electrode. The sensing electrode provides a potential that is dependent on pH of the sample while the reference electrode ideally provides a pH independent potential. Thus the potential difference across the sensing and reference electrode provides a measure of pH. Glass pH combination electrodes are widely used for pH measurement. However, they are easily affected by alkaline solutions, have high cell resistance (in the order of 10^7 to 10^9 Ω) and are difficult to miniaturize and planarize. Because of their brittle nature, they have a risk of breakage [28], [29], [3]. Due to

these disadvantages, iridium/iridium oxide (Ir/IrO_x) and silver/silver chloride (Ag/AgCl) electrodes were chosen as sensing electrode and reference electrode, respectively, for the combination electrode in our sensor. The advantages of an iridium/iridium oxide sensing electrode are discussed in section 3.3 [29]. Ag/AgCl electrode is the most widely used reference electrode in industry and research due to its simple construction and cheap manufacturing cost [7], [28], [31], [32].

The iridium/iridium oxide sensing electrode was prepared according to the method described in section 3.4.1 [30]. The silver/silver chloride reference electrode was prepared from silver wire by electroplating method. 10 mm of Ag wire (1 mm in diameter, 99.8% purity, obtained from Alfa AESAR) was polished using sandpaper. An insulated wire was connected to a small area of the polished Ag wire (about 2 mm in length) using silver epoxy. High temperature epoxy was applied over the connection area for electric insulation. A layer of AgCl was formed on the remaining 8 mm of the polished Ag wire by applying +0.5 V for 50 s in a 0.1 M potassium chloride (KCl) solution. An immobilized electrolyte was freshly prepared by saturating 12 mL of tetrahydrofuran (THF) with KCl at room temperature and then adding 0.4 g of polyvinyl chloride (PVC). The Ag/AgCl wire was dip-coated in the immobilized electrolyte solution and dried in a house vacuum-evacuated desiccator for 48 hr. After drying, the electrode was dip-coated with a protective Nafion layer to prevent the leakage of chloride ions. Following the dip-coating the electrode was cured in a pump-evacuated oven for 1 hour at 140°C, stored in a desiccator for seven days, placed in DI water for 24 hours and then stored in a desiccator until it was used. Nafion was selected because it is a cation-exchange polymer that prevents anion exchange. Thus, transport of chloride ions through the Nafion film is blocked and leakage is eliminated. Nafion stability was greatly enhanced by thermal curing at a high temperature which protects the

reference electrode and provides increased reproducibility and stability [33]. High temperature (120°C-150°C) curing also makes the Nafion membrane stronger and more resistant to cracking than non-heat treated Nafion [34]. Fig. 4.3 shows the potential of the Nafion coated Ag/AgCl quasi-reference electrode with respect to a commercial glass Ag/AgCl reference electrode (CH Instruments 111). It can be seen that an initial stabilization time of around 3.5 hours was required for the Nafion to act as an ion exchanging membrane after the electrode was removed from the desiccator and placed in the fluid [33]. The response for different pH shows that after initial stabilization the potential has a very small deviation , maximum 6 mV, over the 4-10 pH range (see inset of Fig. 3 where pH 4, 7, 10 exhibits potentials of 166±0.53, 168.07±1.7 mV, 170.58± 0.95 mV, respectively).

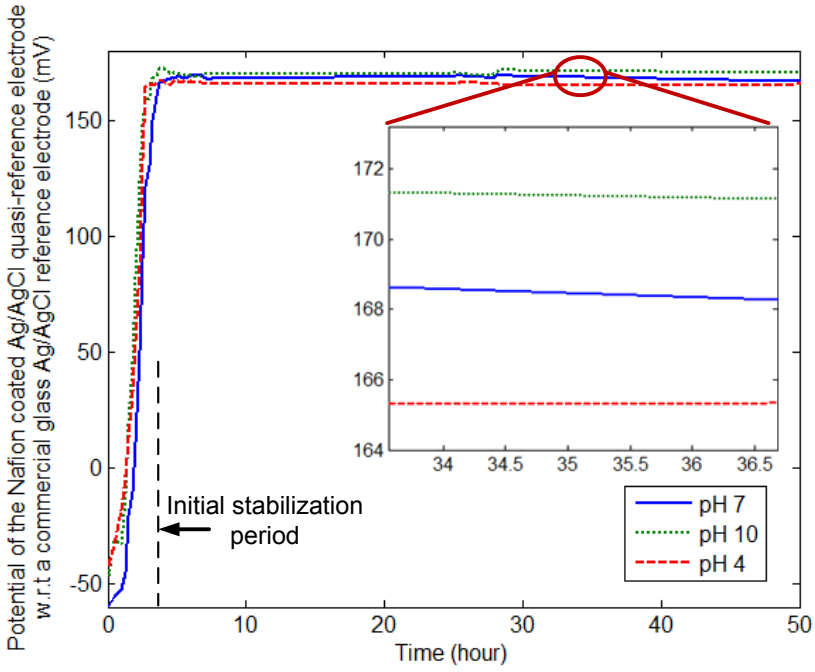

Figure 4.3. Voltage Nafion coated Ag/AgCl quasi-reference electrode potential with respect to a commercial glass Ag/AgCl reference electrode (CH Instruments 111) as a function of time and medium pH. An initial period of approximately 3.5 hours is required for stabilization in buffer solution after removal from a desiccator.

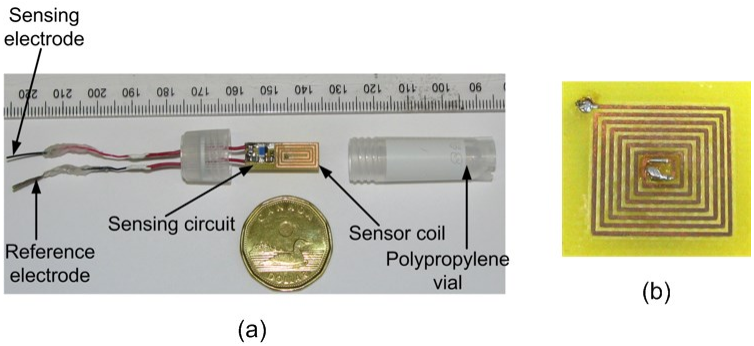

Figure 4.4. (a) Prototype coupled coil sensor for bioprocess pH monitoring and (b) Interrogator coil.

4.4.2 Sensor and Interrogator Description

A prototype sensor, as shown in Fig. 4.4a, was constructed using the Ir/IrO_x and Ag/AgCl electrodes described above. For our study the prototype was fabricated as individual components. The electrodes, sensor electronics and encapsulation can latter be integrated in a more compact manner. The sensor was designed to have a resonant frequency, f_0, near 77 MHz. The sensor inductor and the voltage sensing circuit were fabricated on a 20 mm x 6 mm single sided FR4 printed circuit board (PCB) with surface mount capacitors and resistors. The encapsulation is described latter. The inner and outer dimensions of the rectangular, four-turn planar spiral inductor were 6.5 mm x 1.2 mm and 12 mm x 5.5 mm, respectively, producing L_S=0.13 μH and R_S= 1.25Ω and C_f =0.98 pF at 77 MHz in air and f_{res}=445.89 MHz (measured with a network analyzer HP 8753). The junction built in potential of the varactor (NXP BB202) used in the voltage sensing circuit is 0.7 V. The junction capacitance of the varaactor, C, as a function of bias voltage was measured at 77 MHz and is shown in Fig. 4.5a. It provides a voltage sensitivity of dC/dV= 0.02 pF/mV at a bias voltage of 111 mV (corresponding to a pH of 7). Fig. 4.5b shows the IrO_x electrode potential with respect to the Nafion coated Ag/AgCl quasi-reference electrode, V_{pH}, for pH solutions in the range of 2-12 (the Nafion coated Ag/AgCl quasi-reference

and Ir/IrO_x electrode potential was measured with a high impedance voltmeter). V_{pH} has a slope of 58 mV/pH which is very close to the ideal slope (~59 mV/pH). The electrode resistance, R_{pH}, was approximately 3.16 MΩ. The Ag/AgCl and Ir/IrO_x electrodes were connected to the positive and negative terminals of the voltage sensing circuit (Fig. 4.2), respectively. The sensor along with the electrodes is normally stored in a desiccator to prevent leakage. Since an initialization stabilization time of around 3.5 hours is required, as seen from Fig. 4.3, the electrodes were stored overnight in DI water before the experiments.

The interrogator coil was fabricated on a 32 mm x 32 mm single sided FR4 printed circuit board. The inner and outer dimensions of the square, eight-turn planar spiral inductor were 3 mm x 3mm and 13 mm x 13 mm, respectively, producing L_S=0.82 μH, R_S= 2.2 Ω at 77 MHz and a self-resonant frequency, f_{res}=97.3 MHz. The sensor's resonant frequency was determined by measuring the real part of the impedance of the interrogator coil, Re{Z_{in}}, when inductively coupled to the sensor coil. The interrogator inductor coil impedance was measured using an impedance analyzer (Agilent 4294A) with the voltage source level of the analyzer set to 25 mV.

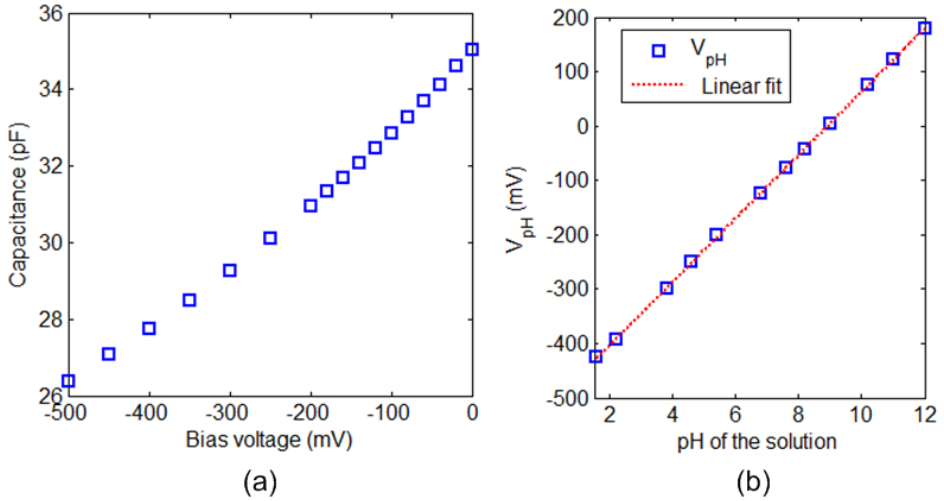

Figure 4.5. (a) Measured junction capacitance of the varactor at 77 MHz as a function of the bias voltage and (b) potential of IrO_x electrode with respect to Nafion coated Ag/AgCl quasi-reference electrode, V_{pH}, versus pH of the contact solution.

4.5 Experiment and Result

4.5.1 In-fluid Monitoring

For bioprocess pH monitoring, the sensor needs to be immersed in a fluid medium inside the bioreactor. We assume the medium inside bioreactor is a non-ferrous fluid with relative permeability of the fluid, μ_r=1 for all cases. One issue for in fluid monitoring is protection of the electronics from the fluid. This is typically solved by putting a thin passivation layer or encapsulation material on the sensor electronics. Another important issue is the effect the lossy fluid has on the sensor coil fields. Wireless sensors embedded in lossy media can experience loss in the interrogator-sensor coupling, especially in the ultra-high-frequency (UHF) band of operation [35]. The loss is significantly less at the lower frequencies our sensor operates at, where the coupling is through magnetic field induction [35]. Further to this, the sensor coil field can impinge into the lossy fluid. As shown in Fig. 4.6a, for a thin passivation layer, this results in a change of interwinding capacitance, C_f, and an added conductance loss. The resonant frequency becomes medium dependant, and the quality factor, Q of the sensor resonator is dramatically reduced. This parasitic effect is often advantageously used in many sensors that monitor the dielectric properties of the medium [27]. In our sensor it is undesirable and a thick encapsulation layer (a low loss dielectric spacer between the sensor coil and the passivation layer), as shown in Fig. 4.6b, can be used to remove the effect of the fluid medium. Fig. 4.6c shows the responses of the sensor for a thin layer of passivation (0.5 mm thick layer of polypropylene, ε_r=2.1) and thick dielectric spacer when the sensor was immersed in a standard fermentation medium of pH 5.3 (measured with a commercial pH probe) at 30°C. The dielectric spacer (see Fig. 4.4a) was constructed by hermetically sealing the sensor coil/electronics in a polypropylene vial, which provided a 2.5 mm air gap between the sensor coil and the thin

polypropylene layer. Locations where the electrodes came out of the vial were sealed with high temperature epoxy. The experimental set up is shown in Fig. 4.7. The interrogator coil was concentrically placed outside of the beaker at a distance, *d*= 3 cm from the sensor coil. Even though the fermentation medium is a fairly low loss fluid (ε_r=74.48, σ=0.04 S/m) it can dramatically affect the response of the thin passivation layer sensor. It can be seen that the thick dielectric spacer improves the *Q* of the sensor by removing the effect of the fluid medium.

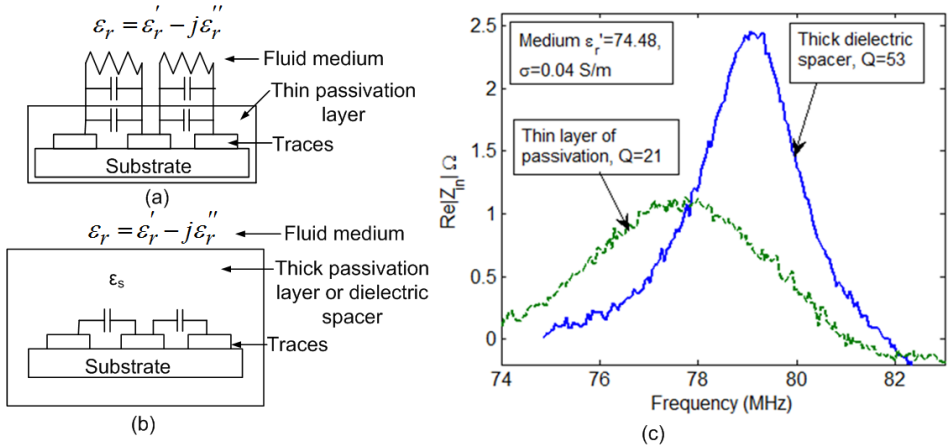

Figure 4.6. Effect of lossy fluid on sensor coil and sensor response. Illustrations of (a) fluid influence for a thin passivation layer (interwinding capacitance change and conductance addition) and (b) removal of that effect by thick dielectric spacer. (c) Response of the sensor for both cases.

The sensitivity of the prototype sensor (with thick dielectric spacer) to the electrical parameters of the medium was tested by using the sensor in fluids with different permittivity and conductivity at 30°C (shown in Fig. 4.7). All the media have a pH of 5.3 (measured with a commercial pH probe). The interrogator coil was placed concentrically outside of the beaker at a distance, *d*= 3 cm from the sensor coil. Fig. 4.8 shows the impedance frequency response when the sensor was in the air (only the electrodes are in contact with the medium of ε_r=74.48, σ=0.04

S/m at the bottom of the beaker) and when it was fully immersed in different fluids. Results show that the Q and f_0 of the sensor did not depend on the relative dielectric permittivity of the fluid. Only a very highly conductive medium reduces the Q and changes the f_0 of the sensor. In this worst case, this corresponds to an error of 0.11 pH. This prototype sensor with thick dielectric spacer was used for the rest of the experiments in this paper.

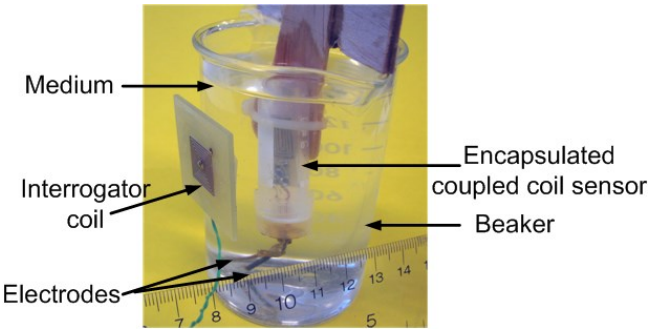

Figure 4.7. Encapsulated coupled coil sensor immersed in a fluid medium.

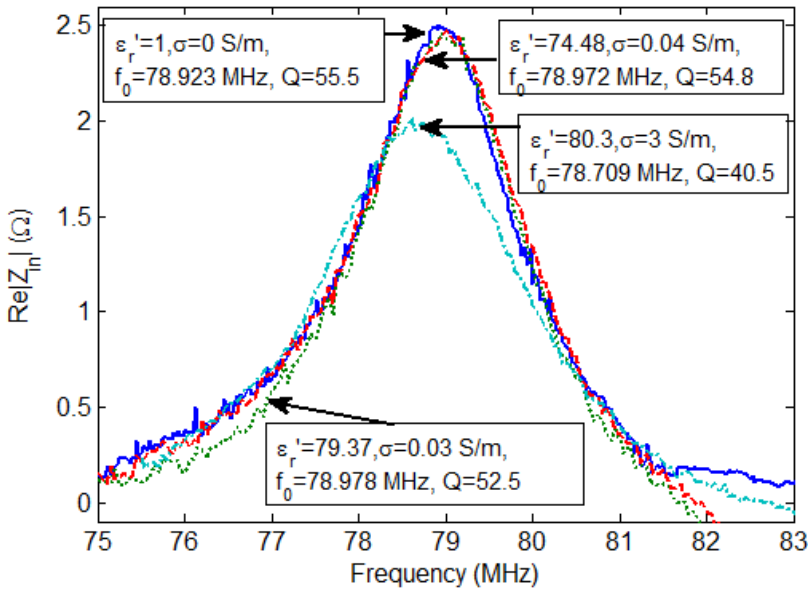

Figure 4.8. Impedance frequency response when the prototype sensor (encapsulated with thick dielectric spacer) is in air and completely immersed in different fluids for a constant pH of 5.3.

4.5.2 Calibration

The sensor along with the electrodes were immersed in a series of varying pH solutions (values between 2-12) in a 250 mL Schott bottle at 30°C. For the calibration test, solutions of different pH were prepared by adding KOH to HCl. During the tests, the pH of the solutions was continuously monitored using a commercial pH probe. The sensor coil was aligned concentrically with the interrogator coil, which is placed outside of the bottle, with a separation distance d= 2 cm. Fig. 4.9 plots the resonant frequency, f_0, for the different pH solutions as determined from the peaks of their impedance response. A linear fit given by

$$f_0(MHz) = -2.477pH + 92.139 \tag{4.3}$$

over the 2-12 pH dynamic range indicates a sensitivity of 2.477 MHz/pH.

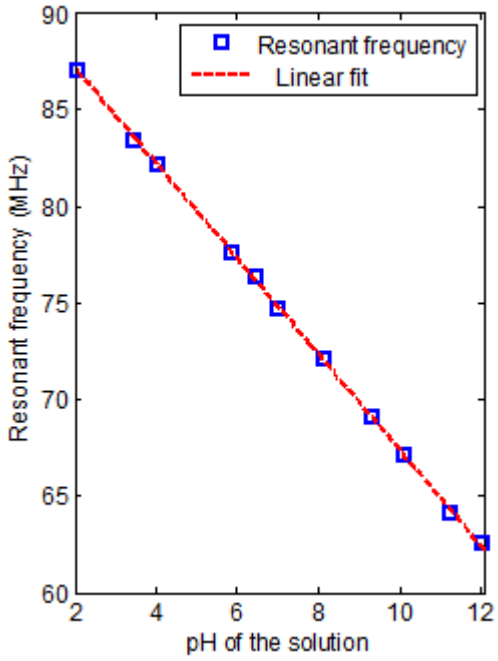

Figure 4.9. Resonant frequency of the sensor as a function of measured pH of the prepared solutions.

4.5.3 Fermentation Experiments

Fermentations of *Yarrowia lipolytica* and *Saccharomyces cerevisiae* were conducted in a 250 mL Schott bottle, which served as a bioreactor in this study. The sensor was embedded in the bioreactor containing the medium. A commercial pH probe (connected to a data logger) was also used to monitor and log the pH inside the bioreactor. Fig. 4.10 shows the experiment set up. It should be noted that the same sensor was used for both fermentation experiments. Media preparation, experiment and results for each fermentation are described below.

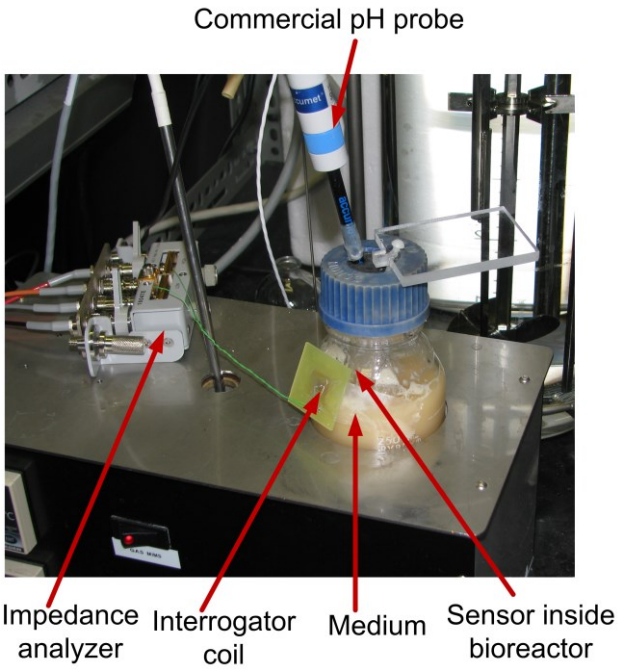

Figure 4.10. Fermentation experiment with the sensor mounted inside the bioreactor.

4.5.3.1 *Yarrowia lipolytica* Fermentation

The medium was prepared from 10 g/L Yeast extract, 20 g/L peptone and glycerol (13 mL of 50% glycerol solution to give a final concentration of 440 mM). Glycerol was used as the carbon source. The total volume of the medium and carbon source was 200 mL. The shake flask and the sensor were both sterilized using an autoclave. The pH probe and oxygen tubing were

sterilized separately and inserted into the bioreactor to track the pH of the medium and supply oxygen, respectively. The organism used was Yarrowia lipolytica, one of the most extensively studied yeasts. It is a strictly aerobic microorganism capable of producing important metabolites and has an intense secretory activity, which justifies efforts to use it in industry (as a biocatalyst), in molecular biology and in genetics studies. 40 mL of *Yarrowia lipolytica* cells were harvested during mid-exponential growth stage. This was centrifuged to separate the cells from the supernatant, and the liquid volume was reduced to 10 mL, concentrating the biomass in the inoculum by a factor of 4. Then 2 mL of *Yarrowia lipolytica* cells were used to inoculate the medium for fermentation. The medium was stirred at a constant speed of 100 rpm at 30°C. The resonant frequency, f_0, of the sensor was monitored at half hour intervals at a distance of 2 cm using the interrogator coil. Fig. 4.11 shows examples of the impedance frequency response of the sensor for two different medium pH values.

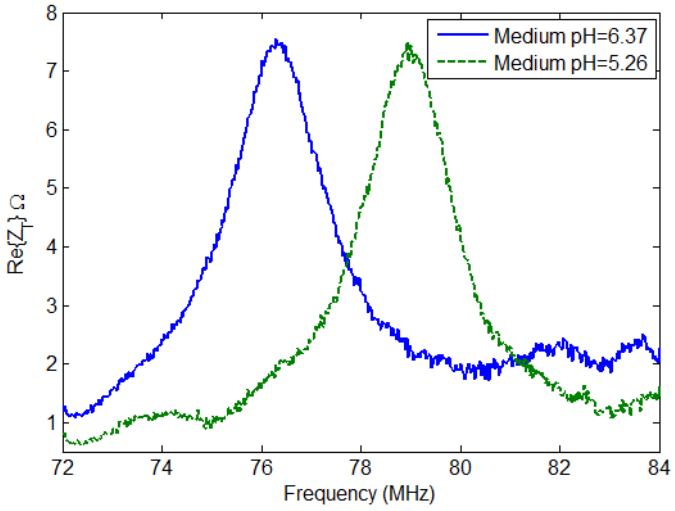

Figure 4.11. Example impedance frequency responses for two different medium pH values.

Variation of the sensor's resonant frequency and medium pH (measured using the sensor and commercial pH-probe) over 63 hours is shown in Fig. 4.12. The medium pH measured by

the sensor was obtained using the resonant frequency and the calibration (eqn. 4.3). It can be seen that the pH monitored by the sensor was always in good agreement with that measured by the commercial pH probe over the course of the fermentation period, with a maximum deviation of 0.08 pH.

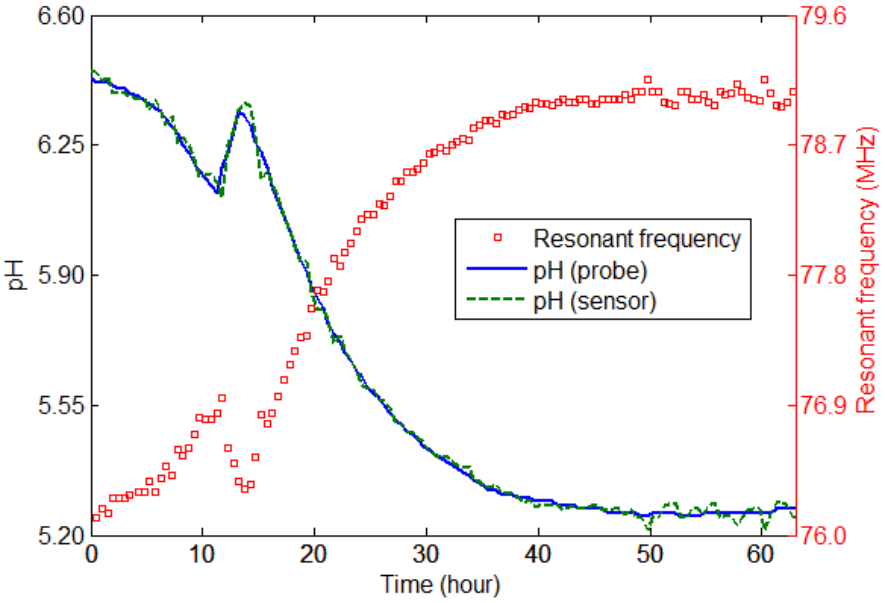

Figure 4.12. Resonant frequency of the sensor and medium pH as measured with a commercial pH probe and with the sensor using eqn. 4.3 and the resonant frequency for *Yarrowia lipolytica* fermentation.

4.5.3.2 *Saccharomyces cerevisiae* Fermentation

The media used in this study was prepared using a purchased mixture of yeast extract, peptone, and dextrose (YPD) (Bacto^{TM} obtained from Becton, Dickinson and Company). To prepare the media, 12.5 g YPD was dissolved into 250 mL deionized water (50 g L^{-1}). The pH of the media was adjusted to 6.5 by the addition of potassium hydroxide. A volume of 200 mL of YPD media was placed in the bioreactor. The media and sensor inside the bioreactor were sterilized using an autoclave. The commercial pH probe was also sterilized and inserted into the bioreactor to monitor the pH. The organism used was a recombinant strain of the yeast

Saccharomyces cerevisiae, a well-studied organism that exhibits ability to produce high yields of ethanol from fermentation of glucose. Five grams of pelletized *S. cerevisiae* yeast was added to the reaction vessel with a 200 mL working volume just prior to the test. The reaction was kept at 30° C and gentle stirring was applied using magnetic stir-plate for a period of 25 hours. The sensor's resonant frequency, f_0, was observed at a distance of 2 cm with the interrogator coil. Fig. 4.13 plots the variation of the sensor's resonant frequency and medium pH as measured with the commercial pH probe and with the sensor using the resonant frequency and calibration (eqn. 4.3). Over the 25 hours fermentation period the sensor pH measurement conforms with the commercial probe pH measurement with maximum deviation of 0.07 pH.

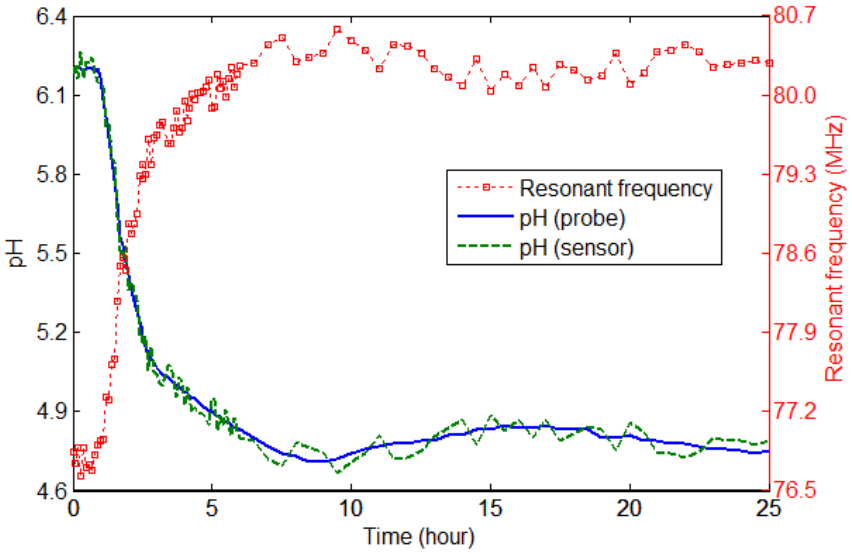

Figure 4.13. Resonant frequency of the sensor and medium pH as measured with a commercial pH probe and with the sensor using (eqn. 4.3) and the resonant frequency for *Saccharomyces cerevisiae* fermentation.

4.5.4 Repeatability and Cyclic Stability

To test the repeatability of the sensor, base was added to the medium after 63 hours in the case of the *Y. lipolytica* fermentation. In this manner, the pH of the medium was increased from 5.26 to 5.94 and then 6.43 in two steps. The resonant frequency obtained for medium pH 5.94

and 6.43 after 63 hours was then compared with the resonant frequency obtained for medium values of pH 5.94 and 6.43 measured at 21.25 hour and 1 hour, respectively during fermentation. The results, shown in Table 4.1, shows that the sensor produced repeatable results (<0.05 pH) after the 63 hours test. This also indicates that sensor was not affected or damaged inside bioreactor by the medium or the bioreactor stirring process.

Table 4.1. Variation of resonant frequency with time for same medium pH

Time (hour)	Medium pH (Commercial pH probe)	Resonant frequency, f_0 (MHz)	pH measured from f_0 and (eqn. 4.3)
1	6.43	76.122	6.46
63.25	6.43	76.048	6.49
21.25	5.94	77.371	5.96
63	5.94	77.494	5.91

The cyclic stability of the sensor was determined by repeatedly immersing the sensor in solutions of pH 2, 7 and 12 at 25°C in the 250 mL Schott bottle. The sensor's resonant frequency was measured at each step for a separation distance d = 2 cm from the interrogator coil. pH was obtained using the resonant frequency and calibration (eqn. 4.3). The results, shown in Fig. 4.14, indicate that the sensor has high cyclic stability with a maximum deviation of 148.62 kHz (corresponding to a maximum deviation of 0.06 pH).

4.5.5 Effect of Interrogator-Sensor Separation Distance

As the separation distance between the sensor and the interrogator coil increases, the mutual inductance between the sensor and interrogator coil, M decreases, reducing the received signal amplitude, Z_T, from the sensor. Also, position of the sensor inside the fluid may affect the

resonant frequency. The dependence on location in fluid and distance to the interrogator was measured using a setup shown in Fig. 4.7. For all tests the sensor was immersed in a medium (ε_r=74.48, σ=0.04 S/m) of pH 5.3 (measured with a commercial pH probe) at 30°C in the beaker. The sensor coil was aligned concentrically with the interrogator coil which was placed on the surface of the beaker. Only the sensor was moved inside the beaker to obtain different separation distances. Theoretical values for the resonant frequency were calculated by eqn. 4.2 using measured values of L_1, R_1, L_s, R_s, C_f, $C(V_{pH})$ and an approximation for coupling factor, M. The value of M was calculated using the theoretical coupling factor for two concentric coils [36]. Table 4.2 shows the measured and theoretical resonant frequency, f_0 along with the theoretical coupling, M, values for different distances. For separation distances ranging from 1.5 cm to 4 cm, the theoretical f_0 value did not change since the coupling factor was small in all cases. The measured f_0 varied 245 kHz (corresponding to 0.1 pH). This is due to the noise of the system, which sets an upper limit for the operating distance of this type of sensor. As the separation distance increases the signal-to-noise ratio decreases rapidly reducing the measurement accuracy. It should be noted that placing the sensor too close to the interrogator coil can induce a large voltage in the sensor coil and push the varactor into a non-linear operating region [30]. It is also important to have the two coils concentrically oriented to achieve an optimal coupling (the experiments described in this paper do this). The upper limit for the separation distance can be improved by increasing the power at the interrogator coil, or by increasing the number of turns and/or radius of the interrogator coil [27]. Table 4.2 also shows that the circuit behaves the same way as the model given in Fig. 4.2. The differences between the theoretical and measured values of f_0 are due to the printed circuit board parasitic effects on the varactor (the varactor capacitance in Fig. 4.5a was measured before placing it on the PCB).

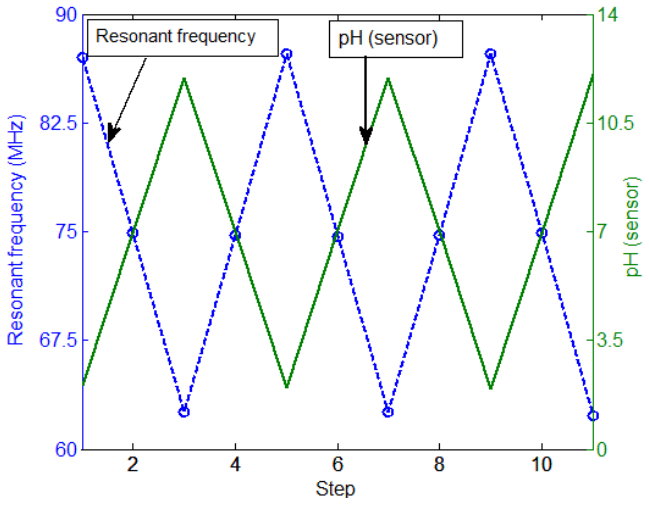

Figure 4.14. Resonant frequency and pH as measured with the sensor using (4) and the resonant frequency when exposed to repeated cycles of pH 2, 7 and 12 solutions.

Table 4.2. Variation of resonant frequency and mutual inductance with interrogator-sensor distance

Distance (cm)	Measured f_0 (MHz)	pH measured from f_0 and (eqn. 4.3)	Theoretical M (H)	Theoretical f_0 (MHz)
1.5	78.957	78.957	$1.26X10^{-8}$	78.785
2	78.923	78.923	$5.31X10^{-9}$	78.784
2.5	79.142	79.142	$2.72X10^{-9}$	78.784
3	78.994	78.994	$1.57X10^{-9}$	78.784
3.5	79.034	79.034	$9.91X10^{-10}$	78.784
4	79.168	79.168	$6.63X10^{-10}$	78.784

4.6 Discussion and Conclusion

This paper presented a coupled coil pH sensor capable of real-time and repeatable in-fluid pH measurement inside bioreactor. This simple sensor is based on a LC resonator with pH of the medium monitored by measuring the change of sensor's resonant frequency. This sensor has the

advantages of requiring no power source in the sensor, and no physical connection between the sensor and the data acquisition system. The sensor was calibrated over a 2-12 pH dynamic range. Using the calibration the sensor was successfully able to provide continuous remote pH measurement of *Yarrowia lipolytica* and *Saccharomyces cerevisiae* fermentation. The pH recorded by the sensor was repeatable and in good agreement with the values measured with a commercial pH probe. The maximum deviations were 0.08 pH over a 6.83-5.26 pH range and 0.07 pH over a 6.2-4.7 pH range from the commercial pH probe during *Yarrowia lipolytica* and S*accharomyces cerevisiae* fermentation, respectively. Although the accuracy of non-invasive optical pH sensors (optical pH sensors have accuracy of 0.05 pH [17]) is slightly better than the accuracy of the proposed sensor, narrow operating range and long-term drift due to photobleaching are the two concerns [14], [20]. Since the proposed sensor is based on a pH combination electrode, it operates over a wider dynamic range and does not have a long-term drift problem.

For general use, temperature should be taken into consideration when using electrode based pH sensors. The potential difference developed at the pH combination electrode, V_{pH}, is affected by temperature. Since bioprocesses are carried out at different constant temperatures, the sensor has to be calibrated every time the process temperature changes to overcome pH measurement error due to temperature dependence of the electrodes [30]. Another concern for the sensor is the sensing electrode made from iridium which is fairly costly. This sensing electrode can be easily replaced by commercially available, low cost and pH sensitive mixed metal oxide (MMO) electrodes [37]. The robust, sterilizable and encapsulated sensor was not affected by the electrically lossy fluid medium. Its size is suitable for pH monitoring inside a shake flask or test tube. In practice, simultaneous monitoring of several bioreactors would need

multiple sensors to be embedded. In this situation the proposed sensor requires the ability to uniquely identify one sensor's response from its neighbor. This issue can be solved by designing sensors to have different resonant frequencies [38]. The Nafion coated Ag/AgCl quasi-reference electrode used in this work has a very small deviation in potential over a 4-10 pH range. The simple design of the sensor makes it suited to integration using printed circuit technology and thus it can be a potential cost effective way to obtain reliable pH information remotely from a bioprocess.

One issue to apply this sensor for food spoilage monitoring is its need for direct contact with food. This is often not desirable due to the risk of electrode fouling and food contamination. Since the sensor can only work for liquid mediums, another issue is detecting spoilage of dry food. To overcome these two issues, the pH sensor has been transformed to an acidic and basic volatile sensor by embedding the electrodes in a hydrogel host electrolyte. The next chapter will discuss the details of the volatile sensor and demonstrate its ability to detect acidic and basic volatiles. In addition, mixed metal oxide (MMO) will be used as a pH-sensitive electrode in the next chapter to make the sensors low cost.

References

[1] P. Harms, Y. Kostov and G. Rao, "Bioprocess monitoring," *Current Opinion in Biotechnology*, vol. 13, no. 2, pp. 124-127, Apr. 2002.

[2] J. B. E. Horton, S. Schweitzer, A. J. DeRouin and K. G. Ong, "A varactor-based inductively coupled wireless pH sensor," *IEEE Sensors J.*, vol. 11, no. 4, pp. 1061-1066, April 2011.

[3] S. Bhadra, G. E. Bridges, D. J. Thomson and M. S. Freund, "Electrode potential based coupled coil sensor for remote pH monitoring," *IEEE Sensors J.*, vol. 11, no. 11, pp. 2813-2819, Nov. 2011.

[4] R.-G. Du, R.-G. Hu, R.-S. Huang and C.-J. Lin, "In situ measurement of Cl^- concentrations and pH at the reinforcing steel/concrete interface by combination sensors," *Anal. Chem.,* vol. 78, no. 9, pp. 3179-3185, Mar. 2006.

[5] J. M. L. Engels and M. H. Kuypers, "Medical application of silicon sensors," *J. Phys. E: Sci. Instrum.*, vol. 16, no. 10, pp. 987-994, Oct. 1983.

[6] J. Lin, "Recent development and applications of optical and fibre-optic pH sensors," *Trends in Analytical Chemistry*, vol. 19, no. 9, pp. 541-552, Sept. 2000.

[7] W. D. Huang, S. Deb, Y. S. Seo, S. Rao, M. Chiao and J. C. Chiao, "A passive radio-frequency pH-sensing tag for wireless food-quality monitoring," *IEEE Sensors J.*, vol. 12, no. 3, Mar. 2012.

[8] A. S. Jeevarajan, S. Vani, T. D. Taylor and M. M. Anderson, "Continuous pH monitoring in a perfused bioreactor system using an optical pH sensor," *Biotechnology and Bioengineering*, vol. 78, no. 4, pp. 467-472, May 2002.

[9] J. Buchs, "Introduction to advantages and problems of shaken cultures," *Biochemical Engineering Journal,* vol. 7, no. 2, pp. 91-98, Mar. 2001.

[10] S. Vuppu, Y. Kostov and G. Rao, "Economical wireless optical ratiometric pH sensor," *Meas. Sci. Technol.*, vol. 20, pp. 045202(7pp), Feb. 2009.

[11] C. Komives and R. S. Parker, "Bioreactor state estimation and control," *Current Opinion in Biotechnology*, vol. 14, no. 5, pp. 468-474, Oct. 2003.

[12] A. Vasala, J. Panula, M. Bollók, L. Illmann, C. Hálsig and P. Neubauer, "A new wireless system for decentralized measurement of physiological parameters from shake flask," *Microbial Cell Factories*, vol. 5, no. 8, pp. 1-6, Feb. 2006.

[13] S. Kumar, C. Wittmann and E. Heinzle, "Minibioreactors," *Biotechnology Letters*, vol. 26, no. 1, pp. 1-10, Jan. 2004.

[14] H. R. Kermis, Y. Kostov, P. Harms and G. Rao, "Dual excitation ratiometric fluorescent pH sensor for noninvasive bioprocess monitoring: development and application," Biotechnology Progress, vol. 18, no. 5, pp. 1047-1053, Sept. 2002.

[15] L. Tolosa, Y. Kostov, P. Harms and G. Rao, "Noninvasive measurement of dissolved oxygen in shake flasks," *Biotechnology and Bioengineering,* vol. 80, no. 5, pp. 594-597, Dec. 2002.

[16] Y. Kostov , P. Harms, L. Randers-Eichhorn and G. Rao, "Low-cost microreactor for high-throughput bioprocessing," *Biotechnology and Bioengineering,* vol. 72, no. 3, pp. 346–352, Feb. 2001.

[17] "Non-Invasive pH Sensors." Internet: http://www.presens.de/fileadmin/user_upload/products/Sensor_Probes/Non-invasive_pH_Sensors/110715_SP-NonInvpH-11-01_w.pdf [June 5, 2012].

[18] "SENSOLUX." Internet: http://www.sartorius.com/en/product/product-detail/dcs09/ [June 9, 2012].

[19] "Ambr-system overview." Internet: http://www.tapbiosystems.com/tap/cell_culture/ambr.htm# [June 9, 2012].

[20] W. -L Tsai, J. L. Autsen, J. Ma, T. Hudson and J. Luo, "Noninvasive optical sensor technology in shake flasks for mammalian cell cultures," *BioProcess International*, vol. 10, no. 1, pp. 50–56, Jan. 2012.

[21] S. Bhadra, W. Blunt , C. Dynowski , M. McDonald , D. J. Thomson , M. S. Freund , N. Cicek and G. E. Bridges, "Fluid embeddable coupled coil sensor for wireless pH monitoring in a bioreactor," *IEEE Transactions on Instrumentation and Measurement*, vol. 63, no. 5, pp. 1337-1346, May 2014.

[22] S. Bhadra, G. E. Bridges, D. J. Thomson and M. S. Freund, "A wireless passive pH sensor based on pH electrode potential measurement," in *Proc. IEEE Sensors*, 2010, pp. 927-930.

[23] J. B. E. Horton, S. Schweitzer, A. J. DeRouin and K. G. Ong, "A varactor-based inductively coupled wireless pH sensor," *IEEE Sensors J.*, vol. 11, no. 4, pp. 1061-1066, April 2011.

[24] B. C. Towe. "Systems and methods for wireless transmission of biopotentials." U.S. Patent 20100198039 A1, Aug. 5, 2010.

[25] S. Bhadra, C. Dynowski, W. Blunt, M. McDonald, D. J. Thomson, M. S. Freund, N. Cicek and G. E. Bridges, "Wireless Passive Sensor for pH Monitoring inside a Small Bioreactor," in *Proc. I2MTC*, 2013, pp. 276-279.

[26] R. Nopper, R. Niekrawietz and L. Reindl, “Wireless readout of passive *LC* sensors,” *IEEE Transaction on Instrumentation and Measurement*, vol. 59, no. 9, pp. 2450-2457, Sept. 2010.

[27] J. B. Ong, Z. You, J. Mills-Beale, E. L. Tan, B. D. Pereles and K. G. Ong, “A wireless, passive embedded sensor for real time monitoring of water content in civil engineering materials,” *IEEE Sensors J.*, vol. 8, issue 12, pp. 2053-2058, Dec. 2008.

[28] S. Yao, M. Wang and M. Madou, “A pH electrode based on melt-oxidized iridium oxide,” *Journal of the Electrochemical Society*, vol. 148, no. 4, pp. 29-36, 2001.

[29] P. Vanýsek. “The glass pH electrode,” *The Electrochemical Society Interface*, vol. 13, no. 2, pp. 19-20, Summer 2004.

[30] S. Bhadra, D. S. Y. Tan, D. J. Thomson, M. S. Freund and G. E. Bridges, "A wireless passive sensor for temperature compensated remote pH monitoring," *IEEE Sensors Journal,* vol.13, no.6, pp. 2428-2436, June 2013.

[31] G. Papeschi, S. Bordi, M. Carlagrave, L. Criscione and F. Ledda, “An iridium-iridium oxide electrode for in *vivo* monitoring of blood pH changes,” *Journal of Medical Engineering & Technology*, vol. 5, no. 2, pp. 86-88, Mar. 1981.

[32] P. Kurzweil, “Metal oxides and ion-exchanging surfaces as pH sensors in liquids: state-of-the-art and outlook,” *Sensors*, vol. 9, pp. 4955-4985, June 2009.

[33] M. A. Nolan, S. H. Tan and S. P. Kounaves, “Fabrication and characterization of a solid state reference electrode for electroanalysis of natural waters with ultramicroelectrodes,” *Anal. Chem.*, vol. 69, pp. 1244-1247, Mar. 1997.

[34] R. C. Mercado and F. Moussy, "*In vitro* and *in vivo* mineralization of Nafion membrane used for implantable glucose sensors," Biosensors and Bioelectronics, vol. 12, no. 2, pp. 133-145, Feb. 1998.

[35] K. Finkenzeller, RFID Handbook - Fundamentals and Applications in Contactless Smart Cards and Identification, 2nd ed, New York: John Wiley & Sons Inc., 2003.

[36] F. M. Tesche, M. V. Ianoz and T. Karlsson, *EMC Analysis Methods and Computational Models*, New York: John Wiley & Sons Inc., 1997.

[37] C. A. MacGregor, S. Bhadra, K. Perveen, M. M. Q. Xing, G. E. Bridges and Douglas J. Thomson, "A wireless volatile organic absorption pH sensor using a nixed metal oxide electrode," in *Proc. I2MTC*, 2013, pp. 83-86.

[38] V. Sridhar and K. Takahata, "A hydrogel-based passive wireless sensor using a flex-circuit inductive transducer," *Sensors and Actuators: A*, vol. 155, no. 1, pp. 58-65, Oct. 2009.

Chapter 5: Monitoring Acidic and Basic Volatile Concentration Using a pH-electrode Based Wireless Passive Sensor

5.1 Abstract

We present a near-field coupled passive sensor capable of detecting acidic and basic volatiles in its surrounding environment. The sensor employs a LC resonant circuit consisting of a spiral inductor connected in parallel with a voltage dependent capacitor (varactor). The volatile detector comprises a hydrogel coated pH-sensitive electrode pair connected in parallel with the varactor. The hydrogel is used as an absorptive medium for the volatiles and acts to contain the electrolyte. On absorption of the acidic or basic volatiles the hydrogel pH changes, which in turn changes the voltage across the pH-sensitive electrode pair shifting the resonant frequency of the sensor. An interrogator coil is inductively coupled to the sensor inductor and remotely tracks the resonant frequency of the sensor. The ability to sense different concentrations of ammonia and acetic acid vapor is demonstrated. The sensor has a linear response to the logarithm of the volatile concentration and a detection limit of 1.5 ppm and 2 ppm for ammonia, and acetic acid vapor, respectively. Effects of varying relative humidity, temperature and hydrogel coating thickness on the sensor's performance are presented. With less than a 20 minutes response time and irreversible operation in a closed environment, the sensor has potential in packaged food freshness monitoring.

5.2 Introduction

Volatile detection sensors have important applications in environmental monitoring and in the food and chemical industries [1]-[4]. In many cases quantitative knowledge of the concentration of acidic and basic volatiles is of great interest. During food spoilage, the growth

of yeasts and microbes results in production of organic acids, and acidic and basic volatiles. Monitoring the increase of these volatiles inside food packages can serve as an indicator for food spoilage [2], [5]-[7]. For example, microbial degradation of fish produces volatile amines such as trimethylamine ($N(CH_3)_3$), dimethylamine ($(CH_3)_2NH$) and ammonia (NH_3). These products are collectively known as total volatile basic nitrogen (TVBN) and its level is a potential indicator of fish spoilage in the food industry [2]. It is crucial to monitor NH_3, a basic volatile, excreted in poultry and livestock farming. To achieve maximum performance and efficiency in animal feeding the NH_3 level should be kept as low as possible. High NH_3 levels result in susceptibility to disease, decreased yield and animal uniformity, and reduced weight gains [8], [9]. In the chemical industry NH_3 is produced and used in high concentration for fertilizer production and refrigeration. A leak in a NH_3 system can be life-threatening and all NH_3 using industries install systems for detecting dangerous NH_3 concentrations. The maximum allowed workplace NH_3 level is considered to be 20 ppm [9]. In museums it is important to detect acidic volatiles as they are harmful to artifacts. Acetic acid (CH_3COOH) and formic acid (HCOOH) are among the most common acidic volatiles (given off by wood, paint, plastics, adhesives, etc) that can cause damage [3]. Monitoring of acidic volatile H_2S is essential in petrochemical and coal manufacturing industries as a concentration above 10 ppm causes damage to the respiratory system [10].

Conducting polymer based gas sensors have been applied in many forms to sense acidic and basic vapors [1], [2], [11]. Acidic vapors of hydrogen chloride (HCl), hydrogen sulphide (H_2S) and carbon dioxide (CO_2, in the presence of water) and basic NH_3 vapor have been detected using Polyaniline (PANI) film based sensors [2], [11]. Polypyrrole (PPy) film based sensors have been used for vapor sensing of weak acids and bases, such as H_2S, CH_3COOH and

NH_3 [11]. Polyaniline boronic acid (PABA) has also been explored as a sensing material for detecting basic vapor of biogenic amines [12]. Conducting polymer based gas sensors operate primarily by conductivity measurement techniques, although some also operate by changing their optical property [2], [13]. Substantial research has been done on metal-oxide gas sensors for monitoring acidic and basic volatiles such as H_2S, CO_2, NH_3, etc. These sensors are rugged and inexpensive. They operate using the principle of conductance change due to the chemisorption of volatile molecules into the sensing layer [9], [14]. Both wired and wireless implementations of the above sensors have been reported. The main advantages of wireless gas sensors, as compared to traditional wired sensors, include the unobtrusive nature of their installation, higher nodal densities and lower installation cost without the need of extensive wiring. Wireless sensors can be remotely interrogated and are suitable for applications where electrical connection to every measuring device is inconvenient or impossible, such as monitoring of containers with toxic industrial chemicals while in transit, medical monitoring of hospitalized and in-house patients and detection of food freshness in individual packages [15].

In this paper we present a hydrogel coated pH electrode based near-field passive wireless sensor for determining of acidic and basic volatile concentration. The sensor is based on a voltage dependant frequency shift technique utilizing a varactor. This approach has been previously used for pH measurement [16], [17] and corrosion monitoring [18]. It employs a passive LC resonator whose resonant frequency depends on the acidic and basic volatile concentration in its surrounding environment. Change in the sensor's resonant frequency is detected by measuring the induced change in the impedance of a remote interrogator coil that is inductively coupled to the sensor. We present experimental results of a prototype sensor capable of detecting different concentrations of NH_3 and CH_3COOH vapor. As the sensor is passive and

can be monitored wirelessly, it is suitable for long-term remote acidic and basic volatile detection and quantitative concentration measurement.

5.3 Sensor Operating Principle

A block diagram of the near-field sensor is shown in Fig. 5.1 and includes the interrogator coil coupled to it. In the sensor, a spiral inductor is connected in parallel with a voltage dependent capacitor (varactor) based voltage sensing circuit and a hydrogel coated pH-sensitive electrode pair. The electrode pair consists of a pH-sensitive electrode and a pH-insensitive reference electrode, with the hydrogel acting as the host electrolyte. The potential difference between the electrodes acts as a biasing voltage to the varactor. In the sensor shown in Fig. 5.1, L_S is the inductance of the spiral inductor, $C(V_{pH})$ is the capacitance of the voltage sensing circuit and V_{pH} is the potential difference across the electrodes. Acidic or basic volatiles produced in a closed environment are absorbed by the hydrogel and react with the water in the hydrogel to increase H^+ or OH^- concentration, respectively. As a result, the hydrogel pH changes which in turn changes the voltage, V_{pH}, across the pH-sensitive electrode pair. The capacitance, $C(V_{pH})$ changes in response to the variation of V_{pH}. The spiral inductor and capacitor form a resonant circuit with a resonant frequency, f_0, given by eqn. 2.1. An interrogator coil is inductively coupled to the sensor inductor and is used to track the resonant frequency of the sensor. In this manner, the measured resonant frequency is directly related to the acidic or basic volatiles absorbed by the hydrogel and indicates their concentration in the environment surrounding the sensor.

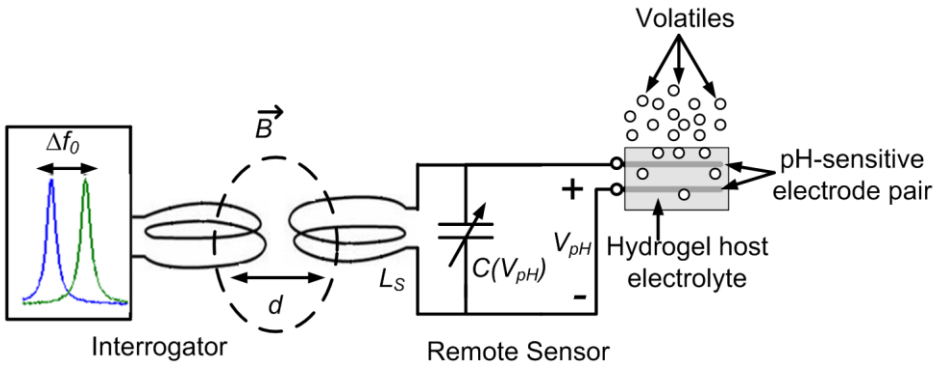

Figure 5.1. Conceptual block diagram of the near-field passive volatile sensor.

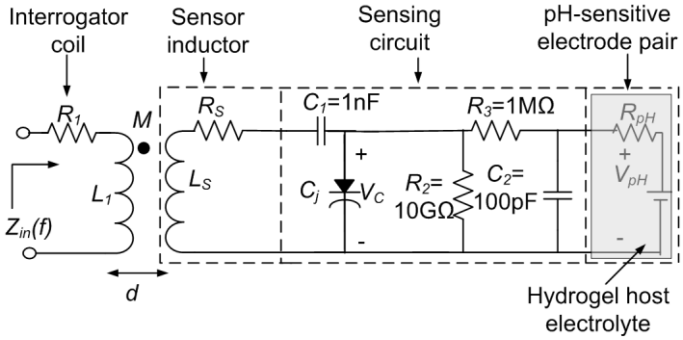

Figure 5.2. Equivalent circuit diagram of the passive sensor and near-field coupled interrogator (separated by a distance, d).

An equivalent circuit diagram of the fabricated near-field passive sensor is shown in Fig. 5.2. All the circuit components are described in section 2.3. The resonant frequency of the sensor was determined using the same method described in section 2.3 [16], [19].

5.4 Prototype Sensor

5.4.1 Hydrogel Coated pH-sensitive Electrode Pair

Mixed metal oxide (MMO) and silver/silver chloride (Ag/AgCl) electrodes were chosen as the pH-sensitive electrode and the pH-insensitive reference electrode, respectively. A MMO electrode was chosen because of its commercial availability, low cost, and pH sensitivity [20]. A MMO electrode manufactured by Titanium Electrode Products (TELPRO) Inc. was used in the

prototype. This consists of titanium wire (1.5 mm diameter) with a coating containing iridium oxide (IrO_2) and tantalum oxide (Ta_2O_5) applied to the wire surface by the manufacturer [21]. Both IrO_2 and Ta_2O_5 are pH-sensitive oxides which respond approximately linearly to changes in pH [22]. Since the MMO was supplied in wire form, it was cut into small (approximately 15 mm long) pieces for use as discrete electrodes. Approximately 3 mm of MMO coating was sanded off lengthwise to expose the bare titanium wire and was connected to an insulated wire using silver epoxy. To ensure that only the pH-sensitive area of the electrode is in contact with the host electrolyte non-conducting epoxy was applied over the connection area for electric insulation. Ag/AgCl was selected as the pH-insensitive reference electrode because of its wide use as a reference electrode in industry, simple construction and low manufacturing cost. The Ag/AgCl reference electrode was prepared according to the method described in section 4.4.1 [23].

The prototype printed circuit board (PCB) sensor, as shown in Fig. 5.3, was constructed using the MMO and Ag/AgCl electrodes. The volatile sensing cell was fabricated by placing the electrode pair on the surface of the PCB separated by 10 mm. The electrode pair was coated with a very thin layer (2.5 mm thick from the PCB surface) of amorphous hydrogel. The amorphous hydrogel (Intrasite gel from Smith and Nephew) is a clear gel containing a modified carboxymethyl cellulose polymer, propylene glycol and water. It has an initial pH of ~7.1. The series resistance of the MMO and Ag/AgCl reference electrode pair when coated with the amorphous hydrogel was found to be approximately 500 kΩ.

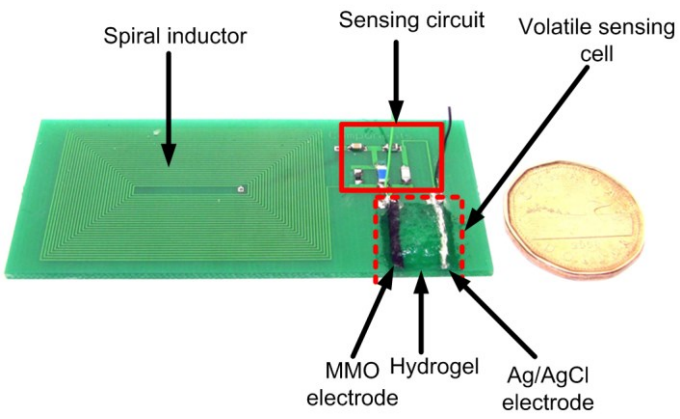

Figure 5.3. Prototype volatile absorption sensor with hydrogel coated MMO and Ag/AgCl electrodes. The prototype is fairly large and can be further miniaturized.

5.4.2 Prototype Sensor and Interrogator

The near-field sensor was fabricated on a 8 cm x 3.5 cm FR4 printed circuit board (PCB) with a 27 turn rectangular coil inductor, surface mount capacitors and resistors. It was designed to have a resonant frequency, f_0, near 6 MHz. The inductor trace width, spacing and thickness are 0.254 mm, 0.254 mm and 0. 15mm, respectively, producing L_S=20.33 µH and R_S= 9 Ω at 6 MHz. The junction capacitance of the varactor (NXP BB202) used in the voltage sensing circuit, C_j, varied in the range of 35.04 pF - 22.95 pF for reverse bias voltages between 0 and 1V, respectively. The Ag/AgCl and MMO electrodes were connected to the positive and negative terminals of the voltage sensing circuit, respectively. The interrogator coil was 5.1 cm in diameter and constructed of 5 turns of insulated copper wire of 1.2 mm diameter, producing L_I=2.35 µH, R_I=334.13 mΩ and a self-resonant frequency, f_{res}=28.32 MHz. The interrogator coil impedance was measured using an impedance analyzer (Agilent 4294A) with the voltage oscillation level of the analyzer set to 25 mV. Previous studies with this type of sensor showed that the sensor's resonant frequency changes linearly with the voltage across the electrode pair and linearly with pH [17], [24]. The sensitivity is 1.65 kHz/mV over -600 to 200 mV range [24].

5.5 Experiment and Results

5.5.1 Ammonia and Acetic Acid Vapor Detection

The absorption of ammonia or acetic acid vapor by the hydrogel and the change of the sensor's response were tested by placing the sensor in different concentrations of NH_3 or CH_3COOH vapor in a closed environment as shown in Fig. 5.4. For each concentration the test was divided into two phases. In phase (i) the sensor was placed in the closed environment with no volatile present and a fixed relative humidity. This was created by placing 40 ml DI water (contained in the small 50 ml beaker) in the closed 1 L beaker. In phase (ii) the sensor was placed in an environment with different concentrations of NH_3 or CH_3COOH vapor. Phase (i), approximately 20 minutes, was immediately followed by phase (ii). Different concentrations of NH_3 or CH_3COOH vapor were produced in the closed 1 L beaker by placing 40 ml ammonium hydroxide or acetic acid solution of known concentrations, respectively (contained in the small 50 ml beaker). The vapor was obtained via ordinary evaporation at room temperature (The mean laboratory temperature was 24.3 °C (σ=0.7 °C) throughout all experiments). In both phases the relative humidity was 100%. The concentrations of gaseous NH_3 or CH_3COOH were calculated using their initial concentration in 40 ml solution and their partial vapor pressure using Raoult's law. Raoult's law was applied here, since the concentration of the solute was not low and an ideal solution was assumed. Moreover, for fish spoilage application, the solute solvent behavior will follow Raoult's law.

Since the sensor is not fully reversible (will be discussed later), the electrodes were cleaned with DI water and coated with fresh hydrogel before beginning phase (i) of each test.

Fig. 5 shows the impedance frequency response of the sensor for different concentrations of NH_3 or CH_3COOH vapor.

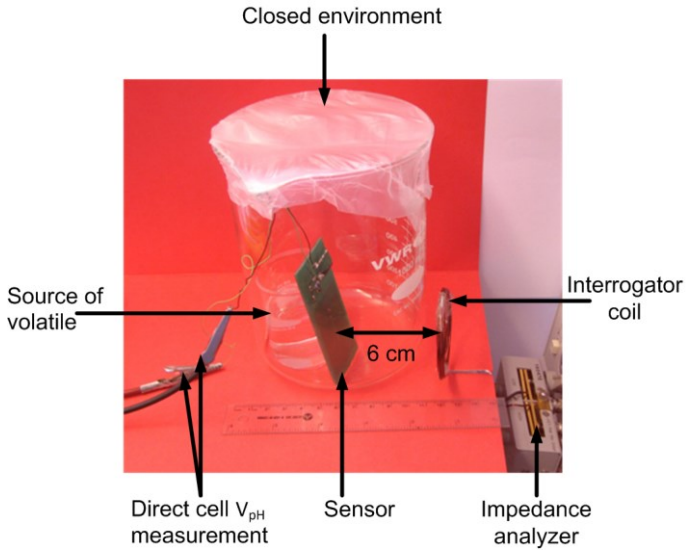

Figure 5.4. NH_3 or CH_3COOH vapor sensing test. A 50 ml beaker containing different ammonium hydroxide or acetic acid concentrations and the sensor is placed in a large sealed 1 L beaker. The sensor resonant frequency is measured using the interrogator coil connected to an impedance analyzer (not shown to the right). The pH electrode pair potential difference is also measured directly using a voltmeter (when the measurements were done, the sensor was aligned concentrically with the interrogator coil).

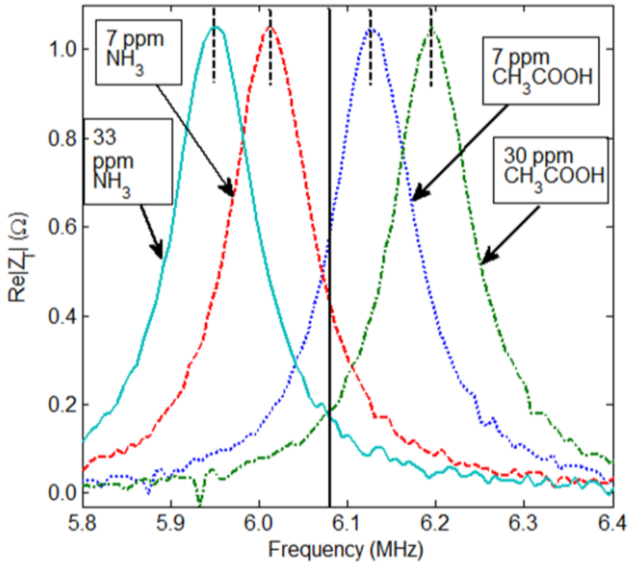

Figure 5.5. Impedance frequency response of the sensor for different concentrations of NH_3 or CH_3COOH vapor. The extracted resonant frequency is shown by the dashed line. The resonant frequency with no volatile (response not shown) was 6.082 MHz.

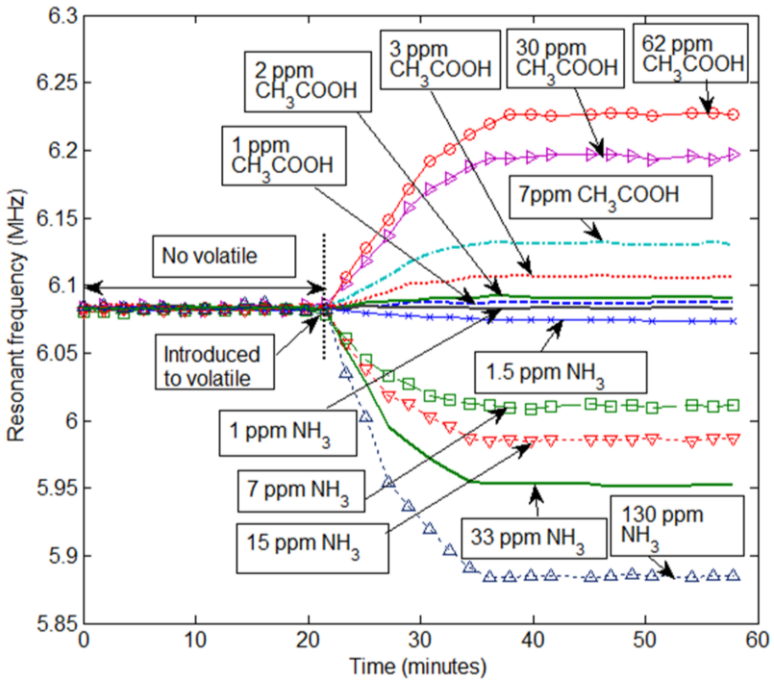

Figure 5.6. Resonant frequency of the sensor measured during both phases for different concentrations of NH_3 or CH_3COOH vapor. 40 ml of a prepared liquid concentration of the volatile is placed in the chamber at the dashed line.

The resonant frequency of the sensor (as obtained from the peak of the quadratic fit to the frequency response - shown in Fig. 5.5 for several concentration examples) was measured as a function of time during both phases for each concentration of NH_3 or CH_3COOH vapor and is shown in Fig. 5.6. It can be seen that when the sensor was introduced to the NH_3 or CH_3COOH vapors, the resonant frequency decreased or increased, respectively. Eventually the resonant frequency stabilized at an equilibrium value related to the concentration. It took approximately 20 minutes for the sensor to reach an equilibrium value after being introduced to the gas. For each concentration of NH_3 or CH_3COOH, the tests were performed three times and results are shown in Fig. 5.7. Each data point consists of an average of 10 resonant frequency measurements, taken at 2 minutes intervals after the sensor reaches its equilibrium state (20 minutes after exposure). The maximum deviation for all 3 tests (30 measurements) for any concentration was 6.1 kHz for NH_3 and 6.6 kHz for CH_3COOH. This corresponds to a sensitivity of 1.5 ppm for NH_3 and 2 ppm for CH_3COOH. From the detection limit to higher concentrations the resonant frequency exhibits a linear relationship with the logarithm of concentration.

The proposed wireless sensor has an NH_3 volatile sensitivity and response time similar to the wired PANI-based sensors (0.25 ppm-10 ppm, 1-5 min.) [25, 26], as well as the wired metal-oxide sensors (10 ppm, 3 min.) [27]. A wireless PANI-based NH_3 sensor was recently reported to have a lower detection limit (20-80 ppb) [1], [28]. Most polymer based sensors work by conductivity/permittivity changes of the polymer film and may be sensitive to water vapor concentration [15]. The proposed sensor requires the relative humidity to be above a threshold, but is not sensitive to high water vapor concentration (explained latter). The sensor has a very linear response with the logarithm of volatile concentration providing a way for direct quantitative measurement.

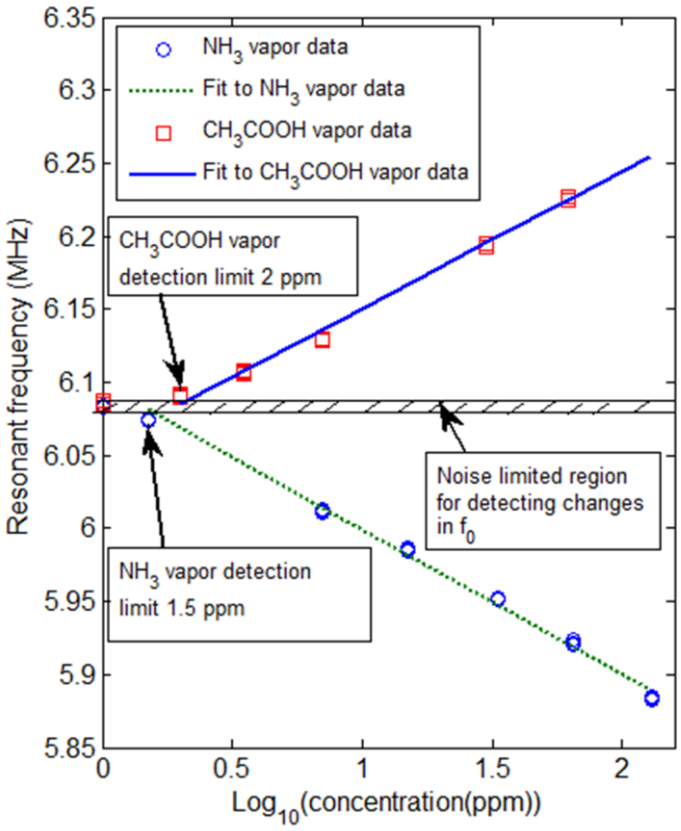

Figure 5.7. Resonant frequency after the sensor has reached an equilibrium state in the closed environment as a function of NH_3 or CH_3COOH vapor concentration (20 mins. after the initial exposure). For each concentration 3 tests are shown (individual markers), each consisting of an average of 10 measurements at 2 mins. intervals.

5.5.2 Effect of Relative Humidity

Under low relative humidity conditions the hydrogel dehydrates and it does not behave as an electrolyte for the pH-sensitive electrode pair [29]. The relative humidity range for which the sensor operates properly was determined using the gas flow management and sensor evaluation system shown in Fig. 5.8. The system can control the flow rate of dry nitrogen (N_2) gas and relative humidity (RH) using mass flow controllers and solenoid valves for delivering dry N_2 and water vapor to a Teflon gas mixing chamber and then to the sensor-testing chamber [29]. The resonant frequency was monitored every hour and the relative humidity level was decreased

every 4 hours. Fig. 5.9 shows the resonant frequency monitored for different relative humidity levels. When the relative humidity fell below 40% the sensor measurement deviated due to dehydration. For RH ≥45%, the sensor performed without any dependence on the relative humidity.

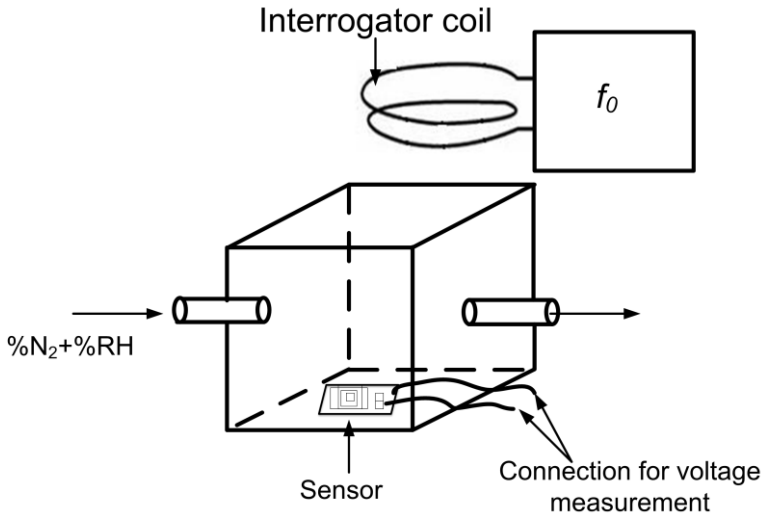

Figure 5.8. Block diagram of the gas flow management and sensor evaluation system used for testing the effect of relative humidity on sensor's performance.

5.5.3 Effect of Temperature

The electrode potential in an electrolyte is dependent on temperature [30]. The influence of temperature on the performance of the sensor was evaluated by exposing the hydrogel coated electrode pair to different concentrations of NH_3 at 4°C and 24°C. Since the temperature dependence of the voltage sensing LC resonator circuit is minimal, only the response of the hydrogel coated electrode pair, V_{pH}, was tested (V_{pH} was measured directly by the wired connection in Fig. 4). The test for each concentration of NH_3 was performed in two phases using

the method described in section 5.5.1 and results are shown in Fig. 5.10. The temperature of the gas inside the closed environment was monitored using a thermistor (Honeywell 112-105PAJ-B01). Each data point (marker) consists of an average of 10 voltage measurements, taken at 2 minutes intervals after the hydrogel coated electrode pair reaches its equilibrium state. It took 20 and 60 minutes for the hydrogel coated electrode pair to reach equilibrium value after being introduced to NH_3 at 24°C and 4°C, respectively. For the no acidic or basic volatile condition, V_{pH} changed from -89 mV at 24°C to -103 mV at 4°C. The slope of the response curve and the V_{pH} value for no acidic and basic volatile decreases with decrease of temperature. This is due to temperature sensitivity of the pH-sensitive electrode pair and the effect of temperature on the mobility of ions inside the hydrogel [30]. The temperature dependence of gas diffusion coefficient increases the sensor response time with decrease of temperature [31].

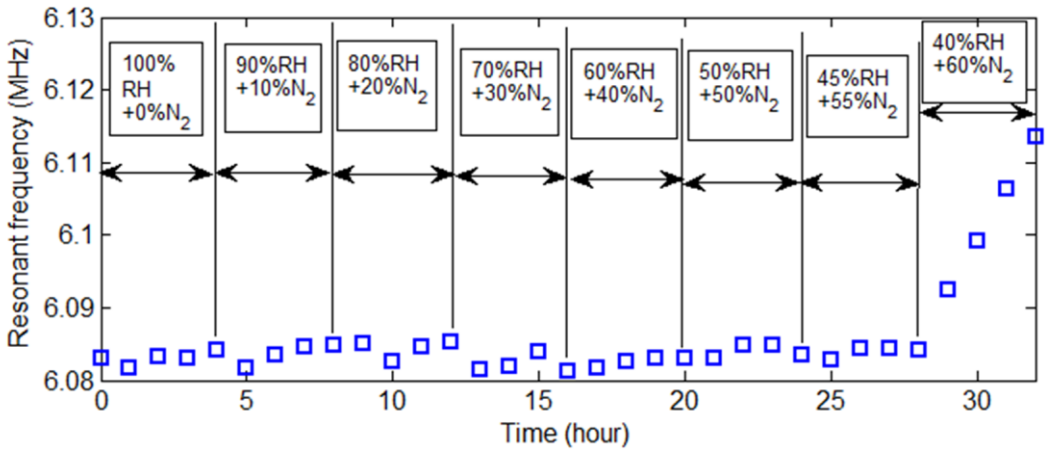

Figure 5.9. Resonant frequency of the sensor measured for different relative humidity levels (no acidic or basic volatile present).

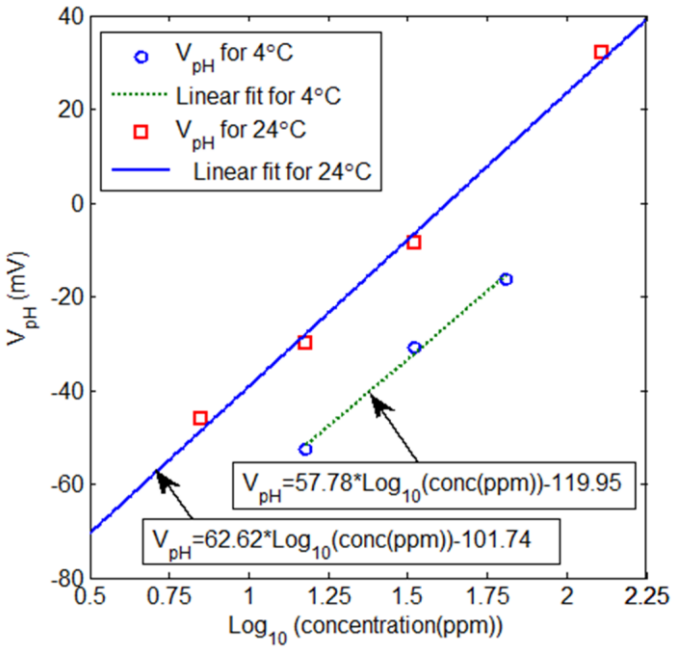

Figure 5.10. Hydrogel coated pH-electrode pair cell potential difference for two temperatures after the cell has reached an equilibrium state in a closed environment (Fig. 5.4) as a function of NH_3 vapor concentration.

5.5.4 Effect of Hydrogel Coating Geometry

The geometry of the hydrogel coating on the electrode pair affects the diffusion time of acidic and basic volatiles in the hydrogel which in turn changes the response time of the sensor. Fig. 5.11 shows a diagram of the hydrogel coated electrode pair used in our prototype cell. When the sensor is exposed to acidic or basic volatiles, the top surface of the hydrogel coating, S, absorbs the permeating volatiles and the volatiles diffuse into the hydrogel [32]. The diffusion time as well as the response time of the sensor increases with thickness, t, of the hydrogel coating. To investigate the variation of response time, two different thickness of the hydrogel coating, were tested for 33 ppm NH_3 vapor concentration. The test for each sensor was done in two phases using the method described in section 5.5.1. The results are shown in Fig. 5.12. The sensors reached an equilibrium value after 20 and 85 minutes after being introduced to the

volatile for hydrogel thickness of 2.5 mm and 5 mm, respectively. Note that the thickness did not affect the final equilibrium value (5.9526 MHz) in both cases.

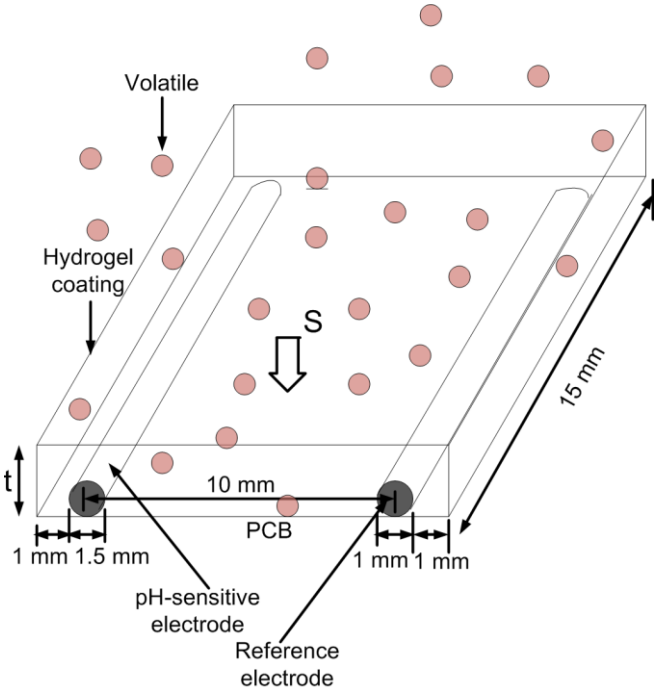

Figure 5.11. Schematic of the hydrogel coated pH-sensitive electrode pair.

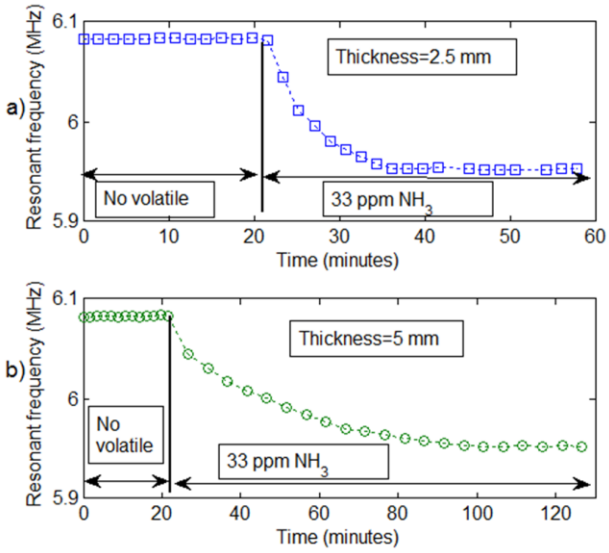

Figure 5.12. Resonant frequency of the sensor measured for two different thickness of hydrogel electrolyte coating; (a) 2.5 mm and (b) 5 mm. The final equilibrium value is the same for both cells.

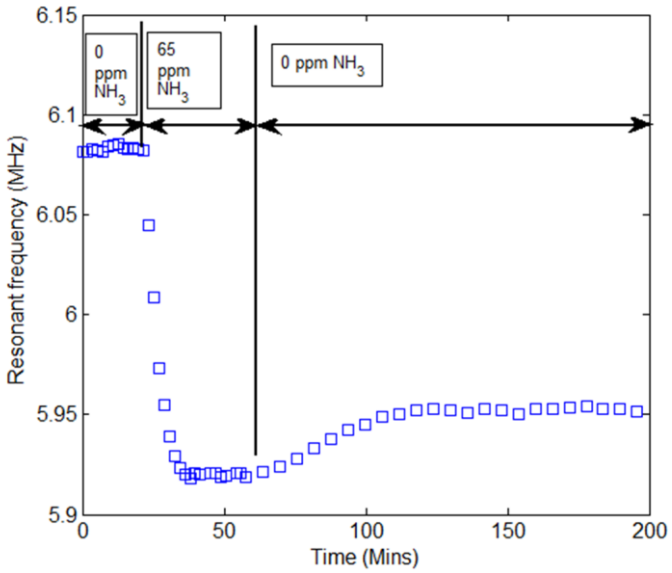

Figure 5.13. Resonant frequency measured during three phases of a reversibility test, where the sensor was successively placed in a chamber with a source producing 0 ppm, 65 ppm and 0 ppm NH_3 concentration.

5.5.5 Reversibility

An An experiment consisting of three phases was conducted to test the reversibility of the sensor. In phases (i), (ii) and (iii) the sensor was exposed to 0 ppm, 65 ppm and then 0 ppm ammonia in a closed 1 L beaker, respectively. The gas concentrations in the 1 L beaker were produced using the method stated in section 5.5.1. The resonant frequencies measured during these three phases are shown in Fig. 5.13. The sensor response during phase (i) and phase (ii) follows the expected trend (see Fig. 5.6), reaching equilibrium in approximately 20 min after introduction of NH_3. When the sensor was exposed to 0 ppm NH_3 in phase (iii), the resonant frequency increased. However, it stabilized at an equilibrium value lower than the original starting value for 0 ppm NH_3 in phase (i). This indicates that the sensor is not fully reversible in this set up (the sensor is placed in an closed chamber with no volatile source after being exposed to acidic/basic volatiles). It is possible that during phase (iii) even though the gaseous NH_3

source was removed from the chamber, the absorbed NH_3 in the hydrogel could diffuse back into the beaker eventually, reaching a new equilibrium, but not the starting 0 ppm value. However, if the sensor is placed in a continuous flow of gas with no acidic/basic volatile, eventually all the NH_3 absorbed in hydrogel will diffuse out and set the sensor reading indicating 0 ppm value.

5.5.6 Long Term Stability

If the sensor resonant frequency drifts over time this will cause error in the volatile concentration measurement, which cannot be eliminated by calibration. A seven day long test was performed to determine the stability of the sensor with time. The sensor was placed in a closed environment with no volatile and 100% relative humidity for 168 hours. The environment was created by placing 40 ml DI water (contained in a 50 ml beaker) in the closed 1 L beaker. After 168 hours the sensor was introduced to the environment with 33 ppm NH_3 and monitored for 10 more hours. Fig. 5.14 shows the resonant frequency of the sensor monitored during the 7 days. The value of resonant frequency for no volatile condition was almost constant, centered at 6.0834 MHz, with a maximum deviation of less than ±3 kHz over 7 days. This deviation falls within the noise limited region (<1.5 ppm) indicated in Fig. 5.7. After 7 days, when the sensor was introduced to 33 ppm NH_3, the sensor's resonant frequency decreased and reached an equilibrium value of 5.9516 MHz within approximately 20 minutes. This is the same value as that measured for 33 ppm NH_3 in Fig. 5.6. This indicates that if the sensor is kept at a relative humidity ≥45%, the sensor performs with high stability, making it suitable for long-term continuous measurement.

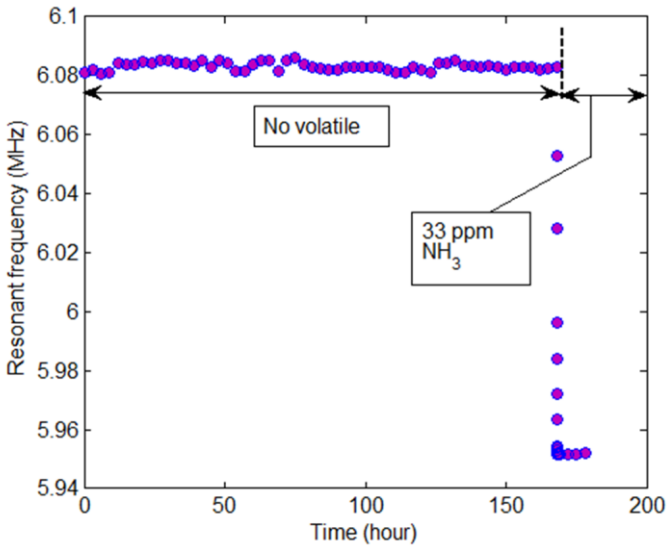

Figure 5.14. Resonant frequency of the volatile sensor showing its stability over 7 days. The sensor was placed in a closed chamber (RH=100%) with no volatile for 168 hours and then introduced to 33 ppm NH_3 concentration. The 33 ppm frequency was 5.9516 MHz.

5.5.7 Interrogator Location and Orientation

Measurement with LC resonator based sensors may be affected by sensor position and orientation with respect to the interrogator coil. The effects of distance, side-to-side orientation and angular orientation have been investigated in [33]-[35]. A large mutual coupling coefficient can affect the resonant frequency and a minimum sensor-interrogator distance should be maintained for weak coupling. On the other hand signal-to-noise ratio decreases with increasing distance between the sensor and interrogator coil, and leads to error in determining the resonant frequency. A detection zone can be defined over which the LC sensor can be monitored within an error tolerance. The detection zone can be increased with interrogator coil power, sensor and interrogator coil size and number of turns [33], [34]. Previous studies employing the sensor described in this paper showed that when the sensor is aligned concentrically with the

interrogator coil, distances in the range of 5 cm to 11 cm achieved a frequency measurement error less than 0.015% (0.9 kHz at f_0=5.9772 MHz) [24].

5.6 Conclusion

This paper presented an inductively coupled wireless passive sensor capable of detecting acidic and basic volatiles in its surrounding. The sensor is based on an LC resonator and hydrogel coated pH-sensitive electrode pair with volatile concentration monitored by measuring the change of sensor's resonant frequency. Tests with NH_3 and CH_3COOH vapor demonstrated the expected Nernstian linear relationship of resonant frequency-to-logarithm of concentration behavior and a detection limit of 1.5 ppm for NH_3 and 2 ppm for CH_3COOH vapor. The response time for the prototype sensor was 20 minutes at 24ºC. This can be improved by miniaturizing the sensing cell geometry. The sensitivity is adequate for many applications, i.e., the maximum NH_3 level for human work environment is 20 ppm [9] and 30 ppm total volatile basic nitrogen (TVBN) is related to the spoilage threshold level in fish condition monitoring [36].

Temperature and relative humidity should be considered when using this sensor. Temperature affects the sensitivity of the pH-sensitive electrode, the mobility of ions inside the hydrogel and the diffusion coefficient of the volatiles. Temperature monitoring/compensation techniques can be incorporated into this sensor using passive components [30]. The sensor requires a relative humidity of 45% or higher to maintain the electrolyte in the hydrogel for proper operation. This limitation could be alleviated by using an encapsulation membrane or an alternate host electrolyte. Since the sensor is based on hydrogel pH change, it responds to all acidic and basic volatiles present in its surrounding environment. Although it was not demonstrated in this paper, a selective gas permeable membrane can be applied on the top of the

hydrogel allowing only a particular gas to pass through the membrane and diffuse through the hydrogel [29]. This pH-electrode based sensor is not reversible. This however, makes it suitable for many detection applications, such as in food spoilage monitoring. The current sensor operates in a near-field coupling regime with interrogation distances on the order of 10 cm. For applications requiring larger read ranges a RF chipless approach can be used [37]. The sensor does not require a custom IC (typical of other passive RFID sensors) which makes it amenable to simple printed electronics techniques and a low cost production. Thus, it has the potential for applications where inexpensive acidic or basic volatile detection techniques are required such as in food packaging.

In the next chapter this volatile sensor will be applied for fish spoilage monitoring. Fish is a widely consumed food worldwide and there is a great interest among the food industries, retailers, consumers and their stakeholders to develop methods for detecting fish spoilage in real-time.

References

[1] R. A. Potyrailo, C. Surman, S. Go, Y. Lee, T. Sivavec and W. G. Morris, "Development of radio-frequency identification sensors based on organic electronic sensing materials for selective detection of toxic vapors," *Journal of Applied Physics*, vol. 106, no. 12, pp. 124902 (6 pages), Dec. 2009.

[2] B. Kuswandi, Jayus, A. Restyana, A. Abdullah, L. Y. Heng and M. Ahmad, "A novel colorimetric food package label for fish spoilage based on polyaniline film," *Food Control*, vol. 25, no. 1, pp. 184-189, May 2012.

[3] J. Tétreault, "Measuring acidity of volatile products," *Journal of IIC-CG*, vol. 17, pp. 17-25, 1992.

[4] C. Elosua, I. R. Matias, C. Bariain, F. J. Arregui, "Detection of volatile organic compounds based on optical fibre using nanostructured films," *International Journal on Smart Sensing and Intelligent Systems*, vol. 1, no. 1, pp. 123-136, Mar. 2008.

[5] A. R. Strom, J. A. Olafsen, K. H. Refsnes and H. Larsen, "Anaerobic fish spoilage by bacteria II. Kinetics of bacterial growth and substrate conversions in herring extracts," *Journal of Applied Bacteriology*, vol. 46, pp. 545-551, 1979.

[6] R. A. Potyrailo, N. Nagraj, Z. Tang, F. J. Modello, C. Surman and W. Morris, "Battery-free radio frequency identification (RFID) sensors for food quality and safety," *Journal of Agricultaural and Food Chemistry*, vol. 60, pp. 8535-8543.

[7] W. D. Huang, S. Deb, Y. S. Seo, S. Rao, M. Chiao and J. C. Chiao, "A passive radio-frequency pH-sensing tag for wireless food-quality monitoring," *IEEE Sensors J.*, vol. 12, no. 3, Mar. 2012.

[8] R. A. Potyrailo, S. P. Golubkov, P. S. Borsuk and P. M. Talanchuk, “pH indicator based ammonia gas sensor: studies of spectral performance under variable conditions of temperature and humidity,” *Analyst*, vol. 119, pp. 443-448, Mar. 1994.

[9] B. Timmer, W. Olthuis and A. V. D. Berg, “Ammonia sensors and their applications—a review,” *Sensors and Actuators B: Chemical*, vol. 107, no. 2, pp. 666-677, Mar. 2005.

[10] J. Gong, Q. Chen, M.-R. Lian, N.-C. Liu, R.G. Stevenson and F. Adami, “Macromachined nanocrytalline silver doped SnO_2 H_2S sensor,” *Sensors and Actuators B: Chemical*, vol. 114, no. 1, pp. 32-39, Mar. 2006.

[11] H. Bai and G. Shi, “Gas sensors based on conducting polymers,” *Sensors*, vol. 7, no. 3, pp. 267-307, Mar. 2007.

[12] J. T. English, B. A. Deore and M. S. Freund, “ Biogenic amine vapour detection using poly(anilineboronic acid) films,” *Sensors and Actuators B: Chemical*, vol. 115, no. 2, pp. 666-671, June 2006.

[13] Z. Jin, Y. Su and Y. Duan, “Development of a polyaniline-based optical ammonia sensor,” *Sensors and Actuators B: Chemical*, vol. 72, no. 1, pp. 75-79, Jan. 2001.

[14] K. Wetchakuna, T. Samerjaia, N. Tamaekonga, C. Liewhirana, C. Siriwonga, V. Kruefua, A. Wisitsoraatb, A. Tuantranontb and S. Phanichphanta, “Semiconducting metal oxides as sensors for environmentally hazardous gases,” *Sensors and Actuators B: Chemical*, vol. 160, no. 1, pp. 580-591, Dec. 2011.

[15] R. A. Potyrailo, C. Surman, N. Nagraj and A. Burns, “Materials and transducers toward selective wireless gas sensing,” *Chemical Review*, vol. 111, no. 11, pp. 7315-7354, Nov. 2011.

[16] J. B. E. Horton, S. Schweitzer, A. J. DeRouin and K. G. Ong, “A varactor-based inductively coupled wireless pH sensor,” *IEEE Sensors J.*, vol. 11, no. 4, pp. 1061-1066, April 2011.

[17] S. Bhadra, G. E. Bridges, D. J. Thomson and M. S. Freund, “Electrode potential based coupled coil sensor for remote pH monitoring,” *IEEE Sensors Journal*, vol. 11, no. 11, pp. 2813- 2819, Nov. 2011.

[18] S. Bhadra, G. E. Bridges and D. J. Thomson, “A wireless embedded passive sensor for monitoring the corrosion potential of reinforcing steel,” *Smart Materials and Structures*, vol. 22, no. 7, 075019 (10pp), July 2013.

[19] M. P. Robinson and J. Clegg, “Improved determination of Q-factor and resonant frequency by a quadratic curve fitting method,” *IEEE Transaction on Electromagnetic Compatibility*, vol. 47, no. 2, pp. 399-402, May 2005.

[20] G. S. Duffó, S. B. Farina, C. M. Giordano, "Characterization of solid embeddable reference electrodes for corrosion monitoring in reinforced concrete structures," *Electrochimica Acta*, vol. 54, no. 3, pp. 1010-1020, Jan. 2009.

[21] M. Biagioli and C. Johannessen, "MMO Coatings," internet: http://www.telprocompanies.com/mmo.html, [Oct. 7, 2012].

[22] A. Fog and R. Buck, "Electronic semiconducting oxides as pH sensors," *Sensors and Actuators*, vol. 5, no. 2, pp. 137-146, Feb. 1984.

[23] M. A. Nolan, S. H. Tan and S. P. Kounaves, “Fabrication and characterization of a solid state reference electrode for electroanalysis of natural waters with ultramicroelectrodes,” *Anal. Chem.*, vol. 69, pp. 1244-1247, Mar. 1997.

[24] S. Bhadra, M. McDonald, D. J. Thomson, M. S. Freund and G. E. Bridges, “An inductively coupled passive tag for remote basic volatile sensing,” in *Proc. IEEE RFID, 2014*, pp. 147-152.

[25] Z. Wu, X. Chen, S. Zhu, Z. Zhou, Y. Yao, W. Quan and B. Liu, “Enhanced sensitivity of ammonia sensor using graphene/polyaniline nanocomposite,” *Sensors and Actuators B: Chemical*, vol. 178, pp. 485-493, Mar. 2013.

[26] B. Kuswandi, Jayus, A. Restyana, A. Abdullah, L. Y. Heng, M. Ahmad, “A novel colorimetric food package label for fish spoilage based on polyaniline film,” *Food Control*, vol. 25, no. 1, pp. 184-189, May 2012.

[27] I. M. Szilagyi, L. Wang, P. I. Gouma, C. Balazsi, J. Madarasz and G. Pokol, “Preparation of hexagonal WO_3 from hexagonal ammonium tungsten bronze for sensing NH_3,” *Mater. Res. Bull.,* vol. 44, no. 3, pp. 505–508, Mar. 2009.

[28] R. A. Potyrailo, N. Nagraj, Z. Tang, F. J. Mondello, C. Surman and W. Morris, “Battery-free radio frequency identification (RFID) sensors for food quality and safety,” J Agric Food Chem., vol. 60, no. 35, pp. 8535-8543, Aug. 2012.

[29] S. Neethirajan, M.S. Freund, D.S. Jayas, C. Shafai, D.J. Thomson and N.D.G. White, “Development of carbon dioxide (CO_2) sensor for grain quality monitoring,” *Biosystems Engineering*, vol. 106, no. 4, pp. 395-404, Aug. 2010.

[30] S. Bhadra, D. S. Y. Tan, D. J. Thomson, M. S. Freund and G. E. Bridges, "A wireless passive sensor for temperature compensated remote pH monitoring," *IEEE Sensors Journal,* vol.13, no.6, pp. 2428-2436, June 2013.

[31] Crank, J. Methods of measurement. In *Diffusion in Polymers*; J. Crank and G. S. Park, Eds.; Academic Press: New York, 1968; pp 1-39.

[32] S. C. George and S. Thomas, "Transport phenomena through polymeric systems," *Progress in Polymer Science,* vol. 26, no. 6, pp. 985-1017, Aug. 2001.

[33] J. C. Butler, A. J. Vigliotti, F. W. Verdi and S. M. Walsh, "Wireless, passive, resonant-circuit, inductively coupled, inductive strain sensor," *Sensors and Actuators A: Physical*, Vol. 102, no. 1–2, pp. 61-66, Dec. 2002.

[34] K. G. Ong, C. A. Grimes, C. L. Robbins and R. S. Singh, "Design and application of a wireless, passive, resonant-circuit environmental monitoring sensor," *Sensors and Actuators A: Physical*, Vol. 93, no. 1, pp. 33-43, Aug. 2001.

[35] R. A. Potyrailo, H. Mouquin and W. G. Morris, "Position-independent chemical quatitation with passive 13.56-MHz radio frequency identification," *Talanta*, vol. 75, no. 3, pp. 624-628, May2008.

[36] R. S. Singhal, P. R. Kulkarni and D. V. Rege, Handbook of Indices of Food Quality. Cambridge, England: Woodhead Publishing Limited, 1997.

[37] S. Preradovic, S. M. Roy and N. C. Karmakar, "RFID system based on fully printable chipless tag for paper-/plastic-item tagging," IEEE Antennas and Propagation Magazine, vol. 53, no. 5, pp. 15-32, Oct. 2011.

Chapter 6: Non-destructive Detection of Fish Spoilage Using a Wireless Basic Volatile Sensor

6.1 Abstract

A hydrogel-pH-electrode based near-field passive volatile sensor is described for real-time monitoring of fish spoilage. The sensor employs a varactor based LC resonator that can be interrogated remotely using inductive coupling. The sensor's resonant frequency varies in response to the basic volatile spoilage compounds (total volatile basic nitrogen, TVB-N) in the headspace of packaged fish. The sensor is shown to have a linear response to logarithm of the ammonia gas concentration with a detection limit of 0.001 mg L^{-1} (1.5 ppm). Trials on tilapia at 24ºC and 4ºC, employing direct comparison of sensor measurements with microbial analysis, indicate that the sensor response is correlated with the bacterial growth pattern in fish samples. It is shown that the sensor can distinctly identify when the product rejection level (10^7 cfu g^{-1} bacterial population) occurs for both 24ºC and 4ºC storage conditions. This demonstrates a potential for real-time monitoring of fish spoilage. The wireless sensor is suited to embedding in packaging material and does not require an integrated circuit, making it amenable to inexpensive mass production using printed electronic technology.

6.2 Introduction

Food spoilage is an important topic to both the consumer and food processing industry. It is not only a human health concern but also a major economic issue due to food wastage [1], [2]. As the present global economy has led to increased distance between the consumer and production zone, and subsequently a complex supply chain, new methods for monitoring food

quality is needed [3], [4]. Fish is a widely consumed food worldwide and there is a great interest among the food industries, retailers, consumers and their stakeholders to develop methods for evaluating fish freshness in real-time [5]. Various approaches have been used to determine fish freshness. In the fish industry, specialized trained assessors evaluate freshness attributes, such as, appearance, colour, smell and texture. A certain grading scheme is then used by compiling these qualities to produce a quality index [6]. This procedure is labor intensive and unreliable. As microbe growth is the main cause of fish quality degradation, total viable count (TVC) is considered as a definitive index for fish spoilage monitoring. After death, the number of microorganisms on the skin and gill surfaces increases gradually and spreads within various tissues. These microorganisms are known as spoilage organisms and are usually *Pseudomonas spp* [5]-[8]. As the fish deteriorates due to the microorganisms, volatile compounds such as $(CH_3)_3N$ (trimethylamine or TMA), $(CH_3)_2NH$ (dimethylamine or DMA) and NH_3 (ammonia) are produced. These products are collectively known as TVB-N. Therefore, TVB-N levels are an indicator of fish freshness. Headspace methods are among the most reliable methods for volatile compound analysis. They consist of collection and concentration of the volatiles for subsequent chromatographic separation to identify and qualify the separated compounds [5], [6], [9]-[11]. Olafsdottir et al. provided a review of these methods in [6]. Unfortunately, these methods are time-consuming, and require trained personnel and laboratory equipment. They generally involve invasively breaching the package and therefore rendering the individual product useless. Further, this selective sampling does not offer any guarantee that the rest of the batch is fresh [6], [11].

An array of metal oxide semiconductor (MOS) sensors have been used for detecting volatile compounds produced during spoilage of silver cup, salmon, haddock, cod, red fish etc [12-14]. MOS sensors are cheap, have high longevity and electronic simplicity. However, they

require high temperature (200-500°C) and substantial power to operate, and have limited selectivity [2], [13]. Non-destructive tests such as fluorescence spectroscopy and nuclear imaging have also been used for determining fish freshness. The fish muscle exhibits intrinsic fluorescence and the intensity of this fluorescence decreases with storage time on ice [4]. Spectroscopic methods have so far not proven sufficient to fully characterize the properties of fresh fish [6]. Nuclear imaging, a mature diagnosis method for analyzing organ and texture, has been applied to inspect dynamic changes of carp muscle to evaluate the fish freshness [15]. However, nuclear imaging is a costly technique [6]. As the pH of the fish changes during the spoilage process, a custom radio-frequency-identification (RFID) based pH sensor has been demonstrated for fish spoilage monitoring [2]. The sensor employs a pH-sensitive electrode pair which needs to be in contact with the fish, thus posing a risk of electrode fouling and food contamination. Monitoring ambient temperature during transportation and storage is an indirect method of promoting fish quality. However, this approach does not directly monitor the fish product and quality cannot be ensured. pH-sensitive dye and polyaniline (PANI) based colorimetric sensors have been demonstrated as a method to monitor the spoilage of Cod, Cardinal, Roundnose grenadier and Milk fish [6], [11]. These sensors change color in response to the TVB-N level in the headspace of the packaged fish. They are non-destructive, low cost and do not require contact with the fish sample, however, they require visual inspection and are not easily translated to qualitative values. Therefore, there is a pressing demand to develop an electronic based real-time fish spoilage monitoring device that is non-destructive, accurate, simple, low-cost, reliable and does not require contact with the fish.

In this paper we present the use of a hydrogel coated pH-electrode based near-field passive sensor for determining fish spoilage. In previous work we reported a near field passive

sensor for detecting basic volatile concentration [16]. It employs a varactor based passive LC resonator whose resonant frequency depends on the basic volatile concentration in its surrounding environment. During spoilage total volatile basic nitrogen (TVB-N) are produced gradually in the fish package and change in sensor's resonant frequency occurs. The sensor's resonant frequency is detected by measuring the impedance of an external interrogator coil that is inductively coupled to the sensor. We present experimental results of prototype sensors monitoring the spoilage of tilapia fish at 24ºC and 4ºC. Direct comparison is made with microbial analysis. The design of the sensor is simple and suited for inexpensive mass production using printed electronic technology [17]. As this sensor is wireless, passive and does not require any contact with the fish sample, it can be a low cost, non-destructive, consumer friendly and reliable alternative for fish spoilage monitoring in individual packages.

6.3 Experiment

6.3.1 Sensor Fabrication

6.3.1.1 Hydrogel-pH-electrode pair

The electrodes and hydrogel coating were prepared using the method described in [16]. Mixed metal oxide (MMO) and silver/silver chloride (Ag/AgCl) were chosen as the pH-sensitive electrode and the pH-insensitive reference electrode, respectively. A MMO electrode was chosen because of its commercial availability, low cost, and pH sensitivity [18]. The Ag/AgCl electrode was coated with immobilized electrolyte solution and protective Nafion layer. Ag/AgCl was selected as the pH-insensitive reference electrode because of its wide use as a reference electrode in industrial applications, simple construction and inexpensive manufacturing cost. A thin layer (2.5 mm thick) of hydrogel coating is placed on top of the electrodes and acts to contain the

electrolyte. The amorphous hydrogel (Intrasite gel from Smith and Nephew) is a clear gel containing a modified carboxymethyl cellulose polymer, propylene glycol and water. It has an initial pH of ~7.1.

6.3.1.2 Prototype Sensor and Interrogator

The sensor and the interrogator coil were constructed according to section 5.4.2.

6.3.2 Sensor Response to Ammonia

The absorption of ammonia into the hydrogel and subsequent response of the sensor were evaluated by placing the sensor in a closed environment with different concentrations of NH_3. The test for each concentration was divided into two phases. In phase (i) the sensor was placed in a closed environment for 20 minutes with no volatile present. In phase (ii) a particular concentration of NH_3 was introduced in the environment. The two phase test method was discussed in detail in section 5.5.1. The mean laboratory temperature, was 24.3 °C (σ=0.7 °C) throughout all experiments. In both phases the relative humidity was 100%. Since the sensor is not fully reversible [19], the electrodes were cleaned with DI water and coated with fresh hydrogel before beginning phase (i) of each test. The sensor inductor was aligned concentrically with the interrogator coil at a distance of 10 cm.

6.3.3 Fish Spoilage Trials

6.3.3.1 Wireless Tilapia Spoilage Test at 24°C

Two fresh Tilapia fish fillets were supplied by local fish retailer (Gimli fish supplier, Winnipeg) and transported to the lab in a sealed ice container. Aseptic techniques such as disposable gloves, autoclaved cutting board, autoclaved and flame sterilized scalpel, forceps were used to avoid sample contamination. One tissue sample of 25 g was removed from the

fillets and placed in a 500 ml sterilized polycarbonate jar. A prototype wireless sensor (prepared according to section 6.3.1) with fresh hydrogel coating was placed inside the jar. The jar was sealed with a polypropylene screw lid. The jar was kept at room temperature (24°C) throughout the experiment. The sensor's resonant frequency was monitored wirelessly every 3 hours for 33 hours with the interrogator coil and impedance analyzer. The sensor inductor was aligned concentrically with the interrogator coil at a distance of 10 cm. Fig. 6.1 shows the experimental set up.

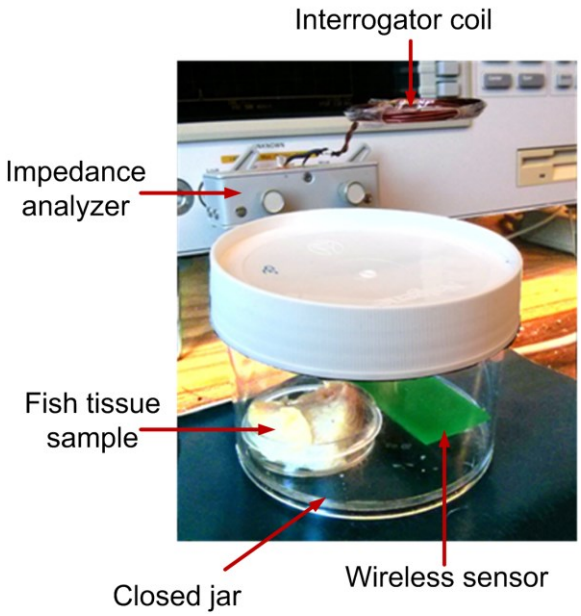

Figure 6.1. Experimental set up for wireless Tilapia spoilage test at 24°C. A 25 g tissue sample of fish and the wireless sensor are placed in a 500 ml polycarbonate jar. The sensor's resonant frequency is measured using the interrogator coil connected to an impedance analyzer.

6.3.3.2 Microbial Analysis of Tilapia Samples at 24°C

Simultaneously to the wireless spoilage trial, 12 samples of 25 g of fish tissue were removed from the same Tilapia fillets, under the same aseptic conditions and placed in 12 polycarbonate jars. A fresh hydrogel coated pH-sensitive electrode pair was placed in each of

these jars. The jars were sealed with polypropylene screw lids. Fig. 6.2 shows some of these jars. In this test direct measurement of the electrode potential, V_{pH}, was performed using wired connections to the hydrogel coated electrode pairs though the lids of the jars. As in the wireless test these samples were allowed to spoil at room temperature (24°C). Every 3 hours one jar was selected at random and the fish sample was taken out for microbial analysis with the first one done at zero hour to determine the initial microbial loads. Before the jar was opened for microbial analysis, voltages across all the hydrogel coated pH-sensitive electrode pairs were monitored. The electrode pair in the opened jar was discarded. For microbial analysis, total viable count (TVC) and *Pseudomonas* count were determined using a spread plate method on plate count agar (Oxoid CM0463) and agar base (Oxoid CM0559) with CFC selective supplement (Oxoid SR0103), respectively. Plates were counted after 48 hour incubation at 30°C. Bacterial population was correlated with wireless sensor measurements and voltages, V_{pH}, across the hydrogel coated electrode-pairs.

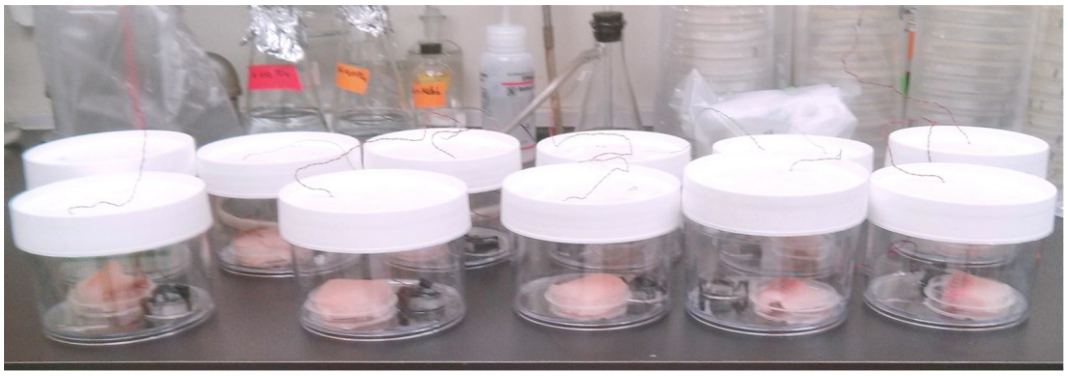

Figure 6.2. Samples of Tilapia tissue kept at 24°C for microbial analysis. Each jar contains a 25 g tissue sample of fish and a hydrogel coated pH-sensitive electrode pair with wired connection to a voltmeter.

6.3.3.3 Wireless Tilapia Spoilage Test at 4°C

The experimental procedure used for the fish spoilage test at 4°C was similar to the one at 24°C (section 6.3.3.1). Two tissue samples of 25 g were removed from the fillets and placed in two 500 ml sterilized polycarbonate jars, each with a prototype wireless sensor (prepared according to section 6.3.1) with fresh hydrogel coating. The jars were sealed with Saran™ food wrap (PVDC with PP coating). The jars were kept in a refrigerator at 4°C. The resonant frequencies of both sensors were monitored wirelessly every 8 hours for 104 hours with the interrogator coil and impedance analyzer. The sensor inductor was aligned concentrically with the interrogator coil at a distance of 10 cm. The test at 4°C was done with Saran™ food wrap to imitate a realistic storage condition of fresh fish.

6.3.3.4 Microbial analysis of Tilapia samples at 4°C

Simultaneously to the above spoilage trial at 4°C, 14 samples of 25 g of fish tissue were removed from the same Tilapia fillets, under the same aseptic conditions and placed in 14 polycarbonate jars. A fresh hydrogel coated pH-sensitive electrode pair was placed in each of these. Direct wired connections to the hydrogel coated electrode pairs were made to monitor V_{pH}. The jars were sealed with Saran™ food wrap (PVDC with PP coating). These samples were also allowed to spoil at 4°C inside the refrigerator. At 8 hour intervals, and at the same time the wireless sensor response was recorded, one of the samples was removed for microbial analysis. The first one was done at zero hour to determine the initial microbial loads. Before the jar was opened for microbial analysis, voltages across all hydrogel coated pH-sensitive electrode pairs were monitored. The electrode sample in the opened jar was discarded. The microbial analysis was done the same manner as described in section 6.3.3.2.

6.4 Results and Discussion

6.4.1 Sensor Response to Ammonia

As described in section 6.3.2, the resonant frequency of the sensor was measured as a function of time for different concentrations of NH_3. The result is shown in Fig. 6.3. It can be seen that when a fixed concentration of NH_3 was introduced to the sensor environment, the resonant frequency decreased, eventually stabilizing at an equilibrium value related to that concentration. It took approximately 20 minutes for the sensor to reach the equilibrium value after being introduced to the NH_3 irrespective of concentration. This response time is adequate for fish spoilage monitoring as the increase in total volatile basic nitrogen (TVB-N) in the fish package will occur over a period of several hours to days. The response time can be reduced by decreasing the thickness of the hydrogel coating as shown in section 5.5.4 [16].

To examine repeatability, for each concentration of NH_3, the response test was performed three times and results are shown in Fig. 6.4. Each data point consists of an average of 10 resonant frequency measurements, taken at 2 minutes intervals after the sensor reaches its equilibrium state (20 minutes after exposure). The resonant frequency exhibits a linear relationship with the logarithm of NH_3 concentration. Fig. 6.4 shows that NH3 concentration can be measured with an accuracy of 13% (based on maximum deviation from the linear fit). Using the standard deviation of the resonant frequency during the initial zero volatile period (first 20 minutes of Fig. 6.3) the sensor has a frequency noise floor of 7.4 kHz. This corresponds to a detection limit of 0.001 mg L^{-1} (1.5 ppm).

Previous studies showed that the slope of response curve and the V_{pH} value for zero acidic/basic volatiles concentration decreased with decrease of temperature as shown in section 5.5.3 [16]. This is due to temperature sensitivity of the pH-sensitive electrode pair and the effect of temperature on the mobility of ions inside the hydrogel [20]. One mechanism is the temperature dependence of the gas diffusion coefficient which increases the sensor's response time with decrease of temperature [21]. Also, under low relative humidity conditions the hydrogel dehydrates and does not act like an electrolyte for the pH-sensitive electrode pair [22]. Previous studies also showed that the sensor requires a relative humidity between 100% to 45% to perform properly [16]. Generally in a sealed fish package environment the relative humidity is higher than this level [23].

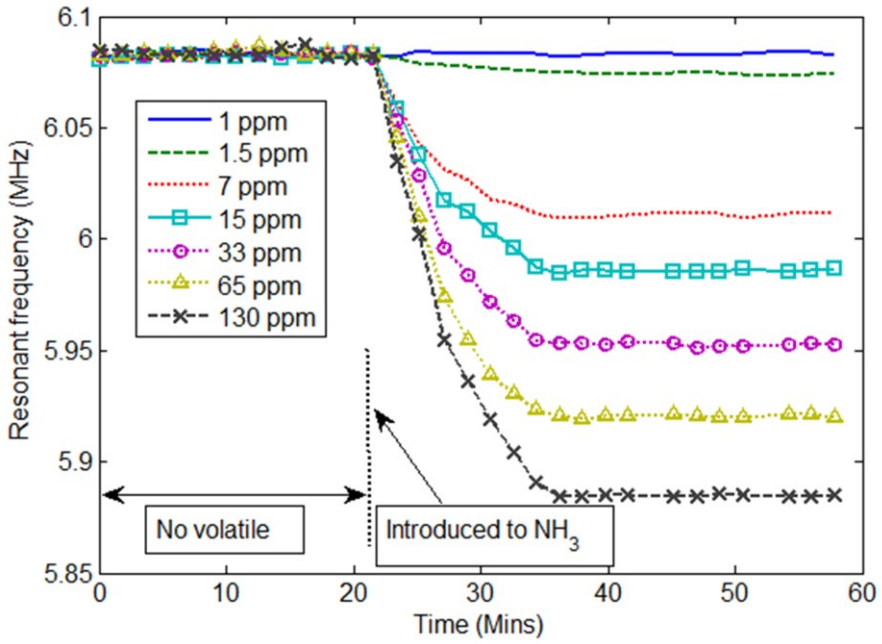

Figure 6.3. Resonant frequency of the sensor measured for different concentrations of NH_3 at 24°C.

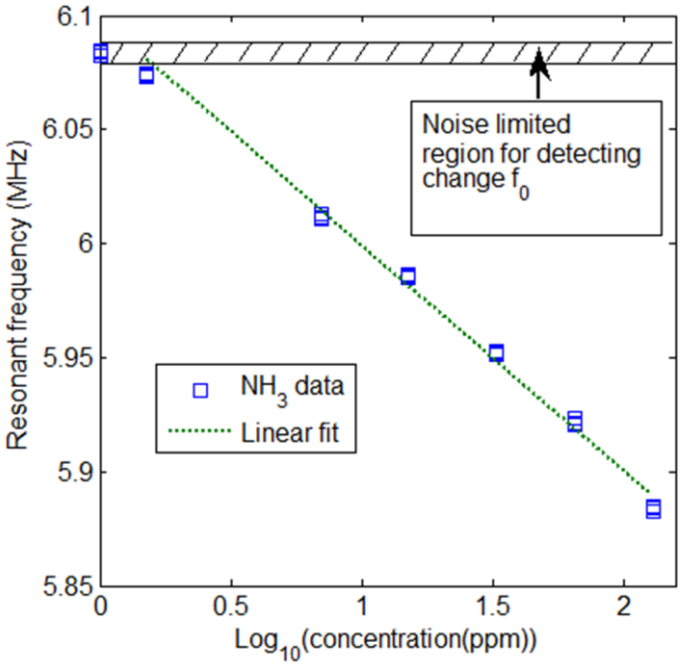

Figure 6.4. Resonant frequency of the sensor after reaching equilibrium state as a function of NH_3 concentration at 24°C (20 mins. after initial exposure-refer to Fig. 5). For each concentration 3 measurements are shown, each consisting of an average of 10 measurements at 2 mins. intervals.

6.4.2 Fish Spoilage Trial at 24°C

Figure 6.5 shows the sensor's resonant frequency and the TVC and *Pseudomonas* count for fish spoilage trials at 24°C. The sensor response is correlated with the bacterial population. The resonant frequency of the wireless sensor (in the same container as the tilapia tissue sample) decreased with increasing total volatile basic nitrogen (TVB-N) generated during tilapia spoilage. The sensor was monitored every 3 hours until no further substantial change in resonant frequency was observed. The TVC slowly increased from a level near 10^5 cfu g^{-1} during the initial 9 hours and then rose sharply before stabilising at approximately 10^9 cfu g^{-1} at 27 hours. Initially the *Pseudomonas* count was approximately 75% of the TVC count and rose to near 100% at after 12 hours. Similarly to the TVC count, the *Pseudomonas* count increased sharply and stabilized at approximately 10^9 cfu g^{-1} at 27 hour. Koutsoumanis and Olafsdottir *et al.* both

reported TVC and *Pseudomonas* values of 10^7 cfu g^{-1} as the level where fresh fish samples have reached their end of shelf life [6], [24]. This level occurred at 15 hours in our experiment. This end-of-shelf-life level can be clearly identified by the 80 kHz change in sensor resonant frequency.

Results of the microbial analysis and wired sensor response at 24°C are shown in Fig. 6.6. Here the TVC and *Pseudomonas* count, and the voltage, V_{pH}, measured across the hydrogel coated pH-sensitive electrode pairs are provided. Sensors were in the same container as the 12 Tilapia tissue samples used for microbial analysis and were measured every 3 hours. Thus at the beginning of the trial 12 V_{pH} data points are indicated. The data points decreased every 3 hours as samples were opened and used for microbial analysis. The response, V_{pH} values, from all 12 wired sensors are very similar with a deviation of less than ±2.8 mV and are correlated with the change in the bacterial population of the fish samples. The similarity of all 12 wired sensor responses demonstrates that the hydrogel-pH-sensitive electrode sensor can be fabricated reproducibly. An initial trial (not shown here), performed in the same manner with wired sensors at 24°C, showed an analogous relationship between sensor response and bacterial population over time.

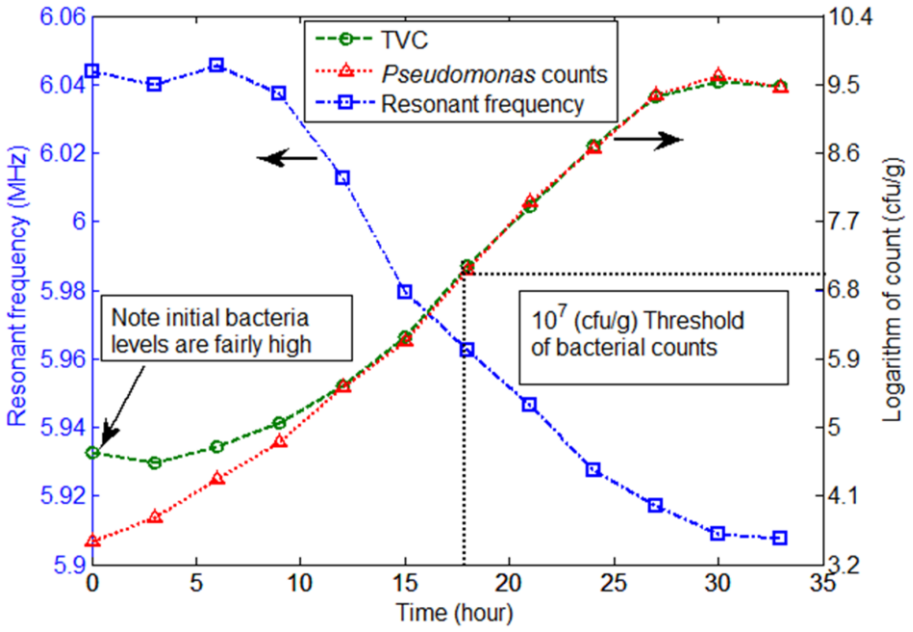

Figure 6.5. Resonant frequency of the sensor and bacterial population in fresh Tilapia kept at 24°C over a period of 1.5 days. Bacterial data are the average of two replicates.

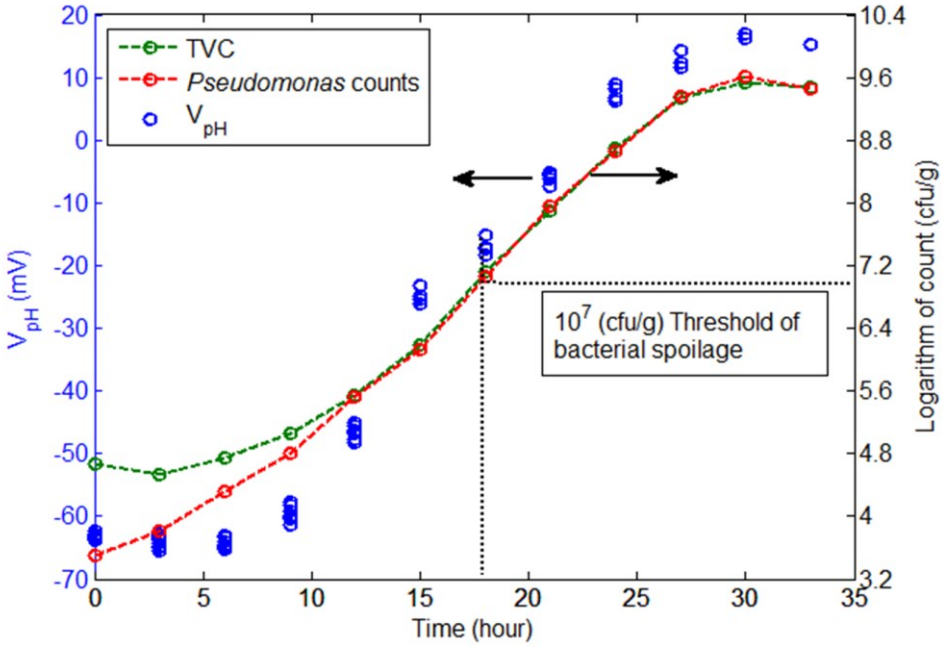

Figure 6.6. Measured voltages across all 12 hydrogel coated pH-sensitive electrode pairs and change in bacterial population for Tilapia at 24°C. Bacterial data are an average of two replicates.

6.4.3 Fish Spoilage Trial at 4°C

Figure 6.7 shows the resonant frequency and the TVC and *Pseudomonas* count for fish spoilage trials at 4°C. Two jars, each with a tilapia sample and a wireless sensor were used. The responses of both sensors are correlated with the change in bacterial population. The resonant frequencies of the wireless sensors decreased with increasing total volatile basic nitrogen (TVB-N) generated during tilapia spoilage. The sensors were monitored every 8 hours until no further substantial change in resonant frequencies was observed. The TVC slowly increased from a level near 10^4 cfu g^{-1} during the initial 16 hours and then rose sharply before stabilising at approximately 10^8 cfu g^{-1} at 88 hours. Initially the *Pseudomonas* count was approximately 78% of the TVC count and rose to near 100% after 32 hours. Similarly to the TVC count, the *Pseudomonas* count increased sharply and stabilized at approximately 10^8 cfu g^{-1} at 88 hours. The end-of-shelf-life level (10^7 cfu g^{-1}) occurred at 48 hours in our experiment. This level can be clearly identified by the 72 kHz change in sensor resonant frequency. The two individual sample tests performed with the wireless sensors showed a very similar resonant frequency behavior, with a deviation of less than ±4.16 kHz, and are correlated with the change in the bacterial population of the fish samples. Similarity of the two wireless sensor responses demonstrates the reproducibility of the sensor.

Results of the microbial analysis and wired sensor response at 4°C are shown in Fig. 6.8. The TVC and *Pseudomonas* count, and the voltage, V_{pH}, measured across the hydrogel coated pH-sensitive electrode pairs are provided. Sensors were in the same container as the Tilapia tissue samples used for microbial analysis and were measured every 8 hours. The response, V_{pH} values, from all 14 wired sensors are very similar with a deviation of less than ±3 mV and are correlated with the change in the bacterial population of the fish samples.

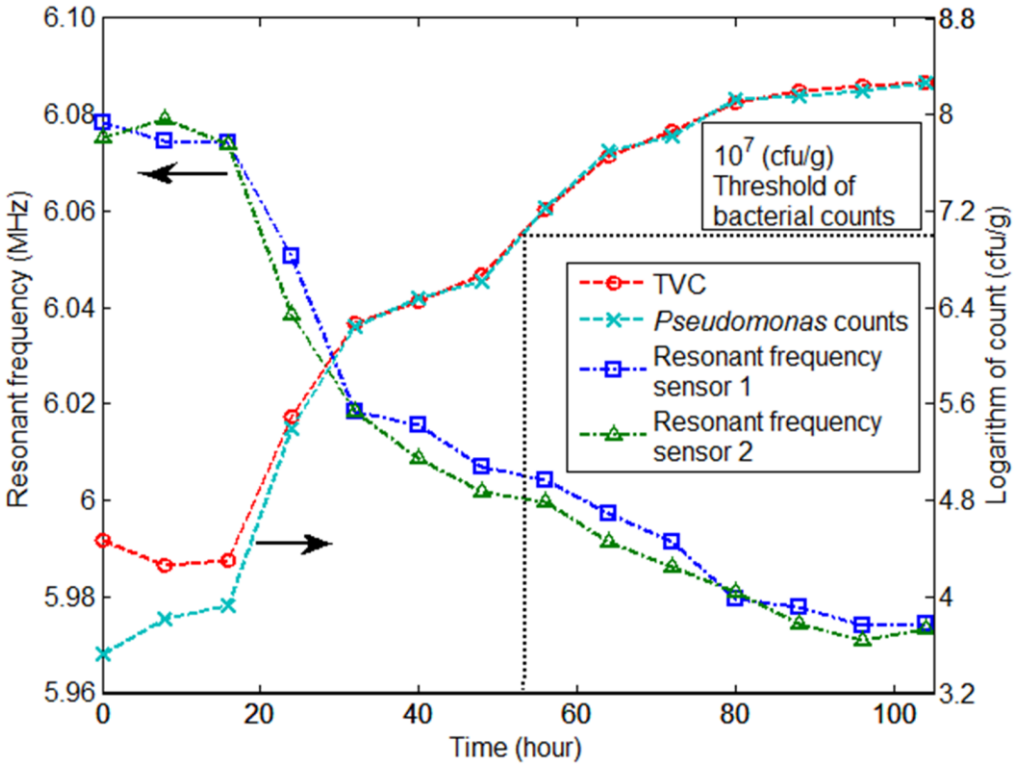

Figure 6.7. Resonant frequencies of the two sensors and bacterial population in fresh Tilapia kept at 4°C over a period of 4.5 days. Bacterial data are the average of two replicates.

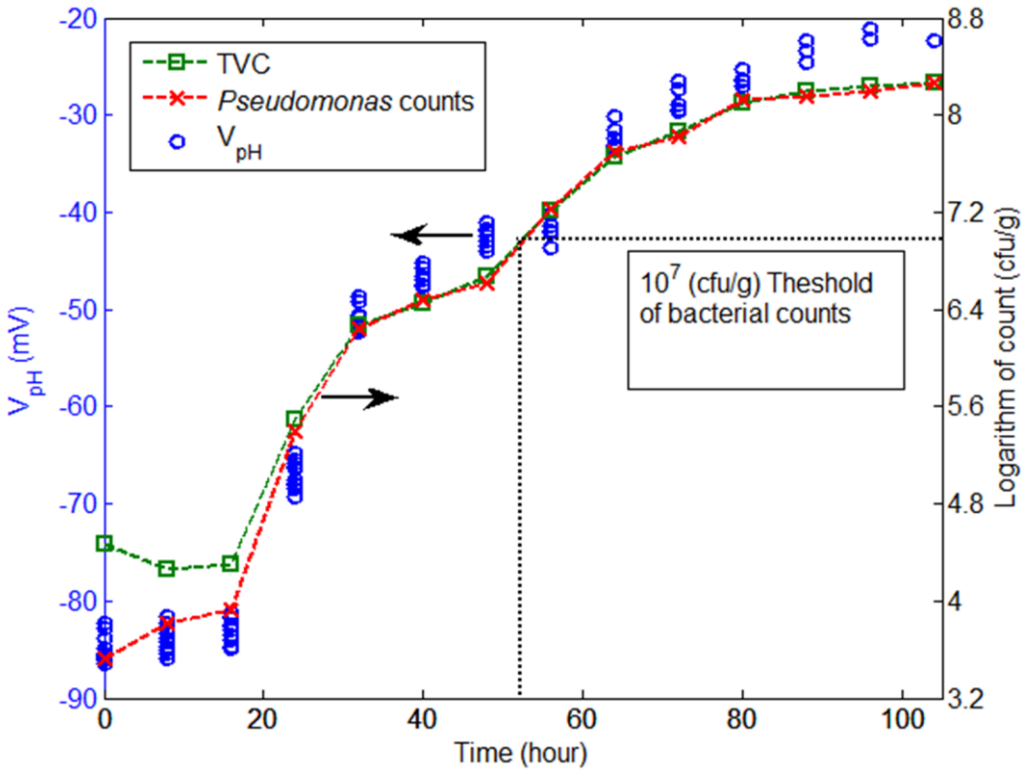

Figure 6.8. Measured voltages across all 14 hydrogel coated pH-sensitive electrode pairs and change in bacterial population for Tilapia at 4°C. Bacterial data are the average of two replicates.

6.5 Discussion and Conclusion

We demonstrated a hydrogel-pH-electrode based wireless sensor as a possible method for food freshness monitoring of packaged fish. The sensor employs a near-field coupled passive LC resonator whose resonant frequency is sensitive to basic volatile concentration. It exhibits a linear response that varies with the logarithm of ammonia concentration and has a detection limit of 0.001 mg L^{-1} (1.5 ppm). Trials of monitoring the spoilage of tilapia over several days at 24°C and 4°C showed that the sensor response was correlated with the bacterial growth in the fish tissue. The sensor was able to identify when the TVC exceeded a level of 10^7 cfu g^{-1}, indicative of end-of-shelf-life.

The sensor demonstrated repeatable results for a constant temperature. However, the sensor's response baseline shifted when temperature decreased from 24°C to 4°C, along with a slight change in sensitivity. This temperature dependence is typical of pH-electrode pair sensors. Previous studies of this particular sensor showed the V_{pH} baseline decreased by 18 mV and the sensitivity decreased by 5 mV/log (concentration (ppm)) when temperature decreased from 24°C to 4°C [16]. This behavior matches the results in Figs. 7 and 9. Thus, in order to reliably correlate bacteria count with sensor response, the temperature of the sample must be known or a temperature compensation method should be employed [20]. In addition the sensor required a relative humidity greater than 45% in order to maintain the electrolyte in the hydrogel [16]. The relative humidity constraint can be alleviated by using an encapsulation membrane, impermeable to water vapor, or an alternate host electrolyte.

The sensor does not require a custom integrated circuitry, making it amenable to low cost mass production using printed electronics technology. The passive components: inductor coil, capacitors and resistors are amenable to several flexible substrate printing approaches [25], [26]. The Ag/AgCl/nafion reference electrode can be fabricated using the inkjet printing/screen printing method [17], as can the pH-sensitive MMO electrode [27]. Even though printed transistor and diode technologies are available, printed RF varactors are still a research topic [26]. The electrodes proposed for this sensor are not toxic and have been previously used in food and biological media applications [2], [28]. The hydrogel used for coating the electrodes is regularly used for medical usage and is biocompatible, even though an encapsulation method still needs to be deployed [29]. Additionally polyamide substrates have been previously used as non-toxic material and would be compatible with food packaging materials by attachment to the inside of the fish package wrap.

References

[1] R.L. Scharff, Economic burden from health losses due to foodborne illness in the United States, J. of Food Protection 75 (2012) 123-131.

[2] W.D. Huang, S. Deb, Y.S. Seo, S. Rao, M. Chiao, J.C. Chiao, A passive radio-frequency pH-sensing tag for wireless food-quality monitoring, IEEE Sensors J. 12 (2012) 487-495.

[3] K.G. Ong, J.S. Bitler, C.A. Grimes, L.G. Puckett, L. G. Bachas, Remote query resonant-circuit sensors for monitoring of bacteria growth: application to food quality control, Sensors 2 (2002) 219-232.

[4] É. Dufour, J.P. Frencia, E. Kane, Development of a rapid method based on front-face fluorescence spectroscopy for the monitoring of fish freshness, Food Research International 36 (2003) 415–423.

[5] A. Pacquit, K.T. Laua, H. McLaughlin, J. Frisby, B. Quilty, D. Diamond, Development of a volatile amine sensor for the monitoring of fish spoilage, Talanta 69 (2005) 515-520.

[6] G. Olafsdóttir, E. Martinsdóttir, J. Oehlenschläger, P. Dalgaard, B. Jensen, I. Undeland, I.M. Mackie, G. Henehan, J. Nielsen, H. Nilsen, Methods to evaluate fish freshness in research and industry, Trends in Food Science & Technology 8 (1997) 258-265.

[7] N. Hamada-Sato, K. Usui, T. Kobayashi, C. Imada, E. Watanabe, Quality assurance of raw fish based on HACCP concept, Food Control 16 (2005) 301-307.

[8] L. Gram, H.H. Huss, Microbiological spoilage of fish and fish products, International Journal of Food Microbiology 33 (1996) 121-137.

[9] K. Crowley, A. Pacquit, J. Hayes, K.T. Lau, D. Diamond, A gas-phase colorimetric sensor for the detection of amine spoilage products in packaged fish, in Proc. IEEE Sensors (2005) 754-757.

[10] A. Pacquit, K.T. Lau, D. Diamond, Development of a colorimetric sensor for monitoring of fish poilage amines in packaging headspace, in Proc. IEEE Sensors (2004), 365-367.

[11] B. Kuswandi, Jayus, A. Restyana, A. Abdullah, L.Y. Heng, M. Ahmad, A novel colorimetric food package label for fish spoilage based on polyaniline film, Food Control 25 (2012) 184-189.

[12] Z. Jun, L.X. Yu, W. Wei, Z. Zhu, Z. Wei, X. Wu, Determination freshwater fish freshness with gas sensor array, in Proc. IEEE World Congress on Computer Science and Information Engineering (2009) 221-224.

[13] X. Li, Electronic Nose to monitor the freshness of Red Fish (*Sebastes marinus*) stored in ice and modified atmosphere packaging (MAP), UNU-Fisheries Training Programme, Final Project 2000, Reykjavik, Iceland, 2000.

[14] J. Hammond, B. Marquis, R. Michaels, B. Oickle, B. Segee, J. Vetelino, A. Bushway, M. E. Camire, K. Davis-Dentici, A semiconducting metal-oxide array for monitoring fish freshness, Sensors and Actuators B: Chemical 84 (2002) 113-122.

[15] L. Zhongdong, G. Benqian, H. Yaqiang, L. Zhenxing, L. Boxiang, A new method for the non-destructive determination of fish freshness by nuclear imaging, in Proc. IEEE Complex Medical Engineering (2011) 165-168.

[16] S. Bhadra, D.J. Thomson, G. E. Bridges, Monitoring acidic and basic volatile concentration using a pH-electrode based wireless passive sensor, Sensors and Actuators B: Chemical (2014) DOI: 10.1016/j.snb.2014.12.021.

[17] B.E. Horton, S. Schweitzer, A.J. DeRouin, K. G. Ong, A varactor-based inductively coupled wireless pH sensor, IEEE Sensors J. 11 (2011) 1061-1066.

[18] G.S. Duffó, S.B. Farina, C.M. Giordano, Characterization of solid embeddable reference electrodes for corrosion monitoring in reinforced concrete structures, Electrochimica Acta 54 (2009) 1010-1020.

[19] S. Bhadra, M. McDonald, D.J. Thomson, M.S. Freund, G. E. Bridges, An inductively coupled passive tag for remote basic volatile sensing, in Proc. IEEE RFID (2014) 147-152.

[20] S. Bhadra, D.S.Y. Tan, D.J. Thomson, M.S. Freund, G. E. Bridges, A wireless passive sensor for temperature compensated remote pH monitoring, IEEE Sensors J. 13 (2013) 2428-2436.

[21] J. Crank, Methods of measurement, in: J. Crank, G.S. Park (Eds.), Diffusion in Polymers, Academic Press, New York, 1968, pp. 1-39.

[22] S. Neethirajan, M.S. Freund, D.S. Jayas, C. Shafai, D.J. Thomson, N.D.G. White, Development of carbon dioxide (CO_2) sensor for grain quality monitoring, Biosystems Engineering 106 (2010) 395-404.

[23] Frozen fish [online]. Retrieved Aug 14, 2014, from http://www.tis-gdv.de/tis_e/ware/fisch/gefroren/gefroren.htm.

[24] K. Koutsoumanis, Predictive modeling of the shelf life of fish under nonisothermal conditions, Appl. Environ. Microbiol. 67 (2001) 1821-1829.

[25] S. Khan, R. Dahiya, L. Lorenzelli, Technologies for printing sensors and electronics over large flexible substrates: a review, IEEE Sensors J. PP (2014) DOI: 10.1109/JSEN.2014.2375203.

[26] T. Ge, J.S. Chang, T. Lin, Z. Lei, L.G. Soon, Fully-additive printed electronics on flexible substrates: a fully-additive RFID tag, in Proc. IEEE International Midwest Symposium on Circuits and Systems (2014) 825-828.

[27] P. Majzlikova, J. Prasek, J. Chomoucka, J. Drbohlavova, J. Pekarek, R. Hrdy, J. Hubalek, L. Trnkova, Cu_2O based electrochemical sensor for direct glucose detection, in Proc. IEEE Sensors (2013) 1-4.

[28] P. Kurzweil, Metal oxides and ion-exchanging surfaces as pH sensors in liquids: state-of-the-art and outlook, *Sensors* 9 (2009) 4955-4985.

[29] INTRASITE◊ Gel [online]. Retrieved July 27, 2013, from http://www.smith-nephew.com/professional/products/advanced-wound-management/intrasite-gel/.

Chapter 7: Conclusions and Future Work

This research studies and develops inductively coupled LC pH sensors based on direct measurement of a pH-sensitive electrode pair's potential difference. In chapter 2, a varactor based LC resonator circuit was developed to measure low frequency potential difference and an RF interrogation technique was demonstrated to wirelessly monitor the resonant frequency of the LC resonator circuit. For wireless pH sensing, the LC resonator circuit was integrated with a pH-sensitive electrode pair. The prototype sensor exhibited linear response to pH over 2-12 pH dynamic range, 0.1 pH resolution, fast response and no long-term drift problem. Thus it overcomes the drawbacks of polymer-based pH sensors (long response time, highly non-linear response and long-term instability [1]-[3]) and optical pH sensors (limited dynamic range and long-term drift due to photobleaching over time [4]-[7]). The sensor presented in chapter 2 has higher resolution and wider dynamic range than other electrode-based LC pH sensor reported in [8]. Therefore this proposed sensor has potential for applications such as bioprocess and food spoilage monitoring, where 0.1 pH accuracy over wide pH dynamic range is needed with long term stability.

The work presented in chapter 3 shows a technique of measuring two parameters (in this case pH and temperature) with a single RLC resonator based sensor by varying the resonant frequency and quality factor. An algorithm is also developed, which applies both pH and temperature measurement to incorporate temperature compensation in pH measurement. The sensor was able to perform temperature compensated pH monitoring with 0.1 pH accuracy for temperature over a range of 25°C-55°C and for pH over a 1.5-12 dynamic range. This temperature and pH range can be improved further. Without temperature compensation the sensor was shown to have < 1 pH accuracy making it unusable in temperature varying

environments such as food monitoring. Temperature compensation was previously demonstrated by other researchers for electrode based wired and active wireless pH sensors [9], [10]. However, no electrode based passive pH sensor has been reported to take the temperature effect into account.

Chapter 4 shows an encapsulation method that can be applied to any LC resonator based sensor for in-fluid applications. The encapsulation reduces the influence of medium permittivity and conductivity on the sensor measurement. The wireless pH electrode-based sensor is scaled down to fit in a small bioreactor and made autoclavable. Non-invasive way to obtain reliable pH information from two yeast fermentation is demonstrated with the fluid embeddable sensor. The sensor can be easily used in any bacterial culture bioprocess for pH monitoring.

The work presented in chapter 5 transforms the pH sensor to a wireless acidic and basic volatile sensor by embedding the pH-sensitive electrode pair in a hydrogel host electrolyte. A simple explanation of how the response varies with sensor geometry is developed and a study of sensor response to acetic acid and ammonia vapor is provided. The sensor demonstrated the expected linear relationship to the logarithm of volatile concentration and a detection limit of 1.5 ppm for NH_3 and 2 ppm for CH_3COOH vapor. This sensitivity is well below or adequate for many applications, i.e., the maximum NH_3 level for human work environment is 20 ppm [11] and fish spoilage can generate 30 ppm total volatile basic nitrogen (TVBN) [12].

Finally chapter 6 reports the use of the wireless acidic and basic volatile sensor as a possible method for detecting fish spoilage. Acidic and basic volatiles are by-products of food spoilage. Applying electrode-based pH sensors to food spoilage monitoring requires the electrodes to be in direct contact with the food. This possesses the risk of electrode fouling and

food contamination, and problems with detection in dry food. The wireless acidic and basic volatile sensors avoid these problems and can distinctly identify when the food spoilage occurs.

The LC sensor technology presented here has promising potential for commercial bioprocess and food quality monitoring. Since the LC-sensors electronics can be reduced in size and implemented with printable electronics technology as described in section 6.5, it is a viable and low-cost method for integration into bioreactors and food packaging.

In the present work the electrode-based pH sensors operate in a near-field coupling regime with interrogation distances on the order of 10 cm. For applications requiring larger read ranges a RF chipless approach in future can be employed [13]. The pH-sensitive electrode pair was made separately and integrated with the LC resonator circuit. Future research can explore printing the electrodes on the LC resonator circuit board. This will enable miniaturizing the sensor further. Relative humidity should be considered when using the volatile sensor. The sensor requires a relative humidity of 45% or higher to maintain the electrolyte in the hydrogel for proper operation. This limitation can be alleviated in future by using an encapsulation membrane or an alternate host electrolyte. Since the volatile sensor is based on hydrogel pH change, it responds to all acidic and basic volatiles present in its surrounding environment. Future research can investigate applying a selective gas permeable membrane on the top of the hydrogel allowing only a particular gas to pass and diffuse through the hydrogel [14].

References

[1] V. Sridhar and K. Takahata, "A hydrogel-based passive wireless sensor using a flex-circuit inductive transducer," *Sensors and Actuators: A*, vol. 155, no. 1, pp. 58-65, Oct. 2009.

[2] M. K. Jain, Q. Cai and C. A. Grimes, "A wireless micro-sensor for simultaneous measurement of pH, temperature, and pressure," *Smart Materials and Structures*, vol. 10, no. 2, pp. 347-353, April 2001.

[3] B. E. Horton, B. D. Pereles, C. Ruan, E. L. Tan and K. G. Ong, "Wireless passive pH sensor based on magnetic higher-order harmonic fields," *Sensor Letters*, vol. 7, no. 4, pp. 599-604, August 2009.

[4] P. Harms, Y. Kostov and G. Rao, "Bioprocess monitoring," *Current Opinion in Biotechnology*, vol. 13, no. 2, pp. 124-127, Apr. 2002.

[5] H. R. Kermis, Y. Kostov, P. Harms and G. Rao, "Dual excitation ratiometric fluorescent pH sensor for noninvasive bioprocess monitoring: development and application," Biotechnology Progress, vol. 18, no. 5, pp. 1047-1053, Sept. 2002.

[6] "Non-Invasive pH Sensors." Internet: http://www.presens.de/fileadmin/user_upload/products/Sensor_Probes/Non-invasive_pH_Sensors/110715_SP-NonInvpH-11-01_w.pdf [June 5, 2012].

[7] W. -L Tsai, J. L. Autsen, J. Ma, T. Hudson and J. Luo, "Noninvasive optical sensor technology in shake flasks for mammalian cell cultures," *BioProcess International*, vol. 10, no. 1, pp. 50–56, Jan. 2012.

[8] J. B. E. Horton, S. Schweitzer, A. J. DeRouin and K. G. Ong, "A varactor-based inductively coupled wireless pH sensor," *IEEE Sensors J.*, vol. 11, no. 4, pp. 1061-1066, April 2011.

[9] P. Kurzweil, "Metal oxides and ion-exchanging surfaces as pH sensors in liquids: state-of-the-art and outlook," *Sensors*, vol. 9, pp. 4955-4985, June 2009.

[10] J. Frisby, D. Raftery, J. P. Kerry and D. Diamond, "Development of an autonomous, wireless pH and temperature sensing system for monitoring pig meat quality," *Meat Science*, vol. 70, pp. 329-336, 2005.

[11] B. Timmer, W. Olthuis and A. V. D. Berg, "Ammonia sensors and their applications—a review," *Sensors and Actuators B: Chemical*, vol. 107, no. 2, pp. 666-677, Mar. 2005.

[12] R. S. Singhal, P. R. Kulkarni and D. V. Rege, Handbook of Indices of Food Quality. Cambridge, England: Woodhead Publishing Limited, 1997.

[13] S. Preradovic, S. M. Roy and N. C. Karmakar, "RFID system based on fully printable chipless tag for paper-/plastic-item tagging," IEEE Antennas and Propagation Magazine, vol. 53, no. 5, pp. 15-32, Oct. 2011.

[14] S. Neethirajan, M.S. Freund, D.S. Jayas, C. Shafai, D.J. Thomson and N.D.G. White, "Development of carbon dioxide (CO_2) sensor for grain quality monitoring," *Biosystems Engineering*, vol. 106, no. 4, pp. 395-404, Aug. 2010.